LBL-14050

LBL--14050

DE82 013004

OBSERVATION OF NEW SPONTANEOUS FISSION ACTIVITIES FROM ELEMENTS 100 to 105

Lawrence Patrick Somerville

Ph.D. Thesis

March 1982

Nuclear Sciences Division
Lawrence Berkeley Laboratory
University of California
Berkeley, CA 94720

This work was supported by the Director, Office of Energy Research, Division of Nuclear Physics of the Office of High Energy and Nuclear Physics of the U.S. Department of Energy under Contract DE-AC03-76SF00098.

Observation of New Spontaneous Fission Activities From Elements 100 to 105

Abstract

Several new Spontaneous Fission (SF) activities have been found. Their half-lives and production cross sections in several reactions have been measured by collecting and transporting recoils at known speed past mica track detectors. No definite identification could be made for any of the new SF activities; however, half-lives and possible assignments to element-104 isotopes consistent with several cross bombardments include ^{257}Rf(3.2 s, 14% SF), ^{258}Rf(13 ms), ^{259}Rf(~3 s, 8% SF), ^{260}Rf(~20 ms), and ^{262}Rf(~50 ms). The 80-ms SF activity claimed by the Dubna group for the discovery of element 104 (^{260}104) was not observed. A difficulty exists in the interpretation that ^{260}Rf is a ~20-ms SF activity: in order to be correct, for example, the SF activities with half-lives between 14 and 24 ms produced in the reactions 109- to 119-MeV ^{18}O + ^{248}Cm, 88- to 100-MeV ^{15}N + ^{249}Bk, and 96-MeV ^{18}O + ^{249}Cf must be other nuclides due to their large production cross sections, or the cross sections for production of ^{260}Rf must be enhanced by unknown mechanisms. Based on calculated total production cross sections a possible ~1% electron-capture branch in ^{258}Lr(4.5 s) to the SF emitter ^{258}No(1.2 ms) and an upper limit of 0.05% for SF branching in ^{254}No(55 s) were determined. Other measured half-lives from unknown nuclides produced in respective reactions include ~1.6 s (^{18}O + ^{248}Cm), indications of a ~47-s SF activity (75-MeV ^{12}C + ^{249}Cf), and two or more SF activities with 3 s$\leq T_{1/2} \leq$60 s (^{18}O + ^{249}Bk). The most exciting conclusion of this work is that if the tentative assignments to even-even element-

104 isotopes are correct, there would be a sudden change in the SF half-life systematics at element 104 which has been predicted theoretically by Randrup et al. and Baran et al. and attributed to the disappearance of the second hump of the double-humped fission barrier. This disappearance of the second barrier also explains the tentative low hindrance factors compared to lighter elements for SF of the odd-mass isotopes ^{257}Rf(~4×10^3) and ^{259}Rf(~2×10^3). On the basis of recent odd-mass alpha-decay energy data, the 152-neutron sub-shell effect is probably weaker for element 104 than for element 102, confirming predictions of Randrup et al., and not strong enough to significantly alter the SF half-life predictions. This weakening sub-shell effect is in contrast to the continuing strong effect assumed in the Ghiorso half-life systematics. The possibilities of enhanced stability against SF with 157 neutrons for ^{261}Rf(65 s) and theoretical arguments concerning the SF-mass distributions for element-104 nuclei are discussed.

I. Introduction and Purpose

According to the charged liquid-drop model of the nucleus, nuclei tend to be stable with respect to Spontaneous Fission (SF) decay if the ratio of Coulomb energy to twice the surface energy is less than one, or equivalently $Z^2/A \leq 50$. Since the Coulomb energy increases roughly as $Z^2/A^{1/3}$ while the surface energy increases more slowly as $A^{2/3}$, fission becomes an increasingly important decay mode for the heaviest elements. The importance of SF decay among the heaviest elements can be seen from the 121 SF activities for which assignments have been suggested in Figure 1. Nuclei with closed shells tend to be more stable against SF than neighboring nuclei; nuclei with odd numbers of protons and/or neutrons are generally more stable against SF than neighboring even-even nuclei. An understanding of the shell effects and the systematic variation in partial half-life for SF decay as a function of the number of neutrons and protons is essential in predicting the half-lives for heavier, unknown nuclei and, in particular, for superheavy elements.

This paper is primarily concerned with the SF properties of isotopes of element 104, and particularly their SF half-lives. For the even-even nuclei up to element 102 inclusive the empirical Ghiorso systematics (GHI70a) fits the partial SF half-lives quite well, as shown in Figure 2a. For element 104, extrapolation of the Ghiorso systematics using an 11-ms half-life for ^{258}Rf and assuming a continuing strong 152-neutron sub-shell effect results in half-life predictions of the order of seconds for ^{256}Rf and $\leq 10^{-6}$ seconds

for isotopes of element 104 with even mass numbers of 260 or higher. But a group at the Joint Institute for Nuclear Research in Dubna, USSR, led by Flerov (FLE64) claimed discovery of element 104 by assigning a 0.3-s SF activity to $^{260}104$, a much longer half-life than predicted by the Ghiorso systematics. The half-life has since been revised by the Dubna group to 0.1 s (OGA69, ZVA70) and later to 80 ms (DRU77). Independent searches for the 100-ms SF activity in the reactions 94-MeV $^{16}O + ^{248}Cm$ (GHI70a) and for the 80-ms SF activity in the reactions 78- to 86-MeV $^{15}N + ^{249}Bk$ (NIT81) have yielded only negative results, however. On the basis of a 100-ms half-life for $^{260}104$ and an 11-ms half-life for ^{258}Rf Flerov (FLE71) then discussed a sudden change in the SF half-life systematics from element 102 to 104, which if confirmed would show a weakening of the 152-neutron sub-shell effect as shown in Figure 2b taken from reference OGA74a. A 5-ms half-life for ^{256}Rf (OGA74a), recently verified by Münzenberg et al. (MÜN80, MÜN81b, MÜN82), was consistent with the notion of a change in SF half-life systematics at element 104. Several authors have since predicted a drastic change in the SF half-life systematics at element 104 (RAN73,76; BAR81) or at element 102 and beyond (PAU74). Randrup et al. attributed this change in half-life systematics to a disappearance of the second hump of the double-humped fission barrier for element-104 isotopes and a weakening of the 152-neutron sub-shell effect in the SF half-lives. Mustafa and Ferguson have also predicted an absence of the second barrier for even-even element-104 nuclei with mass numbers of 260 or higher (MUS78, MUS77).

In attempts to determine the partial SF half-lives of element-104

nuclei and to see if there is indeed a change in the SF half-life systematics at element 104, a recoil tape-transport system was designed by Nitschke. The experiments using this tape system were performed in a collaboration between the heavy-element groups of the Lawrence Berkeley and Lawrence Livermore National Laboratories. In analysis of the experimental data by the author, several new SF activities were found and their production cross sections were measured. The possible assignments which have been suggested in Table 1 include some element-104 isotopes. The way in which these new SF activities were produced is described in the following section.

II. Experimental Procedure

In searches for new SF activities with half-lives between milliseconds and seconds, direct production of relatively large quantities of ^{256}Fm(2.6 hr) and of ^{256}Md(77 min), which decays by electron capture to ^{256}Fm, has led to a substantial SF background in most experiments. To reduce this long-lived background we used a large-area, rotating, scanning drum assembly for the work in reference NIT81. To reduce our SF background by another factor of 20 in search of an 80-ms SF activity, the 2-km-long tape system shown in Figure 3 was constructed. The tape was either 25-μm-thick nickel or 12.5-μm-thick stainless steel, cooled by either contact with a water-cooled post or by a helium gas jet on the back side of the tape. The target, tape, and everything in electrical contact with the tape acted together as a Faraday cup for measuring the beam intensity. Mica track detectors (FLE75) were used to detect SF events from recoils embedded in the tape. The tape moved at a speed of typically 0.05 to 1.0 meter per second, as measured electronically from the capstan drive. The speed was constant to within, typically, one per cent. After the bombardment, the micas were etched for 40 minutes in 48-per-cent hydrofluoric acid at 60°C. The SF tracks were then visible under a microscope with x100 magnification. Knowing the speed of the tape, track distances from the target along the mica strips corresponded to times of SF for nuclei after their production at the target. Knowing the event times, decay curves such as Figures 7-9, and 11-16 could be constructed and the half-lives determined. The overall detection

efficiency including emissivity of the SF fragments from the tape and scanning efficiency was measured with the use of ^{252}Cf sources to be ~70 per cent. Subjective differences in scanning efficiency over time were found to be as large as ten per cent by scanning the same micas at different times.

India-ruby muscovite mica offers a convenient method for detection of SF fragments due to its relative insensitivity to light ions and its low uranium content (FLE75). According to the ion-explosion-spike model developed by Fleischer, Price, and Walker (FLE65), the passage of a heavy ion in mica causes electronic ionization around its path. The remaining positively-charged lattice ions repel and dislodge one another from their sites creating vacancies in the lattice. Price and Walker discovered that the tracks could be observed using a microscope after hydrofluoric-acid etching. This is because hydrofluoric acid attacks and enlarges the damaged regions of mica preferentially (PRI62).

The background effect of SF from natural uranium in the mica is eliminated by annealing the micas for several days at ~500°C and pre-etching them with hydrofluoric acid for 80 minutes at 60°C. prior to use in an experiment. After use in a bombardment the micas were etched again for 50 minutes. The pre-etching causes the tracks from SF of uranium contained in the mica to be larger in size because they have been etched for a longer time than the tracks from SF of nuclei produced in the bombardment. The annealing of the micas also helps to break down the walls of the tracks from uranium SF events in the mica. With these procedures SF tracks from nuclei produced in the

bombardment can be easily distinguished from the larger, "faded" tracks from SF of uranium nuclei contained in the mica.

The targets used in the experiments were prepared either by vaporizing the actinide fluoride onto a heated beryllium backing foil (LOU74, 75) or by molecular electroplating of oxide targets. The actinide-fluoride targets were prepared at Lawrence Livermore National Laboratory by Lougheed and Hulet while the oxide targets were prepared by Moody here in Berkeley (MOO81). In the case of the berkelium-fluoride target, the berkelium (element 97) was chemically separated four days prior to the first bombardment with the 88-inch cyclotron. In many cases the targets were coated with very thin "stopper-foil" coatings of aluminum with ~25- to 50-$\mu g/cm^2$ thickness to reduce the transfer of target material to the tape. Typical target thicknesses were ~0.5 mg/cm^2, close to the calculated compound-nucleus recoil ranges.

For lack of identity of most of the SF activities, compound-nucleus recoil ranges were assumed in determining all of the cross sections. It is important to note that for those SF activities that turn out to be non-compound-nucleus products the cross sections listed in Table 1 and 2 could be quite different. As an example, with 90-MeV ^{12}C ions ^{244}Cf and ^{245}Cf have ranges in the compound-nucleus reactions $^{238}U(^{12}C,5\text{-}6n)^{245,244}Cf$ which are twice as long as when they are produced in the reactions $^{239}Pu(^{12}C;\alpha,2\text{-}3n)^{245,244}Cf$ (HAH74). Thus, for those spontaneously-fissioning products with ranges considerably shorter than compound nuclei, the cross sections listed in Tables 1 and 2 would be too low. On the other hand, if, for

example, the 4.5-s SF activity were a quasi-target product with a long range in the reaction 70-MeV $^{13}C + ^{249}Bk/^{249}Cf$, the quoted cross section would be too high because the target plus aluminum stopper-foil thickness was considerably greater than the assumed compound-nucleus recoil range.

The compound-nucleus recoil ranges were determined from the calculated recoil energies using the range tables of Northcliffe and Schilling (NOR70). Both the radioactive element and the oxygen or fluorine in the target were taken into account. A range calculated in this way agreed with the experimental range measurement of Hahn et al. for the reaction 83.8-MeV $^{12}C + ^{238}U \rightarrow ^{245,244}Cf$ + 5n,6n to within 10 per cent. For target plus aluminum stopper-foil thicknesses somewhat greater than the calculated recoil ranges, the aluminum foil thickness was converted to a target-material-equivalent thickness and subtracted from the calculated recoil range to give an effective target thickness for determining cross sections.

The beam size was collimated to just under the target diameter (usually 6.4 mm) as shown in Figure 3. The tape could be moved left and right at different speeds. At the end of each reel during the slow-down and reversal of the tape motion, the cyclotron beam was turned off electronically. Mica strips totaling one meter in length were mounted on each side of the target. In this way two separate decay curves could be constructed. With the tape moving at two different speeds, tape-speed-independent effects such as beam scattering and neutron-induced fission could be checked. Scattered beam ions near the edges of the first micas could damage the mica

surface and, if the density of scattered tracks was very high, could cause confusion with SF tracks. Glass scrapers were placed in contact with the tape surface on both sides of the target, not to scrape the tape, but to shield the mica from scattered beam ions. However, the tape often became warped with use so that good contact between the scrapers and tape was not always maintained. As a further precaution against scattered beam ions the data from the first several millimeters of mica were usually rejected.

The x and y coordinates of the SF tracks were recorded on punched cards. A computer code converted these coordinates to event times for a given tape speed (EGG78). From the event times the half-life and cross section for each component were computed with the use of the multi-component maximum-likelihood code first written by the late Richard Eggers (EGG81).

The maximum-likelihood code was extensively tested with artificially-generated event-time data including Poisson statistics for a single component and background (SOM82). The mean half-life determined by the maximum-likelihood code from several sets of artificially-generated data was found to accurately reproduce the half-life assumed in generating the data.

For calculation of cross-section upper limits, for example, of the 80-ms SF activity in Table 4, the least-squares computer code FRANTIC (ROG62) was used. The weights for the points in the fit were determined from maximum-likelihood fits assuming no 80-ms component was present.

The error bars for all the cross-section measurements include the

statistical error in the number of counts, a ten-per-cent uncertainty in the scanning efficiency, the uncertainty in the separation of counts into background and events belonging to a short-lived component, and, in one case, the uncertainty in the beam flux measurement. The half-life error bars, however, reflect only the statistical uncertainties. Possible unknown systematic errors have not been included in the errors for the cross-section and half-life measurements.

There are, in fact, three pieces of evidence for unknown systematic effects in the half-life measurements.

(1) Some measurements with the tape system did not repeat too well, for example, in the reactions 95-MeV ^{18}O + ^{248}Cm (1.6±0.1 s, 1.3±0.1 s) and 109-MeV ^{18}O + ^{248}Cm (22.4±1.3 ms, 17.1±2.2 ms). A second possible explanation for the difference in half-lives for the reaction 95-MeV ^{18}O + ^{248}Cm is that there might be another component with a half-life of a few tenths of a second and low production cross section (GHI81b). Due to the 1-cm distance from the target center to the edge of the first mica, the experiments with higher tape speeds are sensitive to earlier decay times than experiments with slower tape speeds. Consequently, a short-lived component might contribute only to data from experiments with higher tape speeds.

(2) For the same reaction ^{15}N + ^{249}Bk the drum experimental half-lives with 90-per-cent confidence limits in Figure 4 also seem to be longer than the tape experimental half-lives with standard deviation errors quoted in Figure 5.

(3) Lastly, the fit for the reaction 96-MeV ^{18}O + ^{249}Cf in

Figure 15 has a value of 1.31 for the chi-square per degree of freedom with only a 2-per cent confidence level. This poor fit, which is easily verified in a visual comparison of Figures 14 and 15, may indicate the presence of an unknown systematic effect in the data.

The cross section measurements, however, may be less subject to systematic error based on the following examples.

(1) In Table 1 two measurements of the cross section for the ~20-ms SF activity in the reaction 109-MeV $^{18}O + ^{248}Cm$ are statistically consistent, although different targets were used and different half-life measurements resulted.

(2) In addition, the drum and tape experimental cross sections are statistically consistent, although different targets and apparatuses were used.

(3) In previous rotating-drum experiments using the reactions 92- to 95-MeV $^{16}O + ^{248}Cm$ the measured cross sections from bombardments that have different targets with thicknesses of 450-500$\mu g/cm^2$ agree well with the cross section measured in the most recent tape experiment for the reaction 92-MeV $^{16}O + ^{248}Cm$.

If range straggling of the recoils were important the range distribution would not be as sharp as assumed in calculating the effective target thicknesses. Then the cross sections presented in Table 1 would be systematically low. This straggling effect was estimated assuming production of compound nuclei including contributions from electronic stopping in the target and the neutron boil-off effect. Since the extent of local variations in the target thickness within the area of the beam was unknown, this possible

contribution was not included in calculating the straggling parameter. Formulas similar to references ALE68 and WIN61, with minor changes discussed in the appendix section VIII.B., were used to calculate the straggling and fraction of recoils escaping the target (ALE82). Since the corrections to the recoil yield from the targets due to straggling were found to be less than 10 per cent, they were not included in determining the cross sections.

The beam energy into the target material was determined from the resonant frequency of the cyclotron and from the calculated energy loss through the Havar beam-window foil, nitrogen cooling gas, and beryllium target backing (NOR70). Measurements of the beam energy after the target using solid-state detectors were found to agree with the energy calculated from the range-energy tables of Northcliffe and Schilling to better than 0.5 MeV (SHI80b).

Since no direct measurements of the beam energy profile after passing through the target were available to the author, the effect of beam energy straggling was estimated for ^{18}O ions. For a mono-energetic beam of 111-MeV $^{18}O^{+8}$ ions passing through a 1.8-mg/cm^2 Havar beam window, 0.47-mg/cm^2 nitrogen target-cooling gas, and a 2.7-mg/cm^2 beryllium target backing the Firsov-Hvelplund expression (HVE71,RUD78) gives ~0.9 MeV for the standard deviation of the energy distribution while the Bohr expression (BOH48,SEG65) gives only ~0.2 MeV. But for ^{14}N ions with the same relative energy loss in beryllium as our ^{18}O ion case, experimental data from reference BEL81 indicate that the straggling should be much larger than either theory predicts, or ~1 MeV from the beryllium backing alone. In our

case, of the three stopping materials in the path of the beam the beryllium backing would give the largest contribution to energy straggling. Possible beam-energy smearing from unknown local variations in foil thickness within the area of the beam have not been included. The energy width of the beam coming directly from the cyclotron was not more than 0.1 MeV (GOU74). The unknown extent of energy straggling and the finite energy width of the beam from the cyclotron have been neglected in plotting excitation functions. But taking into account the beam energy straggling effect the widths of the excitation functions would become somewhat smaller.

The next section presents the results of experiments performed using these procedures.

III. Results

III.A. Introduction

The cross section and half-life measurements as well as possible assignments for the new SF activites are included in the following Table 1. Half-life error bars are standard deviations unless otherwise stated. The possible assignments are suggested largely on the basis of the cross bombardment data of Table 2. Table 3 compares the cross sections for analogous reactions in the two systems $^{18}O + ^{245}Cm$ and $^{18}O + ^{248}Cm$. This information is useful in deciding whether the 1.6-s SF activity produced in the reaction $^{18}O + ^{248}Cm$ could be ^{259}Fm or not. Table 4 compares the fits according to the chi-square values for the data of Figures 13-15 under two assumptions: (1) a single short-lived component and background exist (our interpretation); and (2) a 13.7-ms component (^{242f}Am), an 80-ms component, and background exist (the Dubna interpretation as in section IV.C.5.a.).

Calculations with the JORPLE code, discussed in the appendix section VIII.A., were invaluable in deciding whether or not any of the new SF activities could be compound-nucleus neutron-evaporation products.

III.B. Table 1: The New Spontaneous Fission (SF) Activities And Cross-Section Limits for the 80-ms SF Activity

Reaction	Half-Life	Cross Section Exp.	Cross Section Calc.	Possible Assignment
80-MeV ^{15}N + $^{249}Bk \rightarrow ^{264}Rf^*$	19.8±1.2 ms	14±2 nb	10 nb	^{260}Rf??
92-MeV ^{16}O + $^{248}Cm \rightarrow ^{264}Rf^*$	21.0±1.1 ms	6±1 nb	4.0 nb	^{260}Rf??
96-MeV ^{18}O + $^{249}Cf \rightarrow ^{267}106^*$	19.3±1.4 ms	9±1 nb	–	
80-MeV ^{15}N + $^{249}Bk \rightarrow ^{264}Rf^*$	80 ms	$\leq$0.3±0.4 nb		
	60-100 ms	$\leq$0.3±0.5 nb		
92-MeV ^{16}O + $^{248}Cm \rightarrow ^{264}Rf^*$	80 ms	$\leq$0.4±0.2 nb		
	60-100 ms	$\leq$0.5±0.2 nb		
96-MeV ^{18}O + $^{249}Cf \rightarrow ^{267}106^*$	80 ms	$\leq$0.0±0.5 nb		
	60-100 ms	$\leq$0.0±1.0 nb		
89-MeV ^{18}O + $^{248}Cm \rightarrow ^{266}Rf^*$	52±5 ms	5±1 nb	9 nb(92.5 MeV)	^{262}Rf?
113-MeV ^{22}Ne + $^{244}Pu \rightarrow ^{266}Rf^*$	50±16 ms	1±1 nb	1.5 nb	^{262}Rf??
	14 ms??	1±1 nb??		^{242f}Am(13.7 ms)??

? indicates assignment probable.

?? indicates that not enough evidence is available or that an inconsistency exists in making a definite assignment.

* denotes an excited compound nucleus

Reaction	Half-Life	Cross Section Exp.	Calc.	Possible Assignment
95-MeV ^{16}O + $^{246}Cm \rightarrow ^{262}Rf^*$	13±3 ms	10^{+10}_{-5} nb	3 nb	^{258}Rf(13 ms)?
109-MeV ^{18}O + $^{248}Cm \rightarrow ^{266}Rf^*$	22.4±1.3 ms	10±2 nb		
	17.1±2.2 ms	9±1.4 nb		
100-MeV ^{15}N + $^{249}Bk \rightarrow ^{264}Rf^*$	15^{+6}_{-4} ms**	9±3 nb		
97-MeV ^{15}N + $^{248}Cm \rightarrow ^{263}Lr^*$	15 ms	$\leq$2 nb		
97-MeV ^{15}N + $^{248}Cm \rightarrow ^{263}Lr^*$	20 ms	$\leq$1 nb		
70-MeV ^{13}C + ^{249}Bk(80%) $\rightarrow ^{262}Lr^*$	4.5±0.5 s	7±1 nb	1 μb	$^{258}Lr(4.35\ s) \xrightarrow{EC} ^{258}No(1.2\ ms) \xrightarrow{SF}$??
^{249}Cf(20%) $\rightarrow ^{262}Rf^*$				
89-to 119-MeV ^{18}O+$^{248}Cm \rightarrow ^{266}Rf^*$	1.6±0.1 s	16±2 nb (95 MeV)		
93-MeV ^{18}O + $^{245}Cm \rightarrow ^{263}Rf^*$	3.4±1.7 s	0.6±0.2 nb =8±3% of $\sigma^{calc.}$		8% SF branching in ^{259}Rf??
75-MeV ^{12}C + $^{249}Cf \rightarrow ^{261}Rf^*$	3.8±0.8 s	2±0.4 nb		14% SF branching in ^{257}Rf??
75-MeV ^{12}C + $^{249}Cf \rightarrow ^{261}Rf^*$	47±13 s??	9±1.4 nb??		
72-MeV ^{13}C + $^{245}Cm \rightarrow ^{258}No^*$	50-60 s	$\leq$0.5 nb, or $\leq$0.05% of $\sigma^{calc.}$ for ^{254}No		

** 90-per-cent confidence limits

III.C. Table 2: Cross Bombardments for the ~20-ms, ~50-ms, and 1.6-s SF Activities

Reaction	Cross Sections		
	~20 ms	~50 ms	1.6-s
96-MeV ^{18}O + $^{249}Cf \rightarrow {}^{267}106$*	9±1 nb	≤0.0±1.5 nb	≤12 nb
93-MeV ^{18}O + $^{249}Bk \rightarrow {}^{267}Ha$*	≤0.7 nb	≤0.6 nb	≤2 nb
^{18}O + $^{248}Cm \rightarrow {}^{266}Rf$*	10±2 nb(109 MeV)	5±1 nb(89 MeV)	16 nb(95 MeV)
113-MeV ^{22}Ne + $^{244}Pu \rightarrow {}^{266}Rf$*	≤2 nb	~1 nb?	≤0.6 nb
80-MeV ^{15}N + $^{249}Bk \rightarrow {}^{264}Rf$*	14±2 nb	≤0.3±0.7 nb	≤0.6 nb
92-MeV ^{16}O + $^{248}Cm \rightarrow {}^{264}Rf$*	6±1 nb	≤0.6±0.3 nb	≤0.7 nb
93-MeV ^{18}O + $^{245}Cm \rightarrow {}^{263}Rf$*	-	-	≤11 nb
95-MeV ^{16}O + $^{246}Cm \rightarrow {}^{262}Rf$*	≤7 nb	≤2 nb	≤27 nb
70-MeV ^{13}C + $^{249}Cf \rightarrow {}^{262}Rf$*	-	-	≤5 nb
83-MeV ^{15}N + $^{248}Cm \rightarrow {}^{263}Lr$*	≤4 nb	≤3 nb	≤55 nb
97-MeV ^{15}N + $^{248}Cm \rightarrow {}^{263}Lr$*	≤1 nb	≤1 nb	
97-MeV ^{15}N + $^{248}Cm \rightarrow {}^{263}Lr$*	≤2 nb (15 ms)		
70-MeV ^{13}C + $^{249}Bk \rightarrow {}^{262}Lr$*	-	-	≤1 nb
95-MeV ^{18}O + $^{244}Pu \rightarrow {}^{262}No$*	≤0.3 nb	≤0.3 nb	≤4 nb
81-MeV ^{13}C + $^{248}Cm \rightarrow {}^{261}No$*	≤6 nb	≤6 nb	
95-MeV ^{16}O + $^{244}Pu \rightarrow {}^{260}No$*	≤4 nb	≤0.6 nb	≤2 nb

III.D. Table 3: Comparison of Cross Sections for Analogous Cf and Fm Products in the Reactions $^{18}O + ^{245}Cm$ and $^{18}O + ^{248}Cm$ to Determine If ^{259}Fm Could Be the 1.6-s SF Activity

Pickup Particle	93-MeV $^{18}O + ^{245}Cm$		97-MeV $^{18}O + ^{248}Cm$ (LEE82)	
	nuclide	σ(μb)	σ(μb)	nuclide
+2p -2n	^{245}Cf	-	45±15	^{248}Cf
+2p - n	^{246}Cf	50		^{249}Cf
2p	^{247}Cf	-	850	^{250}Cf
^{3}He	^{248}Cf	3000		^{251}Cf
α	^{249}Cf	-	280	^{252}Cf
		σ(nb)	σ(nb)	
^{6}Be	^{251}Fm	-	2800	^{254}Fm
^{7}Be	^{252}Fm	1800	700	^{255}Fm
^{8}Be	^{253}Fm	800	300	^{256}Fm
^{9}Be	^{254}Fm	-	-	^{257}Fm
^{10}Be	^{255}Fm	-	-	^{258}Fm
^{11}Be	^{256}Fm	≤ 2	16(95 MeV)?	^{259}Fm

III.E. Table 4: Chi-Square Values Under Two Assumptions for Reactions Capable of Producing ^{260}Rf: (1) A Single Short-Lived Component and Background and (2) The Dubna Interpretation---^{242f}Am(13.7 ms) and 80-ms Components With Background

The decay rate A_0 for the short-lived component and background rates at t=0 are given in SF decays per millisecond. The bin size was approximately 10-11 ms for each of the least-square fits using the computer code FRANTIC (ROG62). Weights for points in the calculations were determined from maximum-likelihood code fits to the same data assuming no 80-ms component was present. For each reaction the single-component half-lives determined by the maximum-likelihood code listed in Table 1 are more accurate half-lives than those determined by the least-squares method below. This is because in the binning procedure necessary for the least-squares method, valuable individual event-time information is lost which the maximum-likelihood code can utilize (EGG81).

80-MeV ^{15}N + ^{249}Bk. For the data in Figure 13:

	Short-Lived Component and Background	^{242f}Am(13.7 ms) + 80 ms + Background
	$T_{1/2}$=19.8±1.2 ms	
	$A_0(T_{1/2})$=21.9±2.9	A_0(13.7 ms)=35.5±2.4
		A_0(80 ms)= 0.35±0.11
Background	0.029±0.005	0.024±0.005
Chi-square/freedom	1.02	1.16
Probability	43%	9%

92-MeV ^{16}O + ^{248}Cm. For the data in Figure 14:

	Short-Lived Component and Background	^{242f}Am(13.7 ms) + 80 ms + Background
	$T_{1/2}$=20.7±0.9 ms	
	$A_0(T_{1/2})$=10.9±0.7	A_0(13.7 ms)=15.8±0.8
		A_0(80 ms)=0.390±0.061
Background	0.015±0.004	0.0056±0.0041
Chi-square/freedom	1.10	1.24
Probability	18%	2%

96-MeV ^{18}O + ^{249}Cf. For the data in Figure 15:

	Short-Lived Component and Background	^{242f}Am(13.7 ms) + 80 ms + Background
	$T_{1/2}$=19.9±1.5 ms	
	$A_0(T_{1/2})$=13.3±2.0	A_0(13.7 ms)=25.0±2.0
		A_0(80 ms)=0.275±0.120
Background	0.071±0.010	0.063±0.014
Chi-square/freedom	1.31	1.44
Probability	2%	0.1%

IV. Discussion of Possible Assignments for the New SF Activities

IV.A. Introduction

No certain identifications have been made for any of the new SF activities listed in Table 1. Assigning heavy-element SF activities is extremely difficult for two reasons. (1) The currently-measurable properties of the SF decay process, such as the total kinetic energy of fission, fragment mass and charge distributions, neutron multiplicity, etc., do not change rapidly among neighboring nuclei. In alpha decay, however, a particular nuclide has a specific alpha-decay energy and half-life as well as a genetic relationship to its daughter and granddaughter nuclei, making it possible to prove isotopic assignments. (2) The cross sections for producing these SF activities are in the nanobarn region. From a single tape experiment only two properties of each SF activity can be measured—the half-life and the production cross section, as shown in Table 1. Using several combinations of targets and projectiles possible isotopic assignments can be deduced by determining which isotopes would have estimated production cross sections for each bombardment close to the measured value or limit for the SF activity in question. The JORPLE code discussed in the appendix section VIII.A. can be used to calculate the cross section for compound-nucleus neutron-evaporation reactions. But there is no reliable code for predicting non-compound-nucleus reaction cross sections in the heavy-element region. The available cross-section data for non-compound-nucleus reactions are also severely

limited. In other cases not enough cross bombardments have been performed to narrow the list of candidates down to a single isotope. Because of these limitations often several isotopes may be consistent with the available cross bombardment data. In still other cases, such as for the 1.5- to 1.6-s SF activities and the SF activities with half-lives between 14 and 24 ms, it is difficult to fit all the available data by a single activity; so "twin" SF activities with similar half-lives have been suggested. In section IV.D.2.a. (Future Directions for Experimental Investigations) several methods are suggested in order to experimentally obtain the additional information necessary to positively identify these new SF activities.

The following discussion of the new SF activities listed in Table 1 is divided into two groups: a) activities which are probably not due to element-104 nuclei, most of which have completely unknown assignments; and b) activities which either may be due to element-104 nuclei or have half-lives which are close to other possible element-104 SF activities. For the SF activities with completely unknown assignments the discussion will include the totality of all that is known about them. Some isotopes may be eliminated as possible assignments. For the rest of the SF activities the discussion will include possible assignments and the reasons for and against making those assignments.

IV.B. Discussion of The New SF Activities With Completely Unknown Assignments

IV.B.1. A Possible 47-s SF Activity

In the bombardment 75-MeV ^{12}C +^{249}Cf alone there were indications of a 47±13-s SF activity with a cross section of ~9 nb as shown in the decay curve of Figure 7. There is some difficulty in distinguishing whether the half-life is 47 s or even longer than 65 s, due to the fact that only a little more than one half-life was observed in 65 seconds of observation time. It was initially thought that this SF activity might be due to a 0.4-per-cent SF branching in ^{254}No(55 s). This hypothesis would also be consistent with the 14 SF events that decayed with a half-life of ~70 s observed by Ghiorso et al. (GHI76) in the reactions 197- to 227-MeV ^{48}Ca +^{208}Pb. However, in the reaction 72-MeV ^{13}C +^{245}Cm an upper limit of 0.05 per cent on the fission branch of ^{254}No was established, assuming a calculated production cross section of ~1 μb for ^{254}No. This result is in agreement with the upper limit of 0.06 per cent established in separate experiments comparing the ratio of the cross sections for SF and ^{254}No alpha decay by Donets et al. and Flerov et al. (DON66, FLE67) for the reaction $^{238}U(^{22}Ne,6n)^{254}No$. Thus, largely because of insufficient cross bombardment data, the origin of this possible 47-s SF activity is unknown.

IV.B.2. 1.6-s SF Activity

In the reaction 89-MeV ^{18}O + ^{248}Cm the decay curve of Figure 8 shows clear evidence for SF activities with half-lives of 55±5 ms and 1.3±0.1 s. The 1.3-s component was produced with a rather large 16-nb peak cross section and with an excitation function which was broad when compared to calculations for any compound-nucleus neutron-evaporation product. The half-life of 1.6±0.1 s obtained from the data shown in Figure 9 using the tape system agrees with the half-life of 1.5±0.3 s measured by Hulet et al. (HUL80) for ^{259}Fm produced in the reaction $^{257}Fm(t,p)^{259}Fm$. In our reaction ^{18}O + ^{248}Cm, ^{259}Fm would be a non-compound-nucleus product, in agreement with the broad excitation function shown in Figure 10. The symmetric mass distribution and total kinetic energy for fission of 234±2 MeV measured for our 1.6-s SF activity by Hoffman et al. (HOF81) are also in agreement with the same properties measured for ^{259}Fm in the reaction $^{257}Fm(t,p)^{259}Fm$. However, as will now be shown there are potential difficulties with this assignment.

If our 1.6-s SF activity produced in the reaction ^{18}O + ^{248}Cm is ^{259}Fm, it would be produced in an exotic ^{11}Be-transfer reaction. "^{11}Be transfer" is used here as a formalism to discribe the net particle which must be transferred to the target to reach ^{259}Fm, but does not imply a particular reaction mechanism. Separate experiments were performed subsequent to the discovery of the 1.6-s SF activity to determine whether or not such a ^{11}Be-transfer reaction could have a production cross section as large as 16 nb. With ^{18}O ions

bombarding targets of lower atomic number (Z) the fission competition for ^{11}Be-transfer reactions is expected to be less than with a ^{248}Cm target. But surprisingly low cross sections of ~10 nb in the reaction 110-MeV ^{18}O +^{208}Pb (GHI81a) and $\leq$16±10 nb in the reaction $\leq$124-MeV ^{18}O +^{232}Th were determined for ^{11}Be-transfer products. For the reaction ^{18}O +^{232}Th a useful target thickness for ^{18}O ions degraded from 124 MeV down to the barrier was assumed in determining the cross-section upper limit (McFA80). The possibility suggested by Nitschke (NIT80) and independently by Wilhelmy and Hoffman (WIL80) that the ^{11}Be-transfer products might be produced with excitation energies below the fission barrier has been considered (HOF81). In these cases for ^{11}Be transfers fission competition might not be worse using high Z targets compared to lower Z targets. If so, cross sections for analogous ^{11}Be-transfer reactions might be of similar magnitude using targets in the lead to curium region, in agreement with the above cross-section data.

In order to study the hypothetical ^{11}Be-transfer reaction a ^{245}Cm target was bombarded with ^{18}O ions at 93 MeV and 99 MeV in search of the ^{11}Be-transfer product ^{256}Fm. If the ^{259}Fm assignment to the 1.6-s SF activity produced with a 16-nb cross section in the reaction 95-MeV ^{18}O +^{248}Cm is correct, we would expect that the cross section for ^{256}Fm in the quite similar reaction ^{18}O +^{245}Cm might be of the same order of magnitude. The bombarding energy 93 MeV was chosen to give the same excitation energy as in the system 95-MeV ^{18}O +^{248}Cm. Recoils were caught in a series of ten 100-μg/cm^2 aluminum catcher foils. After the

bombardment each catcher foil was placed over a separate solid-state detector to record alpha particles and SF events from the recoil nuclei. Only upper limits of 2 nb at 93 MeV as shown in Table 3 and 2 nb at 99 MeV could be established for the ^{11}Be-transfer product ^{256}Fm in the reaction ^{18}O +^{245}Cm. Table 3 shows, however, that copious quantities of other alpha-particle-emitting nuclides were produced with cross sections that are higher than the analogous products in the reaction ^{18}O +^{248}Cm. Lee et al. (LEE82) determined the cross sections for the californium and fermium transfer products by measuring the alpha-decay rates and energies from chemically-separated fractions. Since the cross sections for the ^{18}O +^{245}Cm reaction were determined directly from catcher foils without chemical separation, part of the difference between analogous reaction cross sections might also be due to a systematic difference in yields or efficiencies. Nevertheless, there appears to be a correspondence between analogous cross sections. Since the data in Table 3 are quite limited, it is difficult to say whether or not this correspondence is universal to all analogous transfer products. But if the correspondence is universal, a measured cross-section upper limit of 2 nb for the ^{11}Be-transfer product ^{256}Fm in the reaction ^{18}O +^{245}Cm and a cross section of 16 nb for what might be the ^{11}Be-transfer product ^{259}Fm in the reaction ^{18}O +^{248}Cm would be at variance with this correspondence.

In that case ^{259}Fm might not be the 1.6-s SF activity produced in the reaction 95-MeV ^{18}O +^{248}Cm; and one of the two following explanations would be required. (1) There exists a "twin" nucleus to

^{259}Fm with nearly identical properties of half-life, total kinetic energy of fission, and fission-mass distribution: or (2) this 1.6-s SF activity is the same SF activity produced in the original reaction 16-MeV t + ^{257}Fm (HUL80), but the ^{259}Fm assignment is incorrect. Three possibile alternative assignments have been considered--(1) a 1.6-s isomer with an isomeric transition suggested by Ghiorso (GHI81b) or direct fission branch in ^{258}Fm(0.38 ms), (2) a 1.6-s isomer of ^{258}Md, which decays by electron capture to ^{258}Fm, and (3) ^{262}Lr electron-capture decay to ^{262}No or direct SF branching in ^{262}Lr as suggested by Ghiorso (GHI81b). But a cross-section upper limit of 1 barn for 1.6-s SF events in thermal-neutron irradiations of ^{257}Fm by Hulet et al. (HUL71) tends to eliminate the possibility of such a low-spin isomer in ^{258}Fm. A high-spin isomer would not be ruled out by these experiments, however. Also 1.6 s would be an extremely short half-life for electron-capture decay in an actinide isotope. Whether SF events from ^{262}Lr could be produced with a cross section as large as 16 nb in the reaction ^{248}Cm(^{18}O,p3n)^{262}Lr and have an excitation function similar to the 1.6-s SF activity in the reaction ^{18}O +^{248}Cm is unknown; but in order to answer this question the excitation function for the 1.6-s SF activity could be compared with the one for the reaction ^{242}Pu(^{18}O,p3n)^{256}Md (GHI91b). Clearly, further experiments are necessary in order to determine the atomic and mass numbers for the 1.6-s SF activity.

In the next section evidence is presented for new SF activities with half-lives greater than 1.6 s.

IV.B.3. New SF Activities in the Reaction $^{18}O + ^{249}Bk/^{249}Cf$

In the reaction 98-MeV ^{18}O +(82-88% ^{249}Bk/12-18% ^{249}Cf) two or more SF activities with half-lives between 3 s and 60 s were observed. A fit with two components and background yielded half-lives of 5.5±1.5 s and 30±10 s. In the reaction 93-MeV ^{18}O +(94% ^{249}Bk/6% ^{249}Cf) there were also indications of a 6.7±3.0-s component with a production cross section ~1.5 nb, assuming production from the ^{249}Bk portion of the target. The 30-s component might be the element-105 isotope ^{262}Ha (GHI71a, BEM77a, DRU78), although the measured cross section of 5 nb for SF events (6-nb total cross section, assuming a 78-per-cent branch to SF (BEM77a)) considerably exceeds the calculated value of ~1 nb for the reaction 98-MeV $^{18}O + ^{249}Bk \rightarrow ^{262}Ha$ + 5n. A speculation is that the 5.5-s SF activity with a production cross section of ~3 nb (assuming production from ^{249}Bk) might be due, for example, to an electron-capture branch from a new isomer of ^{260}Lr, which could arise from the coupling of the odd proton and odd neutron to form two closely-spaced energy levels with a large difference in spin (HOF79a); if so, based on a measured 6±2-nb production cross section for the ground state of ^{260}Lr (GHI71b) with 93-MeV ^{18}O ions, the product of the electron-capture branch for the isomer and the isomer-to-ground-state ratio might be ~1/4.

IV.C. SF Activities Possibly From Element-104 Nuclei or With Half-Lives Close to Possible Element-104 Nuclei

IV.C.1. 3.8-s SF Activity: Possible SF Branching in ^{257}Rf(4.8 s); 4.5-s SF Activity: Possible Electron-Capture Branch in ^{258}Lr(4.35 s) to ^{258}No(1.2 ms SF)

The bombardment 75-MeV ^{12}C +^{249}Cf was performed in order to search for SF branching in ^{257}Rf, a nuclide which is known to decay primarily by alpha emission (GHI69) with a half-life of 4.8±0.5 s (GHI71). A two-component fit to the data shown in Figure 7 yielded half-lives and cross sections of 3.8±0.8 s (~2 nb) and 47±13 s (~9 nb, see section IV.B.1.). The 3.8±0.8-s half-life is statistically consistent with the 4.8±0.5-s half-life measured for alpha decay of ^{257}Rf. This suggests that the SF and alpha radioactivities may both originate from ^{257}Rf. However, in the bombardment 70-MeV ^{13}C + (80% ^{249}Bk/ 20% ^{249}Cf) a 4.5±0.5-s half-life and a cross section of ~7 nb were measured, assuming production from the ^{249}Bk portion of the target (decay curve in Figure 11). Hoffman et al. (HOF79) found preliminary indications of this activity in experiments measuring fission-mass and total-kinetic-energy distributions in the same reaction. Also in the reaction 98-MeV ^{18}O + (82-88% ^{249}Bk/ 12-18% ^{249}Cf) a 5.5±1.5-s SF activity with a production cross section of ~3 nb (assuming production from ^{249}Bk) might also be produced (see section IV.B.3.). Thus, there are between one and three SF activities with half-lives of ~5 s!

To determine possible assignments for these SF activities it is helpful to compare the cross section and half-life measured for SF with both the same properties measured by alpha decay and the calculated total production cross sections for some candidates. This rather detailed discussion is included in the appendix section VIII.C. (Detailed Arguments for Tentatively Assigning Three 5-s SF Activities). The conclusions are that:

(1) a 14-per-cent SF branch in ^{257}Rf is a possible explanation for the 3.8-s SF activity in the reaction 75-MeV ^{12}C + ^{249}Cf;

(2) a ~1-per-cent electron-capture branch in ^{258}Lr(4.4 s) to the spontaneously-fissioning ^{258}No(1.2 ms) could explain the 4.5-s SF activity in the reaction 70-MeV ^{13}C + ^{249}Bk/^{249}Cf; and

(3) the 5.5-s SF activity produced in the reaction 98-MeV ^{18}O + ^{249}Bk/^{249}Cf is probably not identical to either of the other 5-s SF activities. Its assignment is unknown. But a ^{260}Lr isomer with an electron-capture branch was speculated in the previous section.

The assignment to SF branching in ^{257}Rf could be checked by producing ^{261}106 in the reaction 96-MeV ^{16}O +^{249}Cf$\rightarrow$^{261}106 + 4n and measuring the ratio of SF events to alpha-particle decays in the separated alpha-decay daughter ^{257}Rf nuclei. Keller and Münzel (KEL69) have predicted a half-life of 0.34 ms for ^{261}106 with mostly alpha decay; but their predictions for similar even-odd or odd-even nuclei such as ^{261}Rf and ^{261}Ha are one and two orders of magnitude shorter than the respective experimental half-lives. The low 0.1-nb calculated production cross section and predicted short half-life make this

experiment a difficult one, however.

IV.C.2. ~13-ms SF Activity: Possibly ^{258}Rf

This SF activity was observed using a rotating-drum assembly. Although the measured cross section of 10^{+10}_{-5}nb for production of the 13±3-ms SF activity in the reaction 95-MeV ^{16}O +^{246}Cm (decay curve in Figure 12) is somewhat higher than the calculated 3-nb cross section to produce ^{258}Rf, the half-life agrees with the 13±2-ms half-life determined for ^{258}Rf by Nurmia et al. from the reactions $^{12,13}C$ +^{249}Cf (NUR74, 71, 70; GHI69, 70a). In this early rotating-drum experiment, our beam flux measurement was uncertain by a factor of 2. Consequently, the discrepancy between calculated and experimental production cross sections cannot be regarded as significant. However, the possibility that there may be a contribution from one of the SF activities with half-lives between 14 and 24 ms produced in the reactions 109- to 119-MeV ^{18}O +^{248}Cm, 88- to 100-MeV ^{15}N +^{249}Bk, or 96-MeV ^{18}O +^{249}Cf cannot be excluded.

IV.C.3. ~3-s SF Activity: Possible SF Branching in ^{259}Rf

^{259}Rf is known to be a 3-s alpha-particle emitter. We searched for the 7-per-cent SF branching in ^{259}Rf reported by Druin et al. (DRU73) and suggested by Bemis et al. (BEM81) on the basis of 9±5 SF events. In the reaction 93-MeV ^{18}O +^{245}Cm 20 SF tracks were

detected and a half-life of 3.4±1.7 s was measured. If these SF events are due to ^{259}Rf, the cross section of 0.6±0.2 nb corresponds to a SF branching ratio of 8±3 per cent of the calculated cross section to produce ^{259}Rf, in agreement with the 7-per-cent SF branching reported by Druin. This assignment is not yet proven, however. In particular, ^{256}No, which would be produced in the reaction ^{245}Cm(^{18}O,α3n)^{256}No and has a similar half-life of 3.2 s with a SF branch of 0.3 per cent, might have contributed to the SF events observed. A possible, but difficult way in which a proof of the ^{259}Rf assignment could be made would be to produce ^{263}106 and to measure the ratio of SF events to alpha-particle decays of its alpha-decay daughter ^{259}Rf.

IV.C.4. 80-ms SF Activity Claimed by the Dubna Group to Be ^{260}Rf

For the reaction 82-MeV ^{15}N +^{249}Bk a group in Dubna has observed an 80±20-ms SF activity with a production cross section of 8±2 nb and claimed that it is ^{260}Rf (DRU77, FLE64). New searches have been performed for this SF activity in three different reactions listed in Table 1. The sensitivity has been improved using the tape system due to the reduction of SF background from ^{256}Md and/or ^{256}Fm compared to the rotating-drum experiments of reference NIT81. A glance at the decay curve in Figure 13 obtained using the tape system, however, reveals no 80-ms component. Cross-section upper limits covering the half-life range 60-100 ms, i.e., one standard deviation above and below the Dubna half-life measurement of 80±20 ms, are

quoted in Table 1. The measured cross-section upper limit of 0.3 nb is 1/30 of the calculated cross section to produce ^{260}Rf and 1/24 of the Dubna cross section of 8±2 nb with 82-MeV ^{15}N ions (DRU77). On the other hand, the production cross section for ^{256}Md(77 min), measured from recoil catcher foils (NIT81), agrees with the Dubna value for the same reaction. The JORPLE code has been shown to predict correctly the cross section for the quite similar reaction ^{249}Cf(^{15}N,4n)^{260}Ha within a factor of two (GHI70b). The cross-section upper limit for the reaction 92-MeV ^{16}O + ^{248}Cm from the data of Figure 14 is one-tenth of the cross section calculated for ^{260}Rf.

In summary, a SF activity with a half-life between 60 and 100 ms has not been observed in any experiment in which we expected to produce ^{260}Rf. The cross-section upper limits for the 80-ms SF activity are far below those calculated to produce ^{260}Rf, in agreement with references NIT81 and GHI70a. However, we have found a ~20-ms SF activity, which could be due to ^{260}Rf. The Dubna group has interpreted our data as a mixture of two SF activities---13.7-ms ^{242f}Am and the 80-ms SF activity. These two interpretations will be discussed in the next section. Then in the following sections the reasons for and against making the assignment of the ~20-ms SF activity to ^{260}Rf will be discussed.

IV.C.5. SF Activities With Half-Lives Between 14 and 24 ms

IV.C.5.a. The Dubna Interpretation: The ~20-ms SF Activity is a Mixture of ^{242f}Am(13.7 ms) and the 80-ms SF Activity

In this section the Dubna interpretation (DEM80) of our data presented at the conference in reference SOM80 will be considered: namely, that the ~20-ms SF activity is a mixture of the 13.7-ms isomer ^{242f}Am and the 80-ms SF activity which the Dubna group claims is due to ^{260}Rf. The decay curves in Figures 13-15 show none of the curvature expected for a mixture of two components with half-lives of 13.7 ms and 80 ms, but rather each has the appearance of a single component and background. As Table 4 shows, the chi-square per degree of freedom is larger, indicating a poorer fit to the data, under the Dubna assumptions of 13.7-ms and 80-ms components with background than under the assumptions of a single component and background for each of the reactions 92-MeV ^{16}O +^{248}Cm, 80-MeV ^{15}N +^{249}Bk, and 96-MeV ^{18}O +^{249}Cf. A similar conclusion was reached for the rotating-drum experimental data in reference NIT81. Fits with the Dubna interpretation have probabilities of 9 and 2 per cent, respectively, for the reactions 80-MeV ^{15}N +^{249}Bk and 92-MeV ^{16}O +^{248}Cm. A casual comparison of the fit in Figure 15 with Figures 13 and 14 shows a poor fit with a chi-square value having a 2-per-cent probability, assuming that a ~19-ms component is present. This indicates that there may be unknown systematic effects in these data for the reaction 96-MeV ^{18}O +^{249}Cf.

Also in the reaction 93-MeV ^{16}O +^{248}Cm a cross-section upper limit of 200 nb was established by Ghiorso and Lee for the production of the ^{242}Am(16 hr) ground state (GHI80a). Polikanov et al. and Gangrskiĭ et al. have shown that the ratio of the ^{242}Am isomer-to-ground-state production cross sections of ~$4x10^{-4}$ is nearly independent of the projectile within a factor of three for d, p, and 14 MeV-n projectiles (POL68), and for the reaction ^{11}B +^{238}U (GAN67a). Exceptions are *single-nucleon transfer reactions (GAN67b) with lower ratios and the* very heavy-ion reaction ^{238}U + ^{238}U with a ratio of $2x10^{-5}$ (GÄG80). The ratio also seems nearly constant with bombarding energy in the reaction ^{11}B + ^{238}U (GAN67a) for energies slightly above the Coulomb barrier. These facts can be understood if ^{242f}Am has a low spin so that it is populated readily in both light- and heavy-ion reactions with varying angular momentum (FLE68, POL68). Therefore, it would be very surprising if the production cross section for ^{242f}Am could be much larger than 200 nb x $4x10^{-4}$≅ 0.1 nb, assuming the ratio ~$4x10^{-4}$ is also correct for the reaction 92-MeV ^{16}O +^{248}Cm. As shown in Table 1, a cross-section upper limit of 0.4±0.2 nb for an 80-ms SF activity and an estimated upper limit of ~0.1 nb for 13.7-ms ^{242f}Am make the Dubna interpretation highly improbable that the ~20-ms SF activity with a production cross section of 6 nb could be composed of a mixture of 13.7-ms and 80-ms SF activities. In the rest of this thesis the ~20-ms SF activity is treated as a single SF activity in each nuclear reaction.

IV.C.5.b. Evidence Supporting the Possible Assignment of ^{260}Rf to a ~20-ms SF Activity

A ~20-ms SF activity has been found which could be due to ^{260}Rf. It is produced in the reactions 80-MeV $^{15}N + ^{249}Bk$ and 92-MeV $^{16}O + ^{248}Cm$, both with compound system $^{264}Rf^*$, with cross sections in Table 1 close to those calculated to produce ^{260}Rf. The decay curves from these bombardments are shown in Figures 13 and 14. We hope to test whether or not the ~20-ms SF activity is also produced in another reaction $^{18}O + ^{246}Cm$ with the same compound system $^{264}Rf^*$ in future experiments.

^{260}Rf would be produced in the reaction $^{249}Bk(^{15}N,4n)^{260}Rf$. The excitation functions for the ~20-ms SF activity obtained from the tape apparatus in Figure 5 and from the rotating-drum system of Figure 4 (NIT81) agree well with the calculated excitation function for production of ^{260}Rf for ^{15}N ion energies between 82 and 88 MeV; but for lower energies the measured cross sections are much larger than the calculated values. The experimental excitation function appears to be broader than the calculated one. While it is true that taking into account the unknown extent of beam energy straggling would narrow this excitation function, it is doubtful whether the corrected excitation function would be as narrow as the calculated one. However, other (^{15}N,4n) experimental excitation functions in Figures 6a-c (GHI70b, ESK71, DON66) are also broader than calculated by the JORPLE code. But as discussed in the appendix section VIII.A. (The JORPLE Code for Calculating (HI,xn) Cross Sections and Comparison With

Experimental Cross Sections) and shown in Figure 6a-c, the JORPLE code does not predict the shape of any (^{15}N,4n) reaction excitation function very well. Thus, ^{260}Rf is still a possible assignment for this ~20-ms SF activity.

The ~20-ms SF activity has also been produced in a reaction with 96-MeV ^{18}O ions bombarding a 640-μg/cm^2 ^{249}CfF$_3$ target. A cross section of 9±1 nb was determined from the data of Figure 15 assuming that the recoil range is at least as long as the target thickness plus the ~25-μg/cm^2 aluminum covering over the target. Should the recoil range for the unknown SF activity be less than this amount as in some non-compound-nucleus reactions (HAH74), the cross section would be correspondingly higher. In this bombardment ^{260}Rf could be produced in the reaction ^{249}Cf(^{18}O,α3n)^{260}Rf. The 9-nb cross section for possible production of ^{260}Rf with a ^{249}Cf target is consistent with some other known cross section data.

(1) It is lower, as expected, than the cross section of 20 nb for the similar (^{18}O,α3n) reaction using a ^{248}Cm target with 93-MeV ^{18}O ions (SIL73). This is explainable by increased fission competition for a compound nucleus with 106 protons compared to 104 protons.

(2) It is higher than the ^{249}Cf(^{18}O(~95 MeV),α4n)^{259}Rf reaction cross section of ~0.5 nb derived from the data of reference GHI74a. The maximum (HI,α3n) reaction cross section has also been found to exceed the maximum (HI,α4n) reaction cross section for the reactions ^{16}O +^{248}Cm and ^{12}C +^{249}Cf (GHI69).

The cross section of 9 nb is most probably too high for any

isotope of element 105 or 106 based on the small 0.3-nb cross section measured by Ghiorso et al. for $^{263}106$ (GHI74a). However, there may be a serious inconsistency in a 9-nb cross section for the reaction $^{249}Cf(^{18}O,\alpha 3n)^{260}Rf$ compared to other ($^{18}O,\alpha 3n$) reaction cross-section data. This will be discussed in the following section.

Absence of the ~20-ms SF activity in the cross bombardments with negative results listed in Table 2 is also consistent with the possible assignment of ^{260}Rf.

IV.C.5.c. Possible Inconsistencies in the Assignment of ^{260}Rf to a ~20-ms SF Activity

The assignment of ^{260}Rf as the isotope responsible for the ~20-ms SF activity appears to be inconsistent with the set of data obtained from the reaction 109-MeV $^{18}O + ^{248}Cm$. For this reaction the measured cross section of ~9-10 nb is ~50 times larger than calculated for the (^{18}O,6n) reaction to produce ^{260}Rf. Furthermore, the excitation function is considerably broader than calculated for ^{260}Rf.

Two separate measurements of the half-life of ~22.4±1.3 ms (decay curve in Figure 16) and 17.1±2.2 ms have been made in preliminary measurements at this ^{18}O-ion energy. Since the probability is only 4 per cent that these half-life measurements are two normally-distributed measurements of the same true half-life, there is some evidence for an unknown systematic error, as discussed in the

section II. Experimental Procedure. Future half-life measurements with good statistics will be necessary to determine the ~20-ms half-life more precisely. But at this stage the half-life appears to be quite close to the ~20-ms half-life measured in the reactions 80-MeV ^{15}N +^{249}Bk, 92-MeV ^{16}O +^{248}Cm, and 96-MeV ^{18}O +^{249}Cf. If the SF activity produced in the reactions 80-MeV ^{15}N +^{249}Bk and 92-MeV ^{16}O +^{248}Cm and the ~20-ms SF activity produced in the reaction 109-MeV ^{18}O +^{248}Cm are identical, the single ~20-ms SF activity could not be ^{260}Rf unless the (^{18}O,6n) reaction cross section is enhanced by some, as yet unknown, mechanism. This unknown mechanism would also have to explain why the excitation function of Figure 10 is considerably broader than calculated. No evidence for an enhancement has been observed for quite similar (^{18}O,6n) reactions with up to 100 protons in the compound system (DON66a). Also the very similar $^{248}Cm(^{18}O,5n)^{261}Rf$ reaction cross section shows no enhancement (GHI70c).

Another possible, but less serious inconsistency concerns the ~19-ms SF activity produced in the reaction 96-MeV ^{18}O +^{249}Cf with a cross section of 9±1 nb. If this SF activity is truly ^{260}Rf, it would be produced in the reaction $^{249}Cf(^{18}O,\alpha 3n)^{260}Rf$. The cross section for the quite similar reaction $^{249}Bk(^{18}O,\alpha 3n)^{260}Lr$ is 6±2 nb with 93-MeV ^{18}O ions, based on unpublished data of Ghiorso et al. (GHI71b). The comparison is made at ^{18}O-ion energies near the calculated peaks of the excitation functions for evaporation of four neutrons. But due to increased fission competition one would expect the (^{18}O,α3n) reaction cross section to be smaller using a ^{249}Cf target with higher atomic number compared to using a ^{249}Bk target. This is the trend which

already seems to be established from ^{248}Cm to ^{249}Bk targets, i.e., the maximum $^{248}Cm(^{18}O,\alpha 3n)^{259}No$ reaction cross section near the peak of the $(^{18}O,4n)$ excitation function is 20 nb (SIL73) but only 6±2 nb for the reaction $^{249}Bk(^{18}O,\alpha 3n)$, both with 93-MeV ^{18}O ions. This trend could also be checked by measuring the cross section for the reaction $^{244}Pu(^{18}O,\alpha 3n)^{255}Fm$ (GHI82).

It is well known that fission barriers generally decrease with atomic number so that fission competition increases, thereby lowering the cross sections for similar reaction types. A further reduction in cross section occurs due to an increase in the Coulomb barrier as the product of projectile and target atomic numbers increases. In $(^{18}O,\alpha 3n)$ reactions, assuming for the above reasons that the reduction in cross section is at least as severe going from ^{249}Bk to ^{249}Cf targets as from ^{248}Cm to ^{249}Bk targets, a cross-section upper limit for the reaction $^{249}Cf(^{18}O,\alpha 3n)^{260}Rf$ can be very roughly estimated from this assumption directly as follows:

$$\sigma[^{249}Cf(^{18}O(96\ MeV),\alpha 3n)] \leq \sigma[^{249}Bk(^{18}O(93\ MeV),\alpha 3n)] \times \sigma[^{249}Bk(^{18}O(93\ MeV),\alpha 3n)]/\sigma[^{248}Cm(^{18}O(93\ MeV),\alpha 3n)] \approx (6\pm 2\ nb)^2/20\ nb \approx 2\pm 1\ nb \quad (1)$$

In addition, the ratio of the $^{248}Cm(^{16}O,\alpha 3n)$ and $^{248}Cm(^{16}O,\alpha 4n)$ cross sections is ~3 for 92-MeV ^{16}O ions near the of the peak $(^{16}O,4n)$ reaction cross section (GHI70a). As mentioned in the previous section, the cross section for the reaction $^{249}Cf(^{18}O,\alpha 4n)^{259}Rf$ is ~0.5 nb near the peak of the $(^{18}O,4n)$ reaction cross section. Thus, for similar ions

^{18}O and ^{16}O, if one makes the assumption that

$$\sigma[^{249}Cf(^{18}O,\alpha 3n)]/\sigma[^{249}Cf(^{18}O,\alpha 4n)] \approx \sigma[^{248}Cm(^{16}O,\alpha 3n)]/\sigma[^{248}Cm(^{16}O,\alpha 4n)] \quad ,(2)$$

the cross section for the reaction $^{249}Cf(^{18}O,\alpha 3n)^{260}Rf$ with 96-MeV ^{18}O ions might be estimated as follows:

$$\sigma[^{249}Cf(^{18}O,\alpha 3n)] \approx \sigma[^{249}Cf(^{18}O,\alpha 4n)] \times \sigma[^{248}Cm(^{16}O,\alpha 3n)]/\sigma[^{248}Cm(^{16}O,\alpha 4n)]$$
$$\approx 0.5 \text{ nb} \times 3 \approx 1.5 \text{ nb}$$

Although experimental data are not available to justify an assumption of the type in equation 2 with the use of actinide targets, the estimated cross section of 1.5 nb for ^{260}Rf in the $^{249}Cf(^{18}O,\alpha 3n)^{260}Rf$ reaction is close to the independently-derived estimate of $\leq 2 \pm 1$ nb in equation 1. Note that these estimates are considerably below the 9±1-nb cross section measured for the ~19-ms SF activity. Thus, because the measured cross section may be too high compared to the estimated values, the assignment of the ~19-ms SF activity in the reaction 96-MeV ^{18}O + ^{249}Cf to ^{260}Rf might not be correct.

IV.C.5.d. The Possibility of One or More SF Activities With Z<104 and With Half-Lives Between 14 and 24 ms

IV.C.5.d.i. General

A second possible interpretation is that ^{260}Rf may still be the assignment for the ~20-ms SF activity produced in the reactions 80-MeV ^{15}N +^{249}Bk and 92-MeV ^{16}O +^{248}Cm but one or more SF activities with similar half-lives and atomic numbers less than 104 are produced in the reactions 109- to 119-MeV ^{18}O +^{248}Cm, 88- to 100-MeV ^{15}N +^{249}Bk, and 96-MeV ^{18}O +^{249}Cf. If so, none of these SF activities with half-lives between 14 and 24 ms could be due to nuclides close to the ^{248}Cm or ^{249}Bk targets, unless they are very neutron-rich nuclides, because no SF activity with a half-life in this range was observed in the bombardment 97-MeV ^{15}N +^{248}Cm (see Tables 1 and 2).

The shape of the excitation function for the reaction ^{15}N +^{249}Bk in Figure 4 suggests that either one SF activity is produced in two different mechanisms or two distinct SF activities are produced. The large half-life error bars are 90-per-cent confidence limits, not standard deviations. The probability that all five half-life measurements are due to a single SF activity is only 3 per cent, unless there are large unknown systematic errors. Stated another way, the probability that the ~14-ms SF activity observed with 88- to 100-MeV ^{15}N ions is the same SF activity as the 23±1-ms SF activity produced with 78- to 86-MeV ^{15}N ions is only 3 per cent. Although there may be

unknown systematic errors, this difference in half-lives also suggests that there may be two distinct SF activities--(1) possibly ^{260}Rf with a half-life of 23±1 ms for ^{15}N-ion energies from 78 to 86 MeV and (2) an unidentified 14±3-ms SF activity for 88- to 100-MeV ^{15}N-ion energies.

Possible assignments for this ~14-ms SF activity will now be discussed. The fission isomer ^{242f}Am (13.7 ms) is considered quite an unlikely assignment based on the low cross section of 0.8 μb measured for the analogous product ^{226}Th in a separate bombardment 99-MeV ^{15}N +^{233}U (GHI81). In the reaction 100-MeV ^{15}N + ^{249}Bk the production cross section for the analogous product ^{242g}Am(16 hr) ought to be lower than 0.8 μb due to increased fission competition. Assuming the nearly projectile-independent, energy-independent isomer-to-ground-state production ratio of ~4×10^{-4} for ^{242}Am discussed in section IV.C.5.a., the cross section for producing ^{242f}Am in the reaction 100-MeV ^{15}N +^{249}Bk should not be larger than 0.8 μb x 4×10^{-4} ≈ 0.3 nb. However, the measured cross section for the 14-ms SF activity that was observed was ~9 nb. Clearly, another nuclide besides ^{242f}Am is required to explain the ~14-ms SF activity produced in the reaction 100-MeV ^{15}N +^{249}Bk.

In the reaction 100-MeV ^{15}N +^{249}Bk a measured half-life of 15^{+6}_{-4}ms (90-per-cent confidence limits) is consistent with the possible half-life of 13±2 ms for ^{258}Rf (NUR74), which in this reaction would be produced with the emission of six neutrons. However, in the reaction ^{15}N +^{249}Bk the excitation function for production of the 14-ms SF activity is considerably broader than calculated for ^{258}Rf. The

cross section also exceeds the calculated one by a factor of ~130!

In order for the unknown isotope ^{261}No to be one of the SF activities with half-lives between 14 and 24 ms it would have to be produced in one or more of the reactions ^{249}Cf(^{18}O,^{6}Be)^{261}No, ^{248}Cm(^{18}O,αn)^{261}No, ^{249}Bk(^{15}N,^{3}He)^{261}No, or ^{248}Cm(^{16}O,^{3}He)^{261}No. These reactions are expressed in a purely formal manner and are not meant to imply the ejection of a particular light fragment. In short, none of these reactions is expected to have a cross section large enough to explain any one of the SF activities with half-lives between 14 and 24 ms. ^{260}Md and ^{261}Md are also considered unlikely because the estimated cross sections for the required reactions are markedly lower than the measured cross sections for production of the ~20-ms SF activity.

A possible isomeric transition with a ~20-ms half-life in ^{258}No(1.2 ms) has also been considered. But a measured cross-section upper limit of 0.4 nb for ~20-ms SF events in the reaction ^{244}Pu(^{18}O(~95 MeV),4n)^{258m}No is only 1/200 of the calculated production of the ground state. On the other hand, in the reaction 92-MeV ^{16}O +^{248}Cm the cross section was ~6 nb for the ~20-ms SF activity; Ghiorso's data in reference *GHI70a* would imply a cross section of ~1 nb for ^{258}No(1.2 ms) with 94-MeV ^{16}O ions. Consequently, the cross-section ratio for production of the 20-ms and 1-ms SF activities is ~6, which is very different from $\leq$1/200 obtained from the reaction ^{244}Pu(^{18}O(95 MeV),4n)^{258m}No. Such a small isomer-to-ground-state ratio of $\leq$1/200 and such widely-differing ratios in the two reactions ^{244}Pu(^{18}O,4n)^{258m,g}No and ^{248}Cm(^{16}O,α2n)^{258m,g}No make

the hypothesis of a ~20-ms isomeric transition in ^{258}No(1.2 ms) a very unlikely explanation of any of the ~20-ms SF activities observed in this work.

As discussed in reference NIT81, if the 14-ms SF activity which is produced with 88- and 100-MeV ^{15}N ions is also produced to some extent with 80- to 82-MeV ^{15}N ions, the half-life of the 23±2-ms component in Figure 4 could be a few milliseconds longer. Whether the SF activities made in the reactions 109-Mev ^{18}O +^{248}Cm, 88- to 100-MeV ^{15}N +^{249}Bk, and 96-MeV ^{18}O +^{249}Cf are identical is another open question.

For the above reasons nuclides with masses very close to the ^{248}Cm and ^{249}Bk targets, ^{242f}Am(13.7 ms) (except possibly in the reaction 113-MeV ^{22}Ne +^{244}Pu), and ^{258}Rf(13 ms), as well as the undiscovered isotopes ^{261}No, ^{260}Md, and ^{261}Md have been shown to be unlikely assignments for the SF activities with half-lives between 14 and 24 ms that have been observed in the reactions 88- to 100-MeV ^{15}N + ^{249}Bk, 109- to 119-MeV ^{18}O + ^{248}Cm, and 96-MeV ^{18}O +^{249}Cf. The actual identities of these activities are at the present time unknown.

IV.C.5.d.ii. Evidence Supporting a Possible ^{261}Lr Assignment to a SF Activity With a Half-Life Between 14 and 24 ms

Interpreting ^{261}Lr as the (^{15}N,p2n) reaction product with a half-life between 14 and 24 ms in the reactions 88- to 100-MeV ^{15}N +^{249}Bk would be consistent with the fact that in the reaction

96-MeV ^{15}N +^{244}Pu>^{256}Fm + p2n, the (^{15}N,p2n) reaction product was observed at high bombarding energies. The possible assignment of ^{261}Lr to this ~14-ms SF activity would also be consistent with all the negative results from the cross bombardments of Table 2. A cross-section upper limit of 0.7 nb for the reaction 93-MeV ^{18}O +^{249}Bk>^{261}Lr + α2n is not unexpected, based on the following data.

(1) The cross-section upper limit for the reaction $^{244}Pu(^{18}O(\sim 95\ MeV),\alpha 2n)^{256}Fm$ is 3 nb, based on the unpublished data of Ghiorso (GHI80b). One would expect the cross section for an (^{18}O,α2n) reaction with a ^{249}Bk target to be even lower due to increased fission competition. A cross-section upper limit for the $^{249}Bk(^{18}O,\alpha 2n)^{261}Lr$ reaction cross section of 0.7 nb or lower might not be unreasonable.

(2) Also in the similar reaction ^{16}O +^{248}Cm the ratio of the cross sections for the (^{16}O,α2n) and (^{16}O,α3n) reactions is ~0.1 with ~95-MeV ^{16}O ions (GHI70a). The cross section for the reaction $^{249}Bk(^{18}O,\alpha 3n)^{260}Lr$ is ~6±2 nb with 93-MeV ^{18}O ions, based on unpublished data of Ghiorso *et al.* (GHI71b). These data suggest that a very rough estimate for the $^{249}Bk(^{18}O,\alpha 2n)^{261}Lr$ reaction cross section might be

$$\sigma[^{249}Bk(^{18}O,\alpha 2n)] \approx \sigma[^{248}Cm(^{16}O,\alpha 2n)]/\sigma[^{248}Cm(^{16}O,\alpha 3n)] \times \sigma[^{249}Bk(^{18}O,\alpha 3n)]$$
$$= 6\ nb \times 0.1 = 0.6\ nb \qquad ,(4)$$

with 93-MeV ^{18}O ions, assuming a similar ratio between (HI,α2n) and (HI,α3n) reaction cross sections for ^{16}O and ^{18}O ions with actinide targets. Unfortunately, no experimental data are available to justify this assumption. But since the measured cross-section upper limit for a 20-ms half-life of 0.7 nb lies in this range, the possiblilty of ^{261}Lr having a half-life between 14 and 24 ms for SF decay cannot be excluded.

IV.C.5.d.iii. Evidence Against ^{261}Lr Being a SF Activity With a Half-Life Between 14 and 24 ms

^{261}Lr could not be the ~20-ms SF activity produced with cross sections of 14 nb and 6 nb, respectively, in the reactions 80-MeV $^{15}N + ^{249}Bk$ and 92-MeV $^{15}O + ^{248}Cm$, based on the low cross sections for very similar (HI,p2n) reaction products in the bombardments 81-MeV $^{15}N + ^{249}Cf \rightarrow ^{261}Rf$ + p2n ($\leq$0.4±0.2 nb, GHI70) and 96-MeV $^{16}O + ^{243}Am \rightarrow ^{256}No$ + p2n (~3±3 nb, GHI70).

Whether ^{261}Lr could be produced with a cross section of ~10 nb in the reaction 109-MeV $^{18}O + ^{248}Cm \rightarrow ^{261}Lr$ + p4n is unknown. But according to Oganessian et al. (OGA69) the ratio of the cross section for the similar reaction $^{241}Am(^{16}O,p4n)^{252}No$ to the $^{239}Pu(^{18}O,5n)^{252}No$ reaction cross section is only 1/50. Although the bombarding energies were not quoted in reference OGA69, this would imply a cross section of ~0.8 nb for the reaction $^{241}Am(^{16}O,p4n)^{252}No$, assuming a calculated 37-nb maximum cross section for the reaction $^{239}Pu(^{18}O,5n)^{252}No$ with 97-MeV ^{18}O ions. Thus, the data of Oganessian et al. suggest that the

$^{248}Cm(^{18}O,p4n)^{261}Lr$ reaction may have a cross section much less than ~10 nb and that the ~20-ms SF activity produced in the reaction 109-MeV ^{18}O + ^{248}Cm might not be ^{261}Lr.

^{261}Lr would be produced in the reaction (^{18}O,^{6}Li) using a ^{249}Cf target, a reaction which Ghiorso et al. (GHI81a) found had a cross section of ~300 nb using a ^{208}Pb target and 110-MeV ^{18}O ions. The notation (^{18}O,^{6}Li) used here does not necessarily imply that a ^{6}Li light fragment is ejected, but rather that a net reaction with any combination of three protons and three neutrons released takes place. But using a ^{244}Pu target only an upper limit of 3 nb could be established for the (^{18}O,^{6}Li) reaction product ^{256}Es (GHI80b) with ~95-MeV ^{18}O ions. It is evident from the factor of at least 100 reduction in cross section for (^{18}O,^{6}Li) reactions from ^{208}Pb to ^{244}Pu targets that fission competition plays an important role. The cross section for the (^{18}O,^{6}Li) reaction using a ^{249}Cf target would then be expected to be much lower than 3 nb. But the maximum cross section for the production of the ~20-ms SF activity in the reaction 96-MeV ^{18}O + ^{249}Cf is ~9 nb. Thus, ^{261}Lr, the (^{18}O,^{6}Li) product using a ^{249}Cf target, could not be the ~20-ms SF activity in that reaction.

A SF half-life as short as 14-24 ms may seem unlikely for ^{261}Lr, especially since a SF branch has not been observed for any known isotope of element 103. Also the known odd-mass isotopes of element 103 have half-lives of 0.6 to 22 seconds which also do not change drastically with neutron number. But one might argue that a catastrophic decrease in partial half-life for SF occurs in crossing

the 157-neutron line as has been observed in the isotopes of elements 100 to 102 (NUR81). As discussed in the next section, there is evidence that ^{262}Rf may have a SF half-life of ~50 ms. If that is the case, it might be argued that ^{261}Lr, which ought to be hindered against SF relative to ^{262}Rf due to an odd number of protons, could not have a SF half-life as short as ~20 ms.

IV.C.5.e. Concluding Summary of the SF Activities With Half-Lives Between 14 and 24 ms

Interpreting the available data for SF activities with half-lives between 14 and 24 ms is an extremely complex task. But certain conclusions about these SF activities can be drawn.

(1) The Dubna interpretation that the ~20-ms SF activity produced in the reactions 92-MeV ^{16}O +^{248}Cm and 82-MeV ^{15}N +^{249}Bk is actually a mixture of 13.7-ms ^{242f}Am and the 80-ms SF activity has been shown to be very improbable.

(2) Probably none of the the SF activities are due to nuclides very near the ^{248}Cm or ^{249}Bk targets, ^{242f}Am(13.7 ms) (except possibly in the reaction 113-MeV ^{22}Ne +^{244}Pu), ^{258}Rf(13 ms), ^{261}No, ^{260}Md, ^{261}Md, or a ~20-ms isomeric transition in ^{258}No(1.2 ms). This conclusion is based on the fact that the measured production cross sections differ markedly from the estimated ones.

(3) If all of these SF activities are, in fact, a single ~20-ms SF activity, assigning this SF activity to ^{260}Rf would not be

consistent with all of the data. For example, the measured cross sections in the reactions 109- to 119-MeV $^{18}O + ^{248}Cm$ and 96-MeV $^{18}O + ^{249}Cf$ are much larger than expected for ^{260}Rf, suggesting assignment to a nuclide with Z<104. However, the assignment of ^{260}Rf would be consistent with production of the ~20-ms SF activity in the reactions 80-MeV $^{15}N + ^{249}Bk$ and 92-MeV $^{16}O + ^{248}Cm$, as well as with the negative results from seven other cross bombardments in Table 2. Thus, ^{260}Rf might still be a ~20-ms SF activity if one or more SF activities with Z<104 are produced in the reactions 109- to 119-MeV $^{18}O + ^{248}Cm$ and 96-MeV $^{18}O + ^{249}Cf$, or if the cross sections to produce ^{260}Rf in the latter reactions are grossly underestimated.

(4) In the reaction $^{15}N + ^{249}Bk$ a half-life analysis shows that the purely statistical probability of only one SF activity is only 3 per cent. The presence of as yet, unknown systematic effects could alter this statement, however. The shape of the excitation function could be explained by production of two SF activities with similar half-lives or by production of one SF activity in two different mechanisms.

(5) It is unlikely that ^{261}Lr could be any of the ~20-ms SF activities produced in the reactions 80-MeV $^{15}N + ^{249}Bk$, 92-MeV $^{16}O + ^{248}Cm$, and 96-MeV $^{18}O + ^{249}Cf$. It might be the ~14-ms SF activity produced in the reactions 88- to 100-MeV $^{15}N + ^{249}Bk$; however, the low cross section measured by Oganessian et al. (OGA69) for the reaction $^{241}Am(^{16}O,p4n)^{252}No$ would suggest that a ~10-nb cross section measured for the ~20-ms

SF activity might be too high for the similar reaction $^{248}Cm(^{18}O(109\ MeV),p4n)^{261}Lr$.

IV.C.6. ~50-ms SF Activity

IV.C.6.a. Possibly ^{262}Rf

The 55-ms SF activity shown in the decay curve of Figure 8 was produced in the reaction $^{18}O + ^{248}Cm$ with an excitation function which for ^{18}O ion energies up to 95 MeV agrees reasonably well with the calculated excitation function for production of ^{262}Rf, as shown in Figure 17. The maximum cross section of ~6 nb for the reaction ~91-MeV $^{18}O + ^{248}Cm$ is close to the calculated maximum cross section of 9 nb. But although the large error bars make it difficult to locate the peak precisely, the experimental excitation function may peak slightly below the maximum of the calculated excitation function. As discussed in the appendix section VIII.A., since discrepancies of up to ±3 MeV between experimental and calculated peak positions have been observed for carbon and ^{18}O ions bombarding actinide targets (LEI77), a small energy difference is not considered contradictory to the ^{262}Rf assignment, however. There were indications for production of a 50±16-ms SF activity in a single bombardment of 113-MeV $^{22}Ne + ^{244}Pu$. The measured production cross section of ~1 nb, although based on only 77 SF tracks, is close to the calculated cross section of 1.5 nb to produce ^{262}Rf. There might also be a short-lived component in the data with a half-life close to 14 ms, although a longer bombardment is

necessary to be sure. Since the ~50-ms SF activity was produced only in the reaction $^{18}O + ^{248}Cm \rightarrow ^{266}Rf^*$ and possibly also in the reaction $^{22}Ne + ^{244}Pu \rightarrow ^{266}Rf^*$, absence of this SF activity in the other cross bombardments of Table 2 is consistent with the possible assignment of ^{262}Rf. The weighted-average half-life from our data for the reaction $^{18}O + ^{248}Cm$ is 52±5 ms.

IV.C.6.b. Consideration of Other Possible Assignments for the ~50-ms SF Activity---$^{262,263}Lr$, ^{261}No, and ^{260}Md

^{262}Lr and ^{263}Lr would also be possible assignments for the ~50-ms SF activity consistent with the cross bombardments with negative results in Table 2. However, ^{263}Lr would be expected to have a small production cross section with ^{18}O ions of energies 89 to 95 MeV, based on the 3±3-nb cross section for the similar reaction with less fission competition 96-MeV $^{16}O + ^{243}Am \rightarrow ^{256}No$ + p2n (GHI70). Whether ^{262}Lr, the $^{248}Cm(^{18}O,p3n)$ reaction product, could have a production cross section as large as ~6 nb between 89 and 95 MeV is not known. But (HI,p3n) reactions have been shown to take place more readily at bombarding energies greater than for the energy of the calculated peak cross section for the reaction $^{249}Cf(^{13}C,4n)^{258}Rf$ (ESK81).

^{261}No would be produced in a $^{248}Cm(^{18}O,\alpha n)^{261}No$ reaction. For both ^{12}C and ^{14}N ions bombarding a ^{249}Cf target the (HI,αn) reaction cross sections are at least an order of magnitude below the maximum (^{14}N,α2n) and (^{12}C;α2-3n) reaction cross sections (GHI69). For both

^{12}C (GHI69) and ^{15}N (ESK71) ions bombarding a ^{249}Cf target the maximum (HI,α2n) and (HI,α3n) reaction cross sections are nearly equal. In addition, Lee et al. (LEE82) measured a cross-section upper limit for the $^{248}Cm(^{16}O(98\ MeV),\alpha n)^{259}No$ reaction of 1 nb. For the reaction $^{248}Cm(^{18}O,\alpha 3n)^{259}No$ the maximum cross section is 20 nb (SIL73). Thus, if (HI,αn) reaction cross sections are generally small and an order of magnitude lower than (HI,α2-3n) reaction cross sections, the cross section for the reaction $^{248}Cm(^{18}O,\alpha n)^{261}No$ would be expected to be roughly an order of magnitude or more lower than 20 nb, or less than 5 nb measured for the ~50-ms SF activity.

The possibility that ^{260}Md could be the ~50-ms SF activity has also been considered. It would be produced in the reaction ($^{18}O,^{6}Li$) using a ^{248}Cm target. However, as discussed in the previous section, a cross-section upper limit of 3 nb has been established for the ($^{18}O,^{6}Li$) reaction using a ^{244}Pu target with ~95-MeV ^{18}O ions (GHI80b). The fact that this cross section is 100 times lower than for the same reaction using a ^{208}Pb target shows that fission competition increases with the atomic number of the compound nucleus. The cross section for the ($^{18}O,^{6}Li$) reaction using a ^{248}Cm target is expected to be even lower than the 3-nb cross section obtained using a ^{244}Pu target due to further increased fission competition. This implies that the ~50-ms SF activity, which is produced with a maximum cross section of ~6 nb, is probably not the $^{248}Cm(^{18}O,^{6}Li)$ reaction product ^{260}Md.

IV.C.6.c. Concluding Statements About the ~50-ms SF Activity

The ~50-ms SF activity was produced in the reaction $^{18}O + ^{248}Cm$ and possibly also in the reaction 113-MeV $^{22}Ne + ^{244}Pu$ with cross sections close to those calculated to produce ^{262}Rf. In addition, from the data accumulated thus far for the reaction $^{18}O + ^{248}Cm$ the excitation function in Figure 17 appears to have a maximum and shape close to the same parameters calculated for ^{262}Rf. No evidence from all the cross bombardments of Table 2 has been found that contradicts the possible assignment of this ~50-ms SF activity to ^{262}Rf.

IV.D. SF Properties of Element-104 Nuclei

IV.D.1. Present Status of Experimental Half-Life Investigations

As mentioned at the beginning of the discussion section, the identity of none of the SF activities mentioned in this thesis, with the exception of ^{256}Fm(2.6 hr), is known with certainty. Of the possible element-104 SF activities discussed in this paper the 8-ms SF activity has been shown experimentally to be an isotope of element 104 or element 103 by Münzenberg et al. (MÜN80, MÜN81b, MÜN82). Münzenberg et al. (MÜN80a, MÜN82) assigned this activity to ^{256}Rf, supporting the previous assignment by Oganessian et al. (OGA74a) for the following three reasons: (1) lawrencium (element 103) nuclei are usually highly hindered for SF decay, i.e., SF decay has not been

observed for any isotopes of lawrencium; (2) other decay modes from ^{256}Rf were absent; and (3) the narrow width of 10 MeV for the excitation function would tend to exclude transfer reaction products. Data from nine cross bombardments in Tables 1 and 2 are consistent with a ~20-ms half-life for ^{260}Rf. However, the ~20-ms SF activity produced with a cross section of ~50 times the calculated cross section for producing ^{260}Rf in the reaction 109-MeV $^{18}O + ^{248}Cm$ is an unsolved puzzle. Also the cross section of ~9 nb for the ~19-ms SF activity in the reaction 96-MeV $^{18}O + ^{249}Cf$ appears to be too high for the $(^{18}O,\alpha 3n)$ reaction product ^{260}Rf, based on comparisons with other $(^{18}O,\alpha 3n)$ reaction cross sections.

IV.D.2. Future Directions for Experimental Investigations

IV.D.2.a. Half-Life Measurements for SF of Element-104 Isotopes

IV.D.2.a.i. Future Cross Bombardments Using the Tape System

Future experiments must show whether the SF activities produced in the reactions 109- to 119-MeV $^{18}O + ^{248}Cm$ and 96-MeV $^{18}O + ^{249}Cf$ with half-lives between 14 and 24 ms are the same or different from the ~20-ms SF activity produced in the reactions 76- to 86-MeV $^{15}N + ^{249}Bk$ and 92-MeV $^{16}O + ^{248}Cm$. If they are, in fact, all the same activity, the single activity could not be ^{260}Rf. But if they are different, there would then be no inconsistency in ^{260}Rf being a ~20-ms SF activity. And more precise half-life measurements with good statistics might reveal a small

difference in half-lives.

A remote possibility is that the ~20-ms SF activity produced in the reactions 109- to 119-MeV ^{18}O + ^{248}Cm is ^{260}Rf. But if so, the $^{248}Cm(^{18}O,6n)^{260}Rf$ reaction would have to be enhanced by an unknown mechanism. This possibility could be checked by performing the reaction ^{18}O + $^{246}Cm \rightarrow$ ^{258}Rf(13 ms) + 6n and measuring the production cross section and half-life with good statistics. By chemical means (GHI76a) it can be verified that the cross section for producing the ground state of ^{242}Am(16 hr) is small, and using the assumed ratio of $\sim 4 \times 10^{-4}$ (see section IV.C.5.a. The Dubna Interpretation: The ~20-ms SF Activity Is a Mixture of ^{242f}Am(13.7 ms) and the 80-ms SF Activity) for the isomer-to-ground-state production cross sections, the possible confusing SF activity ^{242f}Am (13.7 ms) with similar half-life can be ruled out. With data from several new cross bombardments using the tape system, including the use of new targets such as ^{246}Cm and ^{254}Es, more precise half-life measurements, and a knowledge of whether the $Cm(^{18}O,6n)$ reaction cross sections are enhanced or not, the question of whether one or more SF activities with half-lives between 14 and 24 ms are required to fit the data should be answerable.

However, even if all the data from many cross bombardments are consistent with the assignments ^{258}Rf(13 ms), ^{260}Rf(~20 ms), and ^{262}Rf(~50 ms), we will not have performed any experiment which shows positively that these fission activities originate from element-104 nuclei. The difficulties of making firm identifications of these new SF activities based on the tape experimental data alone were discussed

at the beginning of the discussion section. Four possible ways that firm identifications could be made will now be discussed.

IV.D.2.a.ii. Four Possible Ways to Make Firm Identifications

IV.D.2.a.ii.(1) Mass Measurements Using a Mass Separator

One approach to positively identifying these SF activities would be to determine the mass numbers using an on-line mass separator. Mass separators such as SHIP (MÜN81a, 79) at GSI in Darmstadt, West Germany, and SASSY (LEI81) and OASIS (NIT81a, NIT82) here in Berkeley are already being used in the identification of new isotopes. However, since it is not possible to produce ^{260}Rf with currently-measurable cross sections by using a very heavy ion ($A \geq 40$), neither SHIP nor SASSY could presently measure its mass number (GHI82). For OASIS the half-life of ~20 ms is too short and the vapor pressure for rutherfordium is quite low at the ion-source operating temperatures. But with modifications OASIS might be capable of measuring the mass number in the future (NIT82a). Ghiorso has a proposal called RAMA II to mass analyze singly-charged recoils which have been magnetically separated from the beam and stopped in helium gas (GHI82). This technique offers the advantages of both high efficiency and rapid mass analysis so that the masses of millisecond-lived SF activities could be measured. If the mass of the ~20-ms SF activity produced in either of the reactions 80-MeV $^{15}N + ^{249}Bk$ or 92-MeV $^{16}O + ^{248}Cm$ is determined to be 260, it would be sufficient evidence for assigning ^{260}Rf to this

activity. A low cross-section upper limit of 0.7 nb has already been measured for possible ~20-ms SF events from ^{260}Lr in the cross bombardment ^{249}Bk(^{18}O(93 MeV),α3n)^{260}Lr; but data from unpublished results of Ghiorso et al. (GHI71b) show that the cross section for the three-minute 8.03-MeV alpha particles from ^{260}Lr is ~6±2 nb. The ~20-ms SF activity was produced in the reactions 80-MeV ^{15}N +^{249}Bk and 92-MeV ^{16}O +^{248}Cm with the compound system ^{264}Rf*. In this system lower-atomic-number mass-260 nuclei such as ^{260}No, ^{260}Md, and ^{260}Fm would not be produced with measurable cross sections, based on the unlikely emission of an alpha particle with no neutrons; n,3p; and 4p; respectively. Mass-260 nuclei with atomic numbers less than 100 have more than 160 neutrons and consequently, are unreachable in reactions for which the compound system is ^{264}Rf*.

IV.D.2.a.ii.(2) Element-104 X-Rays

Another approach to identification becomes possible if ^{262}Ha or ^{260}Ha has an electron-capture branch. Bemis et al. have suggested that ^{262}Ha may have an electron-capture branch (BEM77a). They have established an upper limit of 5 per cent on the electron-capture branch of ^{262}Ha if ^{262}Rf has a half-life of 150μs or less (BEM77b). But as this work shows, ^{262}Rf might have a ~50-ms half-life. In the electron-capture decay of ^{262}Ha coincidences between L or K x-rays of element 104 and subsequent SF events of ^{262}Rf could easily have been missed in those experiments if ^{262}Rf had a half-life as long as ~50 ms, due to the large gamma-ray background associated with such a

long coincidence time. Calculations by Keller and Münzel (KEL69) imply an electron-capture branch of ~6 per cent. The experimental estimate for the total branching to SF is 78 per cent (BEM77a).

The electron-capture branch in ^{260}Ha is experimentally known to be less than or equal to 2.5 per cent, assuming an 80-ms half-life for ^{260}Rf, or less than 0.2 per cent, assuming a half-life for ^{260}Rf that is less than or equal to 100μs (BEM77b). This is consistent with the calculations by Keller and Münzel which imply a 1.5-per-cent electron-capture branch (KEL69).

If either ^{262}Ha or ^{260}Ha does have an electron-capture branch, then one could search for element-104 K x-rays followed by SF events from ^{262}Rf or ^{260}Rf. From the distribution of x-ray-fission coincidence times the half-life for SF could be determined. Recoils could be stopped in helium gas and transported by potassium chloride or sodium-chloride aerosol particles (STE80) to a low-background region where x-rays and SF events could be detected in coincidence using x-ray and solid-state detectors. However, since the required coincidence time of 20 to 50 ms is relatively long, the background from other interfering gamma rays of fission fragments in the element-104 x-ray region must be quite low for this technique to be successful.

IV.D.2.a.ii.(3) Laser-Excited Optical Transitions of Element 104

A third approach would be to use a dye laser tuned to a frequency for optically exciting atoms of element 104. The excited element-104 atoms could then be separated from the recoils stopped in gas by the most efficient of several techniques used in laser isotope separation (ZAR77). Bemis et al. (BEM79) have already demonstrated that a tuned dye laser can be used to saturate an atomic transition in ^{240f}Am(0.94 ms) atoms and that subsequent coincident SF fragments from the nuclei of those excited atoms were detectable with an overall efficiency of ~2.5 per cent, calculated from the data of that reference. The appropriate optical frequency could first be calculated for the initial search and then determined by producing and exciting ^{261}Rf(65 s) atoms. From there the calculable optical isomer shift needed to excite ^{260}Rf or ^{262}Rf could determine the mass number to be 260 or 262. Measurement of the half-life for SF from these separated ^{260}Rf or ^{262}Rf atoms could then be made.

IV.D.2.a.ii.(4) A Possible Alpha-Decay Branch in ^{260}Rf

A fourth approach, which is perhaps the most accessible, would be to identify ^{260}Rf by alpha-particle-decay branching. The alpna-particle decay energy would be ~8.6 MeV (GHI82). But a difficulty would be the estimated low branching ratio of ~1/150 if ^{260}Rf has a ~20-ms half-life. Also since ^{260}Rf cannot be produced with a measurable cross section using a very heavy ion ($A \geq 40$), no detecting

system presently exists for possible ~20-ms alpha particles from ^{260}Rf. But once a detecting system is developed the reaction 72-MeV $^{12}C + ^{252}Cf \rightarrow ^{260}Rf + 4n$ might be used to search for ~20-ms alpha particles from ^{260}Rf with a ~0.3-nb cross section for production of these alpha particles.

IV.D.2.b. Fission-Mass Distribution and Total-Kinetic-Energy Measurements for SF of Isotopes of Element 104

In addition to measuring the half-lives to see if there is a change in the SF half-life systematics at element 104, other SF properties of element-104 isotopes can be investigated. In particular, the fission-mass distribution predictions for element-104 nuclei discussed in section IV.D.3.b. can be tested. The SF properties of ^{257}Rf(4.8 s) and ^{259}Rf(3 s) can be measured. As opposed to the possible millisecond-lived even-even rutherfordium isotopes, these nuclei have half-lives long enough to permit separation from the accelerator beam region and alkali-chloride aerosol transport to pairs of solid-state detectors with 4π-geometry for detection of SF events. An experimental setup of this kind is described in reference HOF81. If the possible SF branches measured in this work are correct, the reactions 75-MeV $^{12}C + ^{249}Cf \rightarrow ^{257}Rf + 4n$ and 93-MeV $^{18}O + ^{245}Cm \rightarrow ^{259}Rf + 4n$ can be used to produce and measure SF events from these nuclei with cross sections of ~2 nb and ~0.6 nb, respectively. The actual production of these nuclei can be monitored by measuring the well-known alpha-particle energies of ^{257}Rf(4.8 s) and ^{259}Rf(3 s) using the same

detectors which record the SF events.

Hulet et al. (HUL81) have developed a system of thin rotating catcher foils in which the fission-mass distribution for possible millisecond-lived rutherfordium isotopes can be measured. For ^{260}Rf and ^{262}Rf both Randrup et al. (RAN76) and Mustafa and Ferguson (MUS78) predict that the second barrier should be below the ground state in energy. Thus, measurements of the fission-mass distribution for these nuclei would serve as tests of whether the fission-mass distribution is determined at the last saddle point, as suggested by Möller and Nilsson (MÖL72, MÖL81), or whether the fission process is adiabatic with the entire potential-energy surface from the second-saddle region to scission being important, as suggested by Mustafa and Ferguson (MUS78) (see section IV.D.3.b.).

To reach the region $A \geq 266$ in rutherfordium nuclei, where Mustafa and Ferguson predict a transition to symmetric fission (MUS78), very exotic reactions are required. Heavy-ion- (HI) transfer reactions such as $^{257}Fm(HI,HI-^{9}Be)^{266}Rf$ and $^{254}Es(HI,HI-^{12}B)^{266}Rf$, where the HI could be ^{18}O, ^{22}Ne, ^{40}Ar, or ^{48}Ca, could be attempted if either ^{257}Fm or ^{254}Es targets were available.

The following section discusses the theoretical reasons why even-even isotopes of element-104 nuclei may have millisecond half-lives, the odd-mass isotopes may have low hindrance factors, and why element-104 nuclei might fission symmetrically or asymmetrically.

IV.D.3. Theoretical Predictions of the SF Properties of Element-104 Nuclei and the Relationship to the Present Experimental Data

IV.D.3.a. Half-Life Predictions

In Figure 18 the tentative half-lives for even-even element-104 nuclei have been plotted for comparison with the predictions of Randrup et al. (RAN76). They fitted the partial SF half-lives for even-even nuclei up to element 102 by adjusting one parameter in their inertial mass function and then extrapolating to elements 104 and beyond. For nuclei with poorly-known potential barriers that extend to large deformations such as for uranium and plutonium nuclei, both for the ground-state and isomeric-state (insert of Figure 18) half-lives the agreement between calculation and experiment is not as good as for heavier nuclei with less extended barriers. Note that the half-lives for tentative element-104 isotopic assignments fit remarkably close to the predictions of Randrup et al! Baran et al. have also predicted the partial half-lives for SF of even-even nuclei from first principles using no adjustable parameters (BAR81). However, the agreement with the tentative element-104 half-lives is not as good compared to the calculations by Randrup et al.

Randrup et al. suggested that there may be a weakening of the 152-neutron sub-shell effect and a disappearance of the second hump of a double-humped fission barrier at element 104. However, Figure 19 shows that a 152-neutron sub-shell effect is observed in the alpha-decay energies for odd-mass element-104 nuclei. There is a significant drop

in the maximum alpha-decay energy from ^{257}Rf (9.00 MeV) with 153 neutrons to the newly-observed ^{255}Rf (8.726 MeV) (MÜN81, MÜN82) with 151 neutrons. However, since the alpha-decay energies can be affected by shell effects both in the parent and the daughter nuclei, Figure 19 does not necessarily imply a 152-neutron sub-shell effect in the parent rutherfordium nuclei.

For this purpose the shell correction, defined as the ground-state mass minus the droplet-model mass (MYE77) has been plotted in Figure 20 for nobelium (element 102) and rutherfordium (element 104) nuclei. The masses of nobelium and rutherfordium nuclei for making these plots were determined from:

(1) experimentally-measured values (square points), as quoted in the Table of Isotopes (TOI78);

(2) alpha-decay energies in a chain leading to an experimentally-known mass (circled "x" points);

(3) alpha-decay energy of the parent and the daughter mass, known from systematic plots (WAP77) (triangled points);

(4) systematics plots, as discussed in reference WAP77 (soild dots).

Ground-to-ground state transitions were assumed for the maximum alpha-decay energies for each of the nuclides; the possible presence of unknown isomers undergoing alpha decay in the parent or daughter nuclei would lead to masses and shell corrections which are incorrect under this assumption.

Figure 20 shows a clear 152-neutron sub-shell effect in nobelium nuclei of ~0.75 MeV. Unfortunately, none of the rutherfordium masses

are experimentally known; precision mass measurements using a mass spectrometer would be very useful in determining the precise magnitude of a 152-neutron sub-shell effect in these nuclei. Nevertheless, from the masses determined by methods 2 to 4 above, it appears from connecting any set of points in Figure 20 that the 152-neutron sub-shell effect is probably $\leq$0.3 MeV, or much weaker (if it is present at all) for rutherfordium nuclei than for nobelium nuclei. This weakening of the 152-neutron sub-shell effect was predicted by Randrup et al. But Ghiorso (GHI70a) assumed a continuing strong 152-neutron sub-shell effect upon the even-even SF half-lives in extrapolating an empirical fit for elements 98-102 to element 104 (Figure 2a).

As shown in Figure 18, the theoretical calculations of Randrup et al. have underestimated the effect of the 152-neutron sub-shell on the SF half-lives for $Z \leq 102$ nuclei. What would be the effect of a 152-neutron sub-shell correction of $\leq$0.3 MeV upon the element 104 SF half-life predictions of Randrup et al?

The shape of the distribution of half-lives versus neutron number is very sensitive to whether the second barrier is above or below the ground state in energy for each isotope of element 104. For thorium to curium nuclei (elements 90 to 96) the second hump of the fission barrier has been observed to monotonically decrease with increasing proton number (BAC74). This trend would suggest that for some proton number the second barrier might drop below the ground state in energy, in agreement with the theoretical predictions. A possible example of this effect can be seen in Figures 18 and 21. For fermium (element

100) isotopes the drastic decrease in partial SF half-life from ^{256}Fm ($T_{1/2}$=2.86 hr) to ^{258}Fm ($T_{1/2}$=0.38 ms) may be the result of a lowering of the second barrier below the ground state in energy. With one barrier to penetrate instead of two barriers the fission probability is drastically increased, which, in turn, decreases the half-life by a factor of ~10^7 (RAN73,76). As shown in Figure 21, Randrup et al. have predicted this effect to occur between ^{258}Fm and ^{260}Fm, whereas the drastic experimental drop in half-lives occurs between ^{256}Fm and ^{258}Fm, as shown in Figure 18. A 152-neutron sub-shell effect might lower the ground state below the second barrier in energy, which would drastically increase the half-life. As mentioned earlier, from Figure 20 the 152-neutron sub-shell effect is quite probably $\leq$0.3 MeV for element-104 nuclei. But according to the calculations of Randrup et al. the second barrier is below the ground state in energy by one or two MeV for all even-even element-104 isotopes with neutron numbers between 150 and 158 (MÖL81). Thus, the calculated half-lives are determined mainly by the penetration of only one barrier and show no dramatic increase at neutron-number 152.

Mustafa and Ferguson (MUS78) have predicted that the second barrier would be below the ground state for even-even rutherfordium nuclei with A $\geq$260. These predictions were made using the asymmetric two-center shell model, which minimizes the potential energy during the fission process with respect to the neck radius, the volume ratio, and other dimensions for the portions of the nucleus on either side of the neck plane. If these barrier predictions are correct, for A<260 with a second barrier above the ground state, if a weak 152-neutron

sub-shell effect is present at element 104, it might have some effect on the SF half-lives. However, probable assignments of an 8-ms half-life to ^{256}Rf and a 13-ms half-life to ^{258}Rf would suggest that the 152-neutron sub-shell effect on these SF half-lives is not very strong.

The experimental half-lives with tentative element-104 assignments in Figure 18 would disagree with the predictions of Ghiorso (GHI70a) shown in Figure 2a. An exception is ^{258}Rf, for which Ghiorso used an 11-ms half-life from experimental results (NUR71, 70; GHI69, 70a) to normalize the element-104 half-life systematics. This value is quite close to our current half-life of 13 ms (NUR74). But for ^{260}Rf and ^{262}Rf, for example, tentative experimental half-lives are ~20 ms and ~50 ms, respectively, while the Ghiorso predictions would be microseconds or less.

The possibility of even-even isotopes of element 104 having millisecond ordinary isomers with either direct fission branches or isomeric transitions to short-lived fissioning ground states cannot be excluded. In such cases, the ground states might still obey the systematics of Ghiorso. For example, ^{260}Rf might have a ~20-ms isomer and a microsecond-lived ground state which decays by SF. Other even-even actinide nuclei such as ^{250}Fm and ^{254}No have isomeric states decaying by isomeric transitions to fissionable ground states (GHI73). However, these possibilities are considered unlikely because, of the known nuclei, only one case of an ordinary isomer with a fission branch is known (^{242m}Am (152 yr), shown in blue in Figure 1). Also there is no case of any isomer decaying by fission with a partial SF half-life

longer than for the ground state.

Another piece of evidence against the millisecond-lived isomer hypothesis comes from the production cross sections for the SF activities. The JORPLE code calculates only the total production cross section for a given neutron-evaporation product without considering whether the nuclide is produced in its ground state or isomeric state. The JORPLE code calculations agree to within a factor of three or better with a large sample of peak cross sections when four neutrons are evaporated. Assuming the JORPLE code calculations are correct, the sum of the ground-state and all isomeric-state production cross sections should be equal to the JORPLE value. Then since the measured peak cross sections for production of the 13-ms (NUR70), ~20-ms, and ~50-ms SF activities all agree with those calculated by the JORPLE code, for these millisecond-lived SF activities to be due to ordinary isomers of element-104 nuclei, the isomers would have to be populated preferentially instead of the ground states in nearly every case that even-even element-104 nuclei are produced.

Still another piece of evidence against the isomer hypothesis comes from the energy dependence of the cross sections. In the reaction $^{29}Si(^{18}O,p2n)^{44m,g}Sc$ the ratio of the high spin 6^+-isomeric-state to the 2^+-ground-state production cross sections at first increases with bombarding energy due to increasing angular momentum carried by the ^{18}O projectile, and later decreases due to the onset of a different reaction mechanism (GRO82). An isomer-to-ground-state ratio which changes with bombarding energy has also been observed for production of the moderately high-spin isomer of ^{149}Tb

($11/2^-$, $T_{1/2}$=4.2 min.) compared to production of the lower-spin ground state ($3/2^+$ or $5/2^+$, $T_{1/2}$=4.15 hr) in the reaction $^{133}Cs(^{22}Ne,5n)^{149}Tb$ by Moody (MOO81). Another changing ratio has been noticed in the production of the 12^- isomer of ^{196}Au compared to the 2^- ground state in the reaction $^{192}Os(^{11}B,\alpha 3n)^{196m}Am$ (FLE68, McGA81). Presumably a changing isomer-to-ground-state ratio would also be observed in production of moderately high-spin isomers of heavier nuclei. Since the isomers ^{254m}No(0.28 s) and ^{250m}Fm(1.8 s) are predicted to have moderately high spins (GHI73), the systems $^{240}Pu(^{18}O,4n)^{254m,g}No$ and $^{236}U(^{18}O,4n)^{250m,g}Fm$ might be used to test whether a changing isomer-to-ground-state ratio persists among the heaviest nuclei. The excitation functions for production of the 13-ms (NUR70) and ~50-ms (Figure 17) SF activities, however, agree roughly with the excitation functions calculated by the JORPLE code for the total production of ^{258}Rf and ^{262}Rf nuclei, whether in isomeric or ground states. Thus, it is unlikely that the 13-ms and ~50-ms SF activities are due to ordinary isomers with moderately high spin. This is because one would expect the ratio of the experimental cross section for the isomer to the calculated total production cross section (isomer plus ground state) to change with bombarding energy. But this argument does not exclude the possibility of a low-spin ordinary isomer, however. In heavy-ion reactions such a low-spin ordinary isomer would probably have a relatively projectile-energy-independent (GAN67a) isomer-to-ground-state ratio as in the case of the probable low-spin (POL68,FLE68) fission isomer ^{242f}Am produced in the reaction $^{238}U(^{11}B,\alpha 3n)^{242f}Am$.

In Figure 18 the tentative partial half-lives for SF of odd-mass isotopes of element 104 are plotted as solid triangles. It is possible that the odd-mass isotopes of element 104 may have hindrance factors relative to the even-even isotopes of $\sim 10^4$ (^{255}Rf (1.4 s, 45±20-per-cent SF) (MÜN81, MÜN82)); $\sim 4 \times 10^3$ (^{257}Rf (4.8 s, ~14-per-cent SF); $\sim 2 \times 10^3$ (^{259}Rf (3 s, 7-per-cent SF); and $\geq \sim 10^4$ (^{261}Rf (65 s, $\leq$10-per-cent SF) (GHI70c). And if the observation of SF branching in ^{263}106 by Druin et al. (DRU78) is correct, the hindrance factor would be $\sim 10^3$ relative to the even-even half-life predictions by Randrup et al. Ghiorso et al. did not, however, observe SF branching in ^{263}106 (GHI74a); but the sensitivity in these experiments for SF events was limited by abundant production of the 2.6-hour SF-emitter ^{256}Fm.

These hindrance factors are generally less than the hindrance factors observed for odd-mass nuclei of lighter elements such as nobelium, fermium, and californium. This can also be understood in terms of the disappearance of the second barrier. In first order the barrier of the odd-neutron-number nucleus is obtained by raising the entire potential barrier for the even-even nucleus by a "specialization energy" associated with the energy of the odd neutron (RAN73). As Figure 22 shows, the increase in both the thickness and height V(r) of the barrier (i.e., the barrier integral $\int \sqrt{2MV(r)}/\hbar \, dr$) which must be penetrated in order to fission is much greater when starting with a double-humped fission barrier than with a single-humped barrier. This means that relative to the corresponding even-even nucleus, the odd-mass nucleus with a single-humped fission barrier such as ^{263}106

will be hindered less compared to an odd-mass nucleus with a double-humped fission barrier such as ^{257}Fm. Since Randrup et al. predict that the second barrier which is present for lighter elements may disappear at element 104, the reason why the odd-mass element-104 isotopes might have lower hindrance factors than odd-mass isotopes of lower elements with even atomic number can now be understood.

As seen from Figure 18 the upper limit of 10 per cent on the SF branching of ^{261}Rf may imply some added stability associated with 157 neutrons relative to the other isotopes of element 104. This 157-neutron effect, as it affects alpha-decay half-lives, has long been noted in our laboratory for elements 101 to 106.

IV.D.3.b. Fission-Mass Distribution and Total-Kinetic-Energy Predictions

IV.D.3.b.i. Introduction

Besides examining the predicted effect of the disappearance of the second fission barrier at element 104 on the half-lives, it would be very interesting to measure the fission-mass distributions for these nuclei. Möller (MÖL81) has suggested that the fissions might be symmetric, while Mustafa and Ferguson have argued that the fissions would be asymmetric (MUS78). The theoretical arguments for symmetric and asymmetric fission will be discussed separately.

IV.D.3.b.ii. Arguments for Symmetric Fission

Möller and Nilsson (MÖL70) have suggested that the fission-mass distribution is directly correlated with the nuclear potential-energy surface. Möller argues that the mass distribution is decided at the saddle point distortions (MÖL72). The calculations from references MÖL72 and MÖL70 have shown that the second saddle point is unstable with respect to asymmetric distortions for many actinide nuclei, which explains the asymmetric mass distributions observed for SF of most heavy nuclei of uranium or above. In the calculations by Möller and Nilsson the reduction in height of the second barrier due to asymmetric distortions decreases from uranium to fermium. This corresponds well to the empirical fall-off in mass asymmetry from

uranium to fermium and to the known decrease in height of the second barrier from thorium to curium nuclei (BAC74). Mosel and Schmitt (MOS71) have argued that the preference for asymmetric or symmetric fission both in the calculations by Möller and Nilsson and in the empirical mass distributions is due to fragment shell effects which affect the second barrier height when one or both of the fragments are close to the doubly-magic nucleus $^{132}_{50}Sn$.

On the other hand, the first saddle point is predicted to be stable against asymmetric distortions for even-even nuclei lower than element 106 (MÖL72). If then for element 104 the second barrier has disappeared, one would expect the fission properties to be largely determined by the first saddle point. Consequently, the fission-mass distribution for SF of element-104 nuclei might be symmetric (MÖL81).

The charged liquid-drop model predicts that the total-kinetic-energy release is a maximum for symmetric fission. It is noteworthy that the nucleus with the probable assignment of ^{259}Fm has a fission total kinetic energy that is considerably higher than for lighter fermium and lower Z nuclei (HUL80). But total-kinetic-energy predictions are more complicated than this, depending upon other effects such as the internuclear separation and relative velocity at the unknown point of scission (RAN82).

IV.D.3.b.iii. Arguments for Asymmetric Fission

Mustafa and Ferguson (MUS78) have argued that the fission-mass

distribution is not necessarily determined by the second saddle point, as suggested by Möller and Nilsson (MÖL72), but rather it is correlated with the potential-energy surfaces between the second-saddle region and the scission point. From this point of view the fission process is adiabatic, i.e., the asymmetric two-center shell model applies at any point on the pathway to fission. According to this model, the primary reason for transition from asymmetric to symmetric SF is due to fragment shell effects, not to the second barrier dropping below the ground state in energy.

This model also explains the symmetric fissions observed for ^{258}Fm and for the probable assignment of ^{259}Fm as due to the formation of two fragments, each close to the doubly-magic $^{132}_{50}$Sn system. But ^{258}Fm does not make a good test between the two arguments presented here for symmetric or asymmetric fission because for ^{258}Fm the second barrier may have disappeared. Randrup et al. (RAN73, 76) predict a disappearance between ^{258}Fm and ^{260}Fm, although they feel that the transition has most probably occurred between ^{256}Fm and ^{258}Fm due to the sudden ~10^7 decrease in half-life; Mustafa and Ferguson (MUS78) predict a disappearance of the second barrier for ^{258}Fm as well.

A better test case is ^{262}Ha. Bemis et al. (BEM77a) have observed SF events which are most probably asymmetric and possibly due mostly to ^{262}Ha(34 s). They admit that ^{262}Ha may have an electron-capture branch, in which case some of the asymmetric SF events observed would be due to ^{262}Rf. For ^{262}Ha Mustafa and Ferguson also predict asymmetric SF events, in agreement with the present experimental data.

But the same asymmetric two-center shell model, which was successful in predicting the fission-mass distributions for fermium isotopes, ^{252}No, and ^{262}Ha also predicts that the second barrier for ^{262}Ha should not be above the ground state in energy. Under the assumption that the second barrier is below the ground state in energy, the notion of Möller that the mass distribution would then be determined by the first saddle point, which is stable against asymmetric distortion, would not agree with the experimental observation of most probably asymmetric SF of ^{262}Ha.

Mustafa and Ferguson predict that rutherfordium nuclei with mass numbers less than 266 should have asymmetric SF while those with masses of 266 or higher should fission symmetrically. Unfortunately, rutherfordium nuclei with masses of 266 or higher are not reachable with measurable cross sections in most conceivable reactions. The close of section IV.D.2.b. discusses ways in which the mass distributions for possible rutherfordium nuclei could be experimentally measured, testing whether the fission process is adiabatic, as suggested by Mustafa and Ferguson, or whether the mass distribution is determined by the saddle-point distortion properties, as suggested by Möller and Nilsson.

V. Summary and Conclusions

Several new SF activities have been found and possible assignments for them have been suggested in Table 1. None of the assignments are certain, unfortunately. In particular, concerning the even-even isotopes of element 104, no evidence was found to contradict a possible ~50-ms half-life for SF decay of ^{262}Rf. ^{260}Rf might have a ~20-ms half-life; but if so, there must be one or more SF activities with atomic numbers less than 104 which have similar half-lives in order to explain the large cross sections in the reactions 109- to 119-MeV ^{18}O +^{248}Cm and 96-MeV ^{18}O +^{249}Cf. An enhancement of the (^{18}O,6n) reaction cross section by a factor of ~50 due to an unknown mechanism would be required if the ~20-ms SF activity produced in the reactions 109- to 119-MeV ^{18}O +^{248}Cm is ^{260}Rf. Otherwise, a single ~20-ms SF activity must be a nuclide with atomic number less than 104. We hope to answer this question in future cross bombardments using the tape system. A very important possible consequence of this work follows if the tentative assignments of half-lives of ~50 ms to ^{262}Rf and ~20 ms to ^{260}Rf are correct: namely, there may be a drastic change in the SF half-life systematics for even-even isotopes at element 104. This possible change in SF half-life systematics would also agree with the same suggestion by Münzenberg et al. (MÜN80, MÜN81b, MÜN82) based on their measurement of an 8-ms half-life for ^{256}Rf, and with the original statement of the change in systematics by Flerov et al. (FLE71). Randrup et al. (RAN76) have predicted this effect theoretically and have attributed it to a disappearance of the

second hump of a double-humped fission barrier. Baran et al. (BAR81) have also predicted a change in the SF half-life systematics at element 104 without the use of any adjustable parameters, but in this case the agreement with the tentative experimental half-lives for element-104 nuclei is not as close as for the predictions of Randrup et al. Mustafa and Ferguson (MUS78) have also predicted the disappearance of the second barrier for isotopes of element 104 with $A \geq 260$ using the asymmetric two-center shell model.

Recent alpha-decay energy data indicate that the 152-neutron sub-shell effect is probably weaker for element 104 than for element 102, as predicted by Randrup et al. In the Ghiorso SF half-life systematics a continuing strong 152-neutron sub-shell effect on the SF half-lives was assumed at element 104. Even if a small 152-neutron sub-shell effect is present at element 104, it is probably not strong enough to significantly alter the theoretical half-life predictions of Randrup et al.

Two SF activities might be due to odd-mass isotopes of element 104: (1) 20 SF events with a half-life of ~3 s in the reaction 93-MeV $^{18}O + ^{245}Cm$ might be due to an 8-per-cent SF branching in ^{259}Rf(3 s), as suggested by previous authors (DRU73, BEM81); and (2) a 3.8±0.8-s SF activity produced in the reaction 75-MeV $^{12}C + ^{249}Cf$ is consistent with a possible ~14-per-cent SF branch in ^{257}Rf(4.8±0.5 s, from alpha decay (GHI71)). If these possible assignments are correct, compared to the half-lives interpolated from the tentative assignments for the even-even isotopes of element 104, the odd-mass isotopes ^{259}Rf and ^{257}Rf would be hindered by respective factors of $\sim 2 \times 10^3$ and

~$4x10^3$ against SF. These tentative hindrance factors would be much lower than for odd-mass isotopes of lighter elements with even atomic number. This surprising effect can also be understood in terms of a disappearance of the second barrier at element 104 (RAN73). The lower limit of ~10^4 on the hindrance factor for ^{261}Rf(65 s) (GHI70c) may imply some extra stability associated with 157 neutrons as is known from the alpha decay of elements 101 to 106.

Future measurements of the SF-mass distributions for the possible element-104 SF activities found in this work will be of great importance. A measured asymmetric mass distribution from, for example, ^{260}Rf or ^{262}Rf would suggest that the fission process is perhaps adiabatic, as suggested by Mustafa and Ferguson (MUS78), i.e., the asymmetric two-center shell model applies during the fission and the mass distribution is correlated to the potential-energy surfaces between the second-saddle region and scission; a measured symmetric mass distribution would suggest that the distribution is determined by the distortion properties of the saddle points above the ground-state energy, as suggested by Möller (MÖL81, 72).

Although several new SF activities have been found in this work, some of which may be due to element 104, the 80-ms SF activity attributed by the Dubna group (DRU77) to ^{260}Rf was not observed in the reactions 80-MeV ^{15}N +^{249}Bk, 92-MeV ^{16}O +^{248}Cm, and 96-MeV ^{18}O +^{249}Cf. The measured cross-section upper limit for this activity in our reaction 80-MeV ^{15}N +^{249}Bk is 1/24 of the cross section measured by the Dubna group for the same reaction using 82-MeV ^{15}N ions; but the results of our experiments as well as the Dubna experiments agree on

the ^{256}Md production cross sections (NIT81). For the reactions 80-MeV ^{15}N +^{249}Bk and 92-MeV ^{16}O +^{248}Cm the cross-section upper limits for the 80-ms SF activity listed in Table 1 are also far below the calculated production cross sections for ^{260}Rf. And the JORPLE code used in making these calculations predicts other (HI,4n) maximum cross sections within a factor of three or better. Furthermore, the Dubna interpretation (DEM80) that the ~20-ms SF activity produced in the reaction 92-MeV ^{16}O +^{248}Cm is actually a mixture of the 13.7-ms fissioning isomer ^{242}Am and 80-ms ^{260}104 is shown to be highly improbable. This conclusion has been reached based on both comparisons of and absolute chi-square values for fits under the different assumptions and on the probable low upper limit for the formation cross section of the 13.7-ms ^{242f}Am (section IV.C.5.a.).

The large number of new SF activities which have been observed in this work confirms that SF is a very probable decay mode for many of the heaviest known nuclei. Future developments in on-line mass separators will hopefully make the task of assigning these SF activities easier and will also permit us to investigate the SF-decay properties of the heaviest elements, such as total kinetic energy, mass distributions, and neutron multiplicities. This will further deepen our understanding of nuclear matter at the extreme reaches of stability.

VI. Figure Captions

Figure 1: Folding chart either located inside the back cover of this thesis or sent to you in a mailing tube. It shows all of the SF activities which have been assigned or for which probable assignments have been suggested in publications to date, including this thesis (February, 1982). Both total half-lives and partial half-lives for SF are listed. For assignments which have not been proven, a single question mark following the half-life measurement indicates a probable assignment; two question marks indicate that insufficient evidence exists for making a definite isotopic assignment. In cases where a nuclide decays by electron capture to a daughter nuclide which is a SF activity, only the daughter nuclide is considered a SF activity on this chart. For example, SF events do arise from samples of ^{256}Md(77 min) nuclei. But since ^{256}Md is known to electron-capture decay to the SF activity ^{256}Fm(2.6 hr), the fission activity is associated with ^{256}Fm, not ^{256}Md.

Figure 2: SF half-life systematics for even-even nuclei extrapolated to atomic number 104 by Ghiorso (left, a) (GHI70a) and according to the experimental half-lives measured by the Dubna group (right, b) (FLE71, OGA74a) for presumed even-even nuclei with atomic number 104.

Figure 3: Recoil tape-transport system for investigation of short-lived SF activities with low SF background. The SF decays of the recoil nuclei transported by the tape are recorded by the mica as

diamond-shaped tracks. The tracks are shown on the mica insert of the figure to decrease in frequency with the time after production. Knowing the tape speed, this time is measured by the distance from the target along the mica.

Figure 4: Excitation functions for the short-lived components produced in the rotating-drum experiments for the reaction $^{15}N + ^{249}Bk$ (NIT81). The values in parentheses give the half-lives observed at each energy. Note that the error bars for these half-life measurements represent 90-per-cent confidence limits, not standard deviations. The cross sections in this figure are 7- to 8-per-cent lower than those quoted in reference NIT81 due to small corrections in the calculation of recoil ranges (see section II. Experimental Procedure).

Figure 5: Excitation function for the ~20-ms SF activity in the reaction $^{15}N + ^{249}Bk$, obtained from the tape experiments. The dashed curve is the excitation function calculated by the JORPLE code; the solid curve is meant to guide the eye through the points of the experimental excitation function.

Figure 6: Experimental (^{15}N,4n) reaction excitation functions. The dotted lines show the (^{15}N,4n) excitation functions calculated by the JORPLE code and normalized to the peak cross sections for each of the experimental excitation functions. Notice how each experimental excitation function is broader than calculated. a) $^{249}Cf(^{15}N,4n)^{260}Ha$, (GHI70b), b) $^{248}Cm(^{15}N,4n)^{259}Lr$ (ESK71),

c) $^{243}Am(^{15}N,4n)^{254}No$ (DON66).

Figure 7: Decay curve for the bombardment 75-MeV ^{12}C + ^{249}Cf. The 3.8-s component might be a ~14-per-cent SF branch in ^{257}Rf. The data also indicate that a 47-s or longer half-life component may be present; the assignment for this activity is completely unknown.

Figure 8: Decay curve for the reaction 89-MeV ^{18}O + ^{248}Cm. The 55-ms component might be due to ^{262}Rf. The 1.3-s component is completely unknown; but a SF or electron-capture branch in ^{262}Lr is a speculation for assignment of this SF activity.

Figure 9: Decay curve for the reaction 95-MeV ^{18}O + ^{248}Cm. The line represents the 1.6-s component only, which has not been identified. Addition of the background to the 1.6-s component line will give a resultant curve which will fit the experimental points better. A SF or electron-capture branch in ^{262}Lr is a speculation for assignment of this activity.

Figure 10: Excitation functions for the SF activities observed in the reaction ^{18}O + ^{248}Cm. The number listed for each point indicates the half-life measured for that energy and cross section. The cross sections for ^{256}Fm have been determined by measuring the SF decay rate from aluminum catcher foils with the aid of a gas-proportional counter. The ~50-ms SF activity might be ^{262}Rf. The ~20-ms SF activity could not be ^{260}Rf unless the cross section is enhanced by

a factor of ~50; its assignment is unknown. The ~1.3-s SF activity is completely unknown; but a SF or electron-capture branch in ^{262}Lr is a speculation for assignment of this SF activity.

Figure 11: Decay curve for the bombardment 70-MeV ^{13}C + ^{249}Bk. A possible assignment for the 4.5-s component is a ~1-per-cent electron-capture branch in ^{258}Lr (4.35 s, from alpha-decay measurements (BEM76)) to the SF activity ^{258}No (1.2 ms).

Figure 12: Decay curve for the bombardment 95-MeV ^{16}O + ^{246}Cm. A possible assignment for the ~13-ms SF activity is ^{258}Rf. More realistic estimates for the cross-section error bars would be 10^{+10}_{-5} nb, including uncertainty in the integrated beam flux.

Figure 13: Decay curve for the bombardment 80-MeV ^{15}N + ^{249}Bk. From this data a cross-section upper limit of 0.3±0.4 nb was established for the 80-ms SF activity, claimed by the Dubna group for the discovery of element 104 and due to the isotope ^{260}Rf. The ~20-ms SF activity which is observed might be ^{260}Rf.

Figure 14: Decay curve for the bombardment 92-MeV ^{16}O + ^{248}Cm. From this data a cross-section upper limit of 0.4±0.2 nb was established for the 80-ms SF activity, claimed by the Dubna group for the discovery of element 104 and due to the isotope ^{260}Rf. The ~21-ms SF activity which is observed might be ^{260}Rf.

Figure 15: Decay curve for the bombardment 96-MeV ^{18}O +^{249}Cf. From this data a cross-section upper limit of 0.0±0.5 nb was established for the 80-ms SF activity, claimed by the Dubna group for the discovery of element 104 and due to the isotope ^{260}Rf. The ~19-ms SF activity which is observed is unknown because its 9-nb production cross section is probably too high for ^{260}Rf.

Figure 16: Decay curve for the reaction 109-MeV ^{18}O +^{248}Cm. The ~22-ms SF activity is unknown, but could not be ^{260}Rf unless its production cross section is enhanced by a factor of ~50 due to an unknown mechanism. Therefore, this SF activity is more likely due to a nuclide with atomic number less than 104. It presents a possible inconsistency in the assignment of ^{260}Rf to a ~20-ms SF activity unless there are at least two SF activities with half-lives between 14 and 24 ms.

Figure 17: Excitation function for production of the ~50-ms SF activity in the reaction ^{18}O +^{248}Cm. This SF activity might be due to ^{262}Rf. The long-dashed curve is the excitation function calculated by the JORPLE code. The solid line and the extrapolated short-dashed curve are meant to guide the eye through the experimental points.

Figure 18: Calculated partial half-lives for SF of even-even nuclei by Randrup et al. (RAN76). These calculations were made by adjusting a one-parameter inertial mass function to give half-lives that fit experimental data for nuclei with atomic numbers less than or equal

to 102. The calculations were then extrapolated to nuclei with atomic numbers 104 and higher. None of the experimental points for either even-even (solid squares) or odd-mass (solid triangles) rutherfordium (element 104) nuclei are known with certainty. But the half-lives suggested by several experiments for element-104 nuclei in this work and also the work of Ter-Akopyan et al. (TER75) (^{254}Rf (0.5 ms)); Münzinger et al. (MÜN81) (^{255}Rf (1.4 s, 45±20-per-cent SF)), (MÜN80) (^{256}Rf (8 ms)); Ghiorso et al. (GHI69, NUR74) (^{258}Rf (13 ms)); Druin et al. (DRU73) (^{259}Rf (3 s, 7-per-cent SF)); and Ghiorso et al. (GHI70c) (^{261}Rf (65 s, $\leq$10-per-cent SF)) have been included for comparison with the theory. Since the possible 1.8-s SF activity ^{253}Rf, based on the unpublished work of Oganessian et al. (OGA75) quoted in reference TER75 (see Figure 1), was not included by Oganessian (OGA80) in a recent figure showing SF half-lives for element-104 nuclei, it has also not been included in this figure. The insert at the lower left shows a comparison between calculated and experimental half-lives for fission isomers.

Figure 19: Alpha-decay energy versus neutron-number systematics. The abrupt discontinuities in alpha-decay energies are due to the 152-neutron sub-shell effect on the parent and/or daughter nuclei.

Figure 20: The shell effect, defined as the mass minus the Myers droplet mass (MYE77), is plotted for nobelium (element 102) and rutherfordium (element 104) nuclei. The square points represent experimentally-measured masses quoted from the Table of Isotopes

(TOI78). Circled "x" points represent masses determined from alpha-decay energies of parent, daughter, granddaughter, etc., nuclei down to an experimentally-known mass. Solid dots represent masses (TOI78) determined from systematics plots, as discussed in reference WAP77. Triangle points represent masses derived from the alpha-decay energy of the parent and the daughter mass determined from systematics plots (TOI78). Ground-to-ground state transitions have been assumed in determining ground-state masses from the maximum alpha-decay energies; in cases with possible isomers in the parent and/or daughter nuclei, the masses derived in this way would be incorrect. The solid and dashed lines are meant to guide the eye through the points. An increase in shell effect of ~0.75 MeV centered around neutron-number 152 is clearly visible in nobelium nuclei. For rutherfordium nuclei, although the masses are less certain, the effect appears to be much weaker, if it is present at all. Connecting any set of points for rutherfordium nuclei, the 152-neutron sub-shell effect appears to be less than or equal to 0.3 MeV.

Figure 21: Calculated fission barriers for heavy isotopes of fermium (element 100) (RAN73). Beyond ^{258}Fm the second peak and second minimum are below the ground state in energy, leading to a drastic decrease in the SF half-lives.

Figure 22: Calculated fission barriers for ^{257}Fm (a) and $^{263}106$ (b) (RAN73). The two upper barriers in each figure correspond to having the odd neutron in the 9/2+ and 3/2+ orbitals while the lower curve

represents the hypothetical even-even system as obtained by interpolation between ^{256}Fm and ^{258}Fm (a) or between ^{262}106 and ^{264}106 (b). In first order the barrier for the odd-mass nucleus is obtained by raising the entire potential barrier for the even-even nucleus by a certain "specialization energy." Note that when the second barrier is absent, as for ^{262}106 (b), the increase in thickness and height of the barrier caused by the odd neutron is less than for ^{256}Fm with a double-humped fission barrier (a), resulting in a lower hindrance factor against SF for ^{263}106 than for ^{257}Fm.

VII. Figures

Figure 1 is a large chart either sent to you in a mailing tube or folded inside the back cover of this thesis.

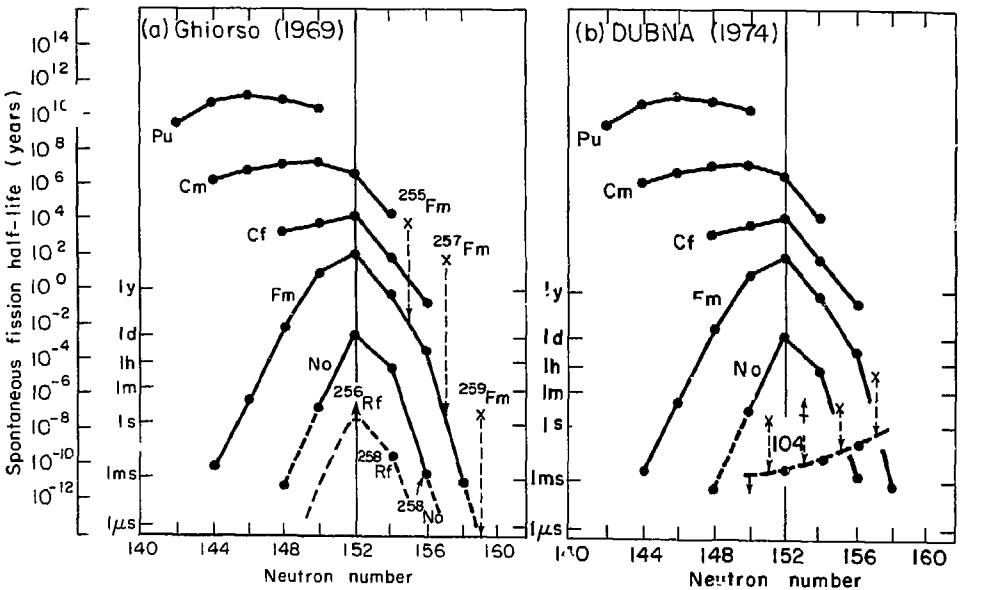

a b XBL759-3852A

Figure 2

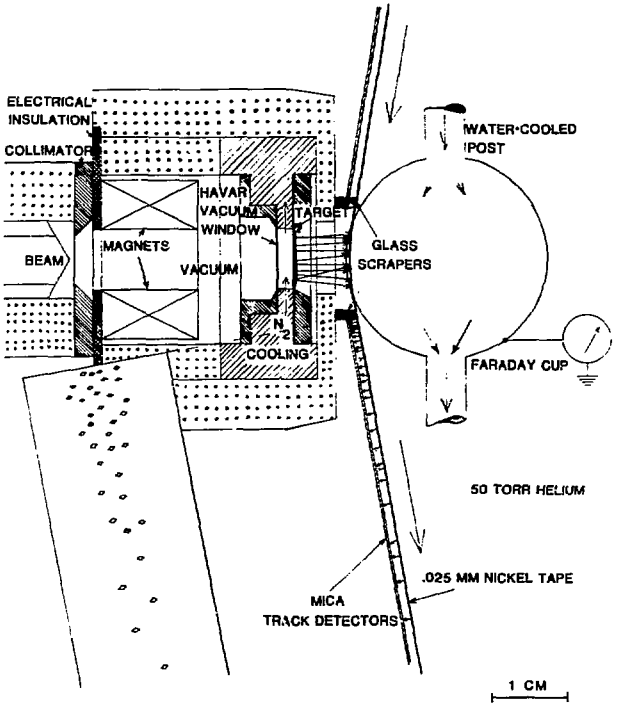
ELECTRICAL INSULATION
COLLIMATOR
BEAM
MAGNETS
HAVAR VACUUM WINDOW
VACUUM
TARGET
N 2
COOLING
GLASS SCRAPERS
WATER-COOLED POST
FARADAY CUP
50 TORR HELIUM
.025 MM NICKEL TAPE
MICA TRACK DETECTORS
1 CM

Figure 3

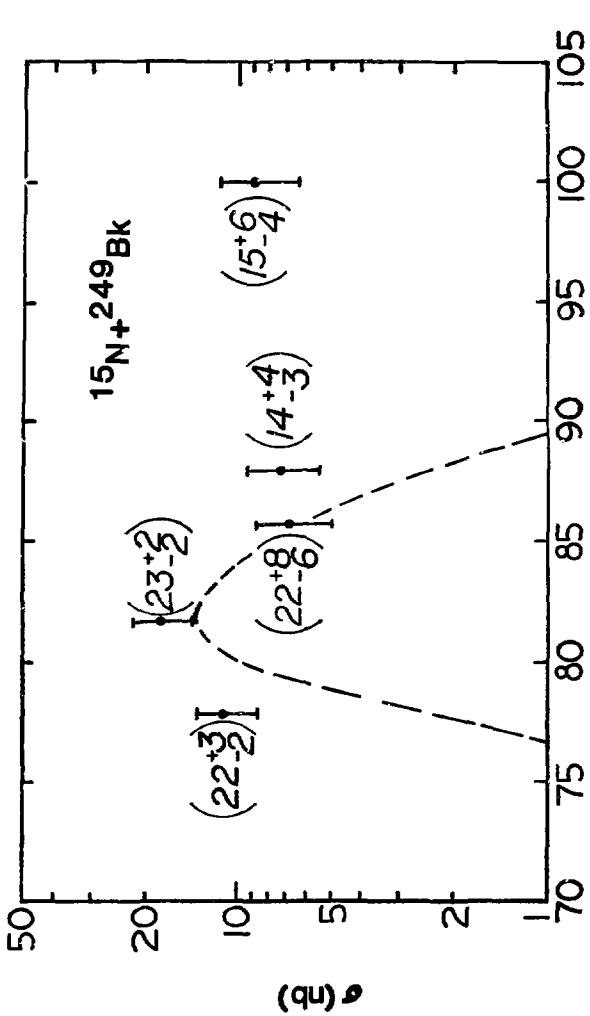
$^{15}N+^{249}Bk$
(22^{+3}_{-2})
(23^{+2}_{-2})
(22^{+8}_{-6})
(14^{+4}_{-3})
(15^{+6}_{-4})
σ (nb)
50
20
10
5
2
1
70
75
80
85
90
95
100
105
^{15}N energy (MeV)

Figure 4

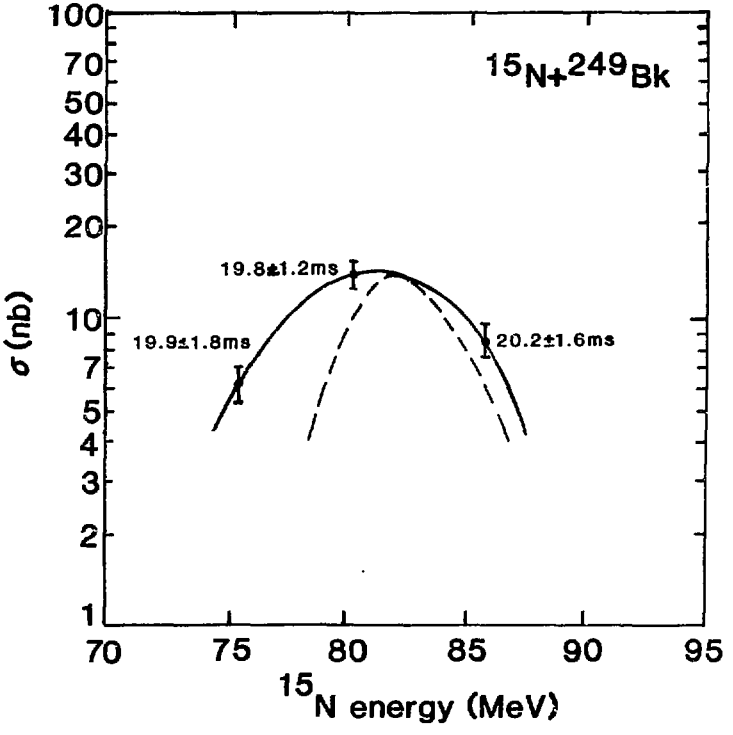
$^{15}N+^{249}Bk$
19.8±1.2ms
19.9±1.8ms
20.2±1.6ms
σ (nb)
100
70
50
40
30
20
10
7
5
4
3
2
1
70
75
80
85
90
95
^{15}N energy (MeV)

Figure 5

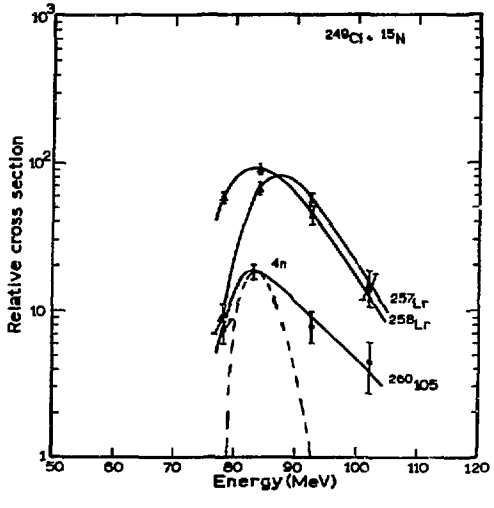
$^{249}Cf + ^{15}N$
Relative cross section
Energy (MeV)
4n
^{257}Lr
^{258}Lr
$^{260}105$

a

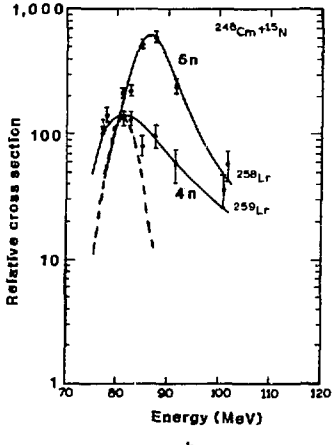
$^{248}Cm + ^{15}N$
6n
4n
^{258}Lr
^{259}Lr
Relative cross section
Energy (MeV)

b

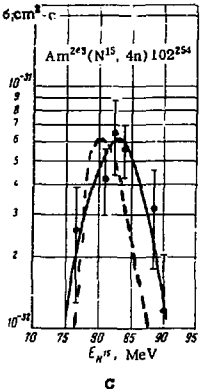
$Am^{243}(N^{15}, 4n)\,102^{254}$
$E_{N^{15}}$, MeV

c

Figure 6

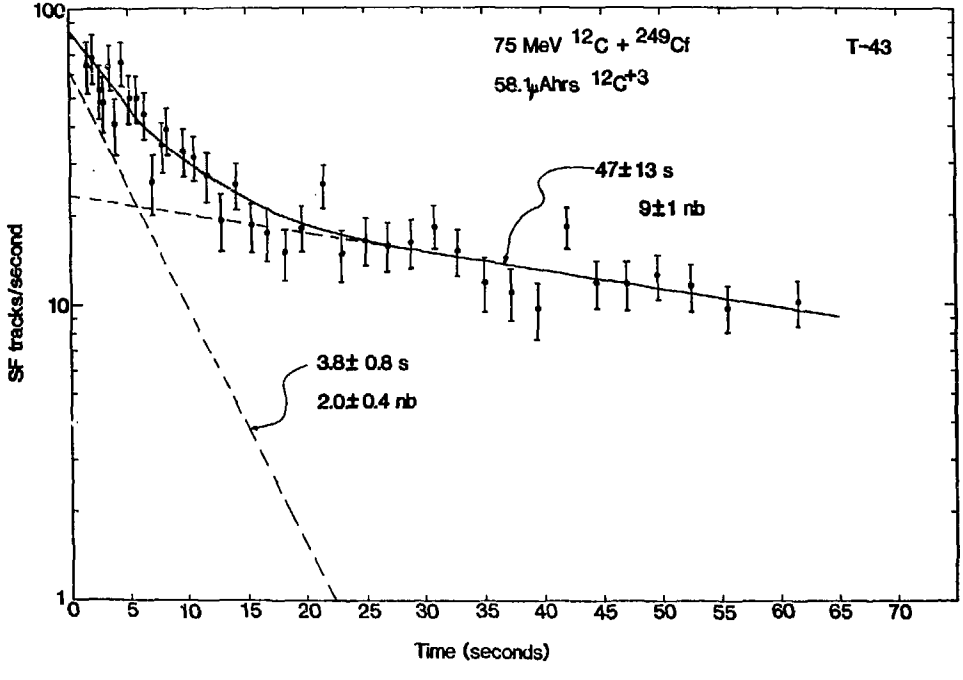
75 MeV ^{12}C + ^{249}Cf
T-43
58.1 μAhrs $^{12}C^{+3}$
47± 13 s
9±1 nb
3.8± 0.8 s
2.0± 0.4 nb
SF tracks/second
Time (seconds)
100
10
1
0
5
10
15
20
25
30
35
40
45
50
55
60
65
70

Figure 7

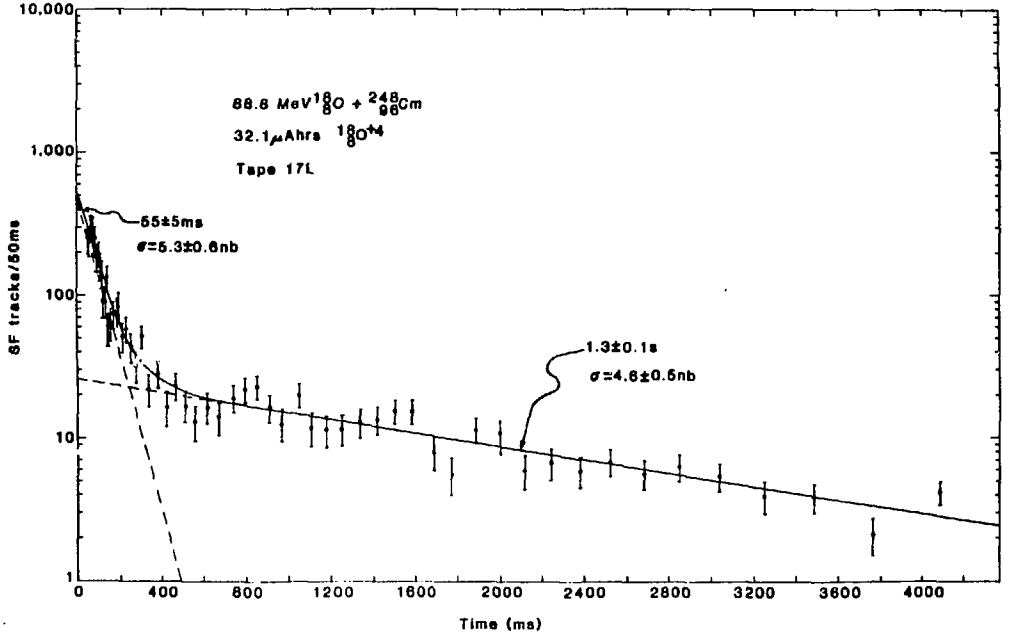
88.8 MeV $^{18}_{8}O$ + $^{248}_{96}Cm$
32.1 μAhrs $^{18}_{8}O^{+4}$
Tape 17L
55±5ms
σ=5.3±0.6nb
1.3±0.1s
σ=4.6±0.5nb
SF tracks/50ms
Time (ms)
10,000
1,000
100
10
1
0
400
800
1200
1600
2000
2400
2800
3200
3600
4000

Figure 8

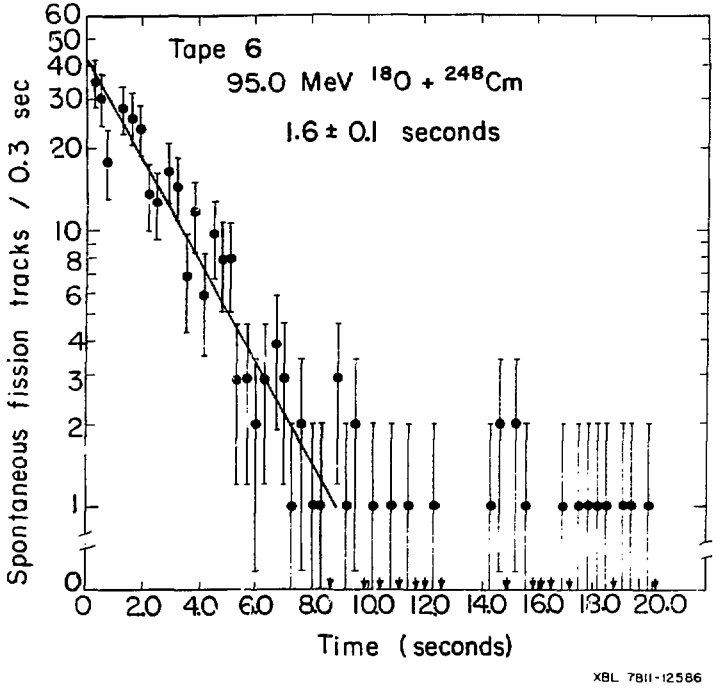
Tape 6
95.0 MeV ^{18}O + ^{248}Cm
1.6 ± 0.1 seconds
Spontaneous fission tracks / 0.3 sec
Time (seconds)
60
50
40
30
20
10
8
6
4
3
2
1
0
0
2.0
4.0
6.0
8.0
10.0
12.0
14.0
16.0
18.0
20.0
XBL 7811-12586

Figure 9

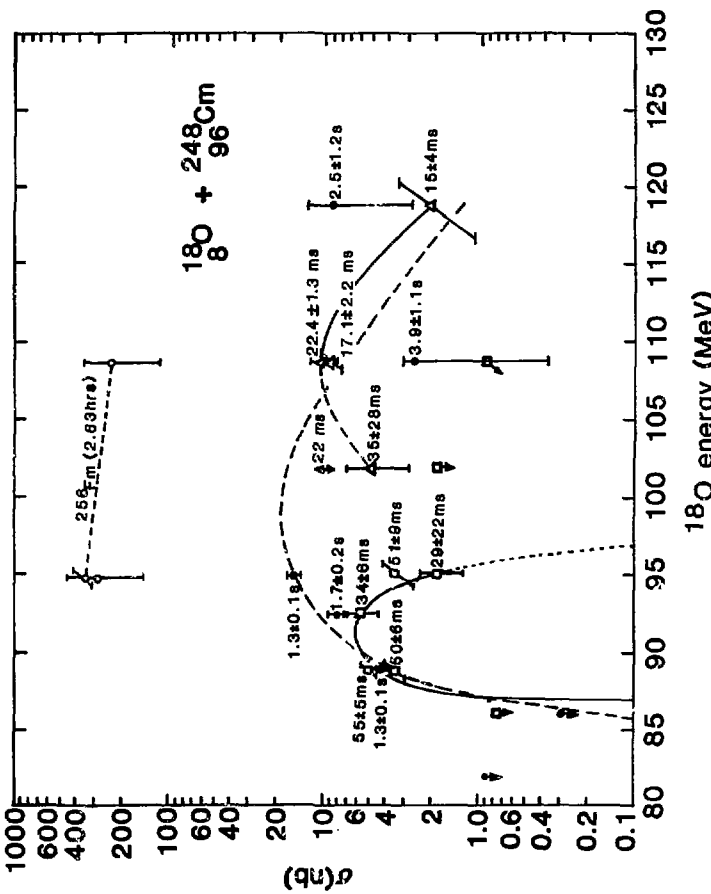
$^{18}_{8}O + ^{248}_{96}Cm$
^{256}Fm (2.63hrs)
1.3±0.1s
11.7±0.2s
134±6ms
55±5ms
1.3±0.1s
60±8ms
61±8ms
22 ms
35±28ms
20±22ms
22.4±1.3 ms
17.1±2.2 ms
3.9±1.1s
2.5±1.2s
15±4ms
σ(nb)
^{18}O energy (MeV)

Figure 10

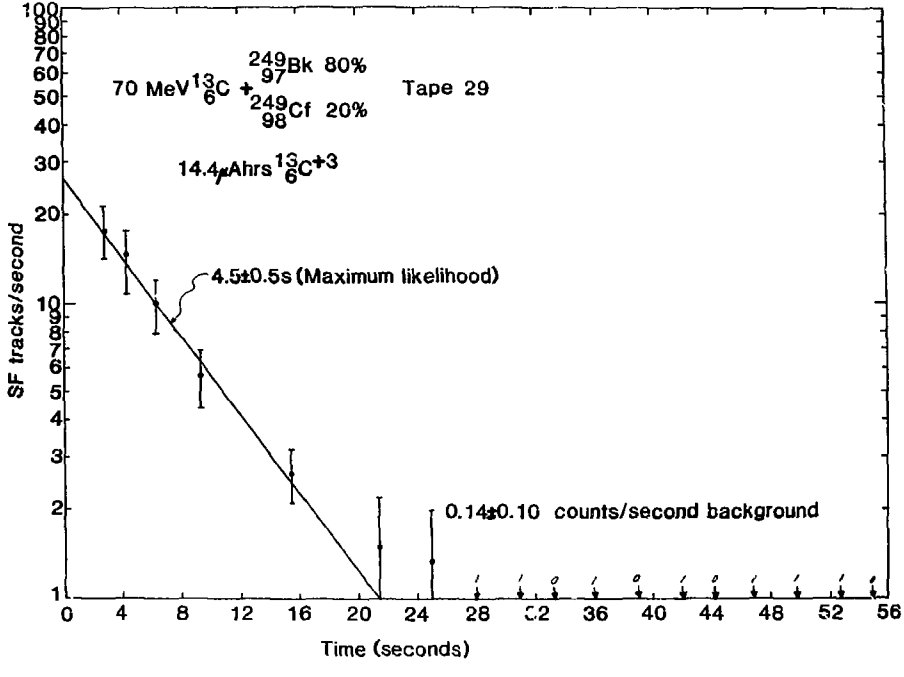
70 MeV $^{13}_{6}C$ + $^{249}_{97}Bk$ 80% $^{249}_{98}Cf$ 20%
Tape 29
14.4μAhrs $^{13}_{6}C^{+3}$
4.5±0.5s (Maximum likelihood)
0.14±0.10 counts/second background
SF tracks/second
Time (seconds)

Figure 11

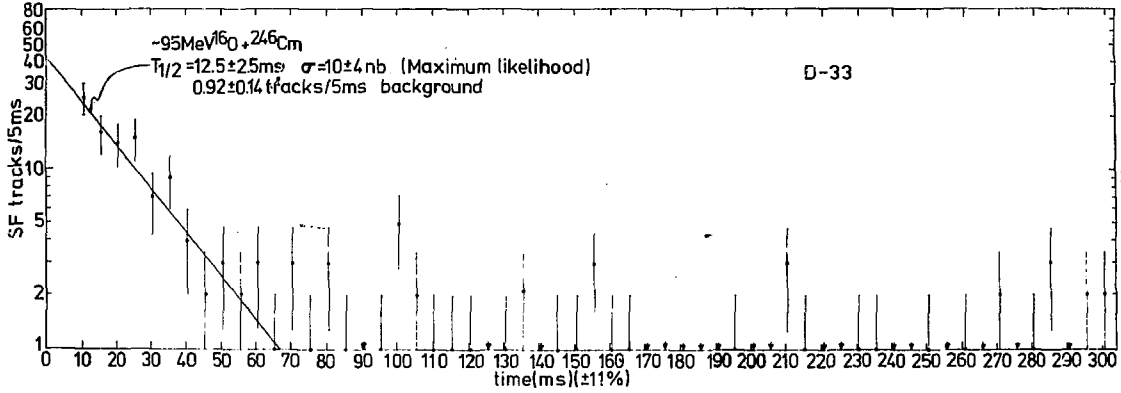
~95MeV 16O + 246Cm
T1/2 =12.5±2.5ms σ=10±4 nb (Maximum likelihood)
0.92±0.14 tracks/5ms background
D-33
SF tracks/5ms
time(ms)(±11%)
105

Figure 12

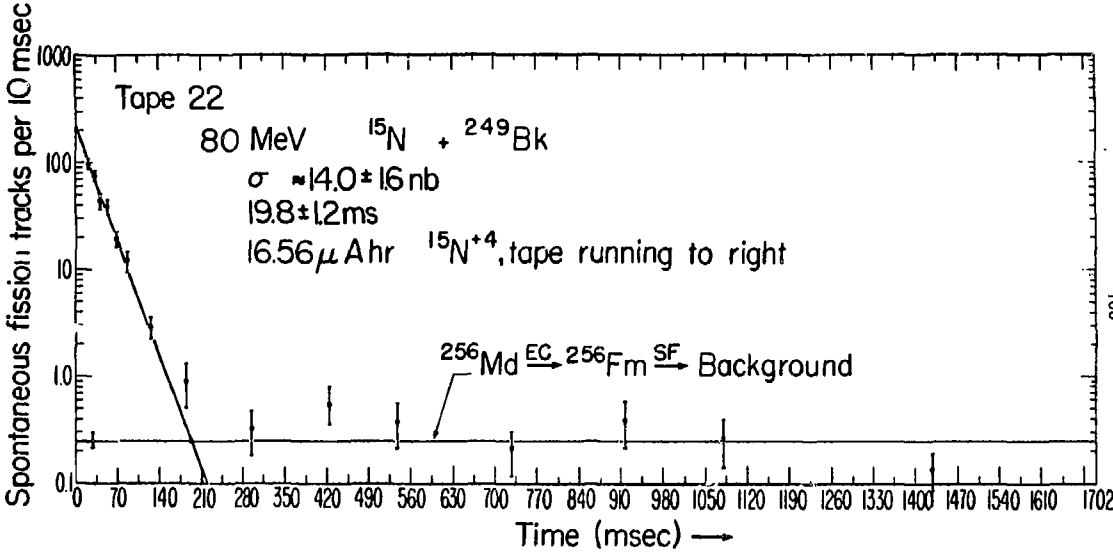
Tape 22
80 MeV ^{15}N + ^{249}Bk
σ ≈14.0±1.6 nb
19.8±1.2 ms
16.56 μA hr $^{15}N^{+4}$, tape running to right
$^{256}Md \xrightarrow{EC} {}^{256}Fm \xrightarrow{SF}$ Background
Spontaneous fission tracks per 10 msec
Time (msec) →
1000
100
10
1.0
0.1
0 70 140 210 280 350 420 490 560 630 700 770 840 910 980 1050 1120 1190 1260 1330 1400 1470 1540 1610 1702

Figure 13

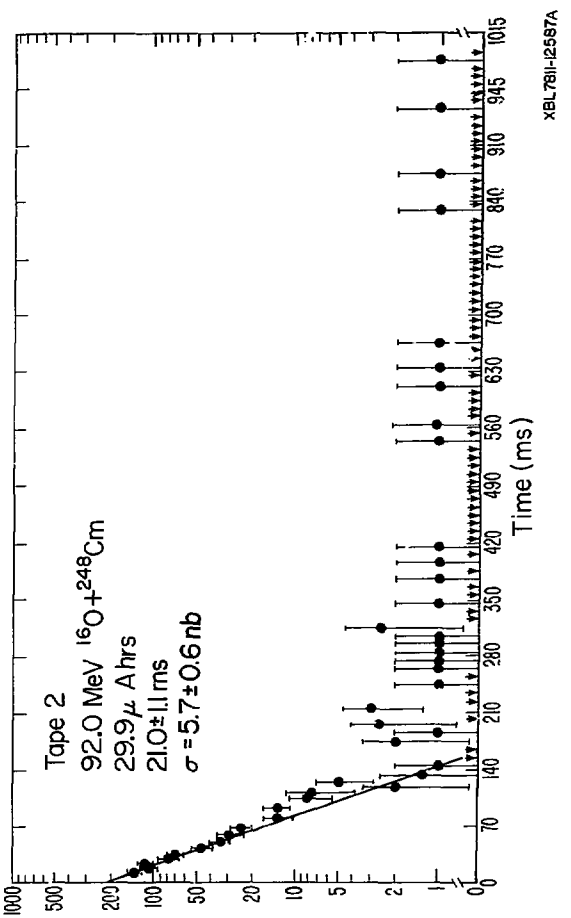
Tape 2
92.0 MeV $^{16}O+^{248}Cm$
29.9 μ A hrs
21.0±1.1 ms
σ = 5.7±0.6 nb
Spontaneous fission tracks/10 msec
Time (ms)
1000
500
200
100
50
20
10
5
2
1
0
0
70
140
210
280
350
420
490
560
630
700
770
840
910
945
1015
XBL781I-12587A

Figure 14

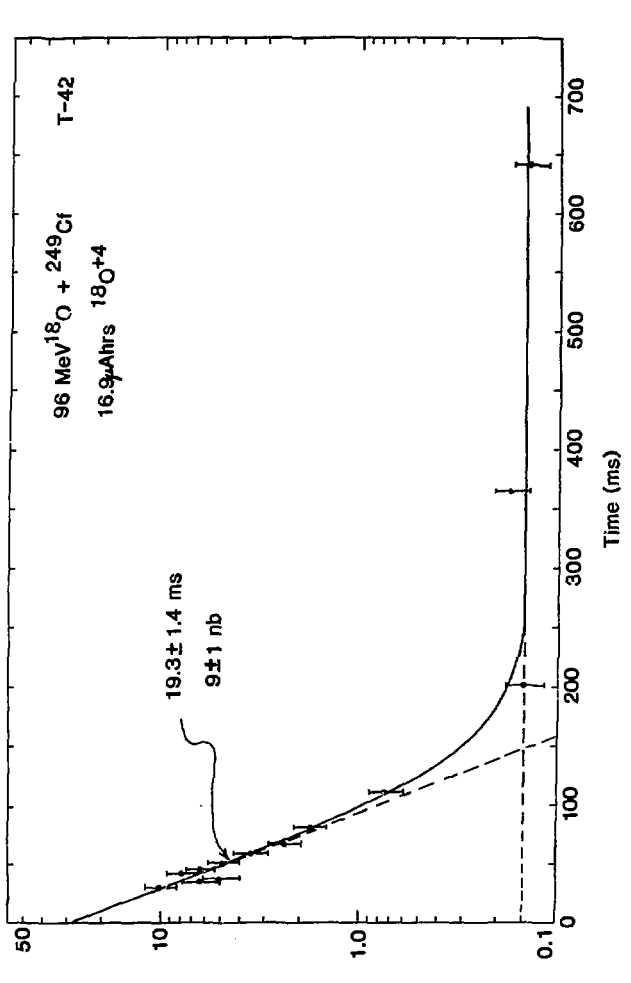
96 MeV ^{18}O + ^{249}Cf T-42
16.9 μAhrs $^{18}O^{+4}$
19.3 ± 1.4 ms
9 ± 1 nb
SF tracks/millisecond
Time (ms)
50
10
1.0
0.1
0
100
200
300
400
500
600
700

Figure 15

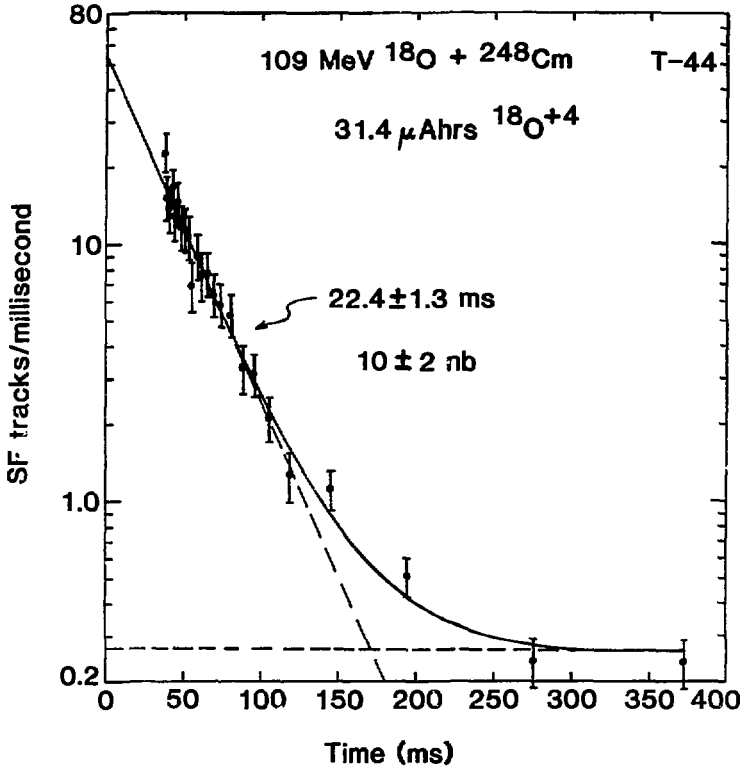
109 MeV 18O + 248Cm
T-44
31.4 μAhrs 18O+4
22.4±1.3 ms
10 ± 2 nb
SF tracks/millisecond
Time (ms)
80
10
1.0
0.2
0
50
100
150
200
250
300
350
400

Figure 16

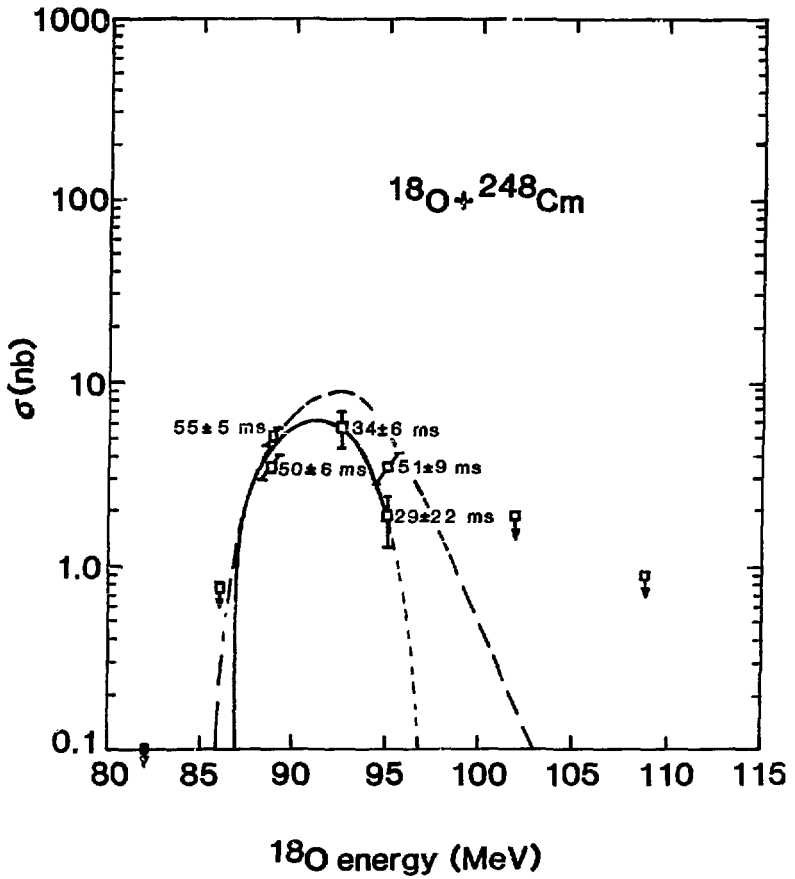
1000
100
10
1.0
0.1
σ(nb)
$^{18}O + ^{248}Cm$
55±5 ms
50±6 ms
34±6 ms
51±9 ms
29±22 ms
80
85
90
95
100
105
110
115
^{18}O energy (MeV)

Figure 17

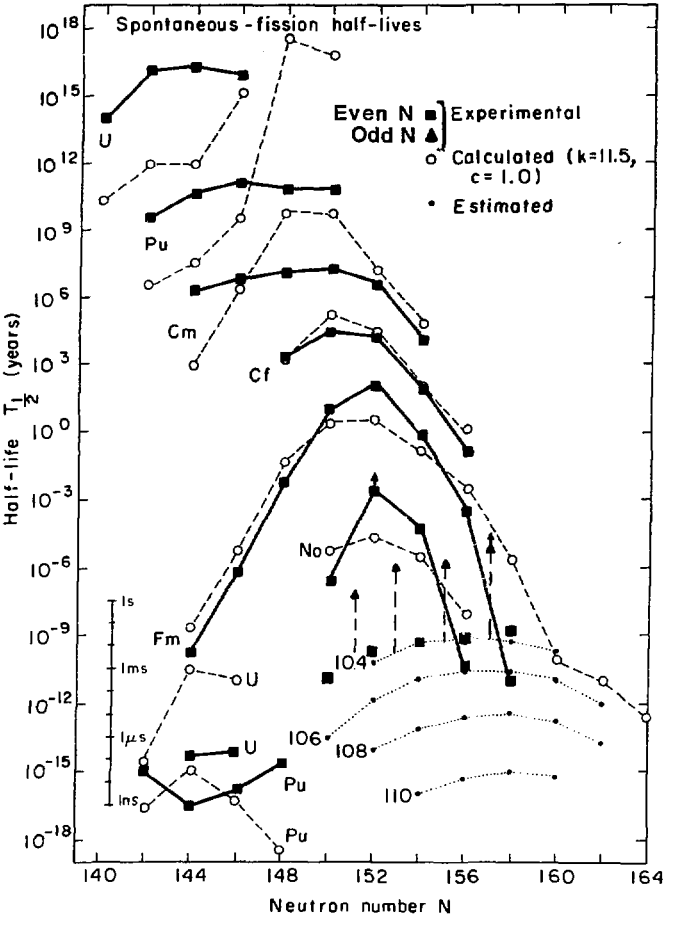
Spontaneous-fission half-lives
Even N ■ Experimental
Odd N ▲
○ Calculated (k=11.5, c=1.0)
• Estimated
U
Pu
Cm
Cf
Fm
No
104
106
108
110
Is
Ims
Iμs
Ins
Half-life $T_{\frac{1}{2}}$ (years)
Neutron number N

Figure 18

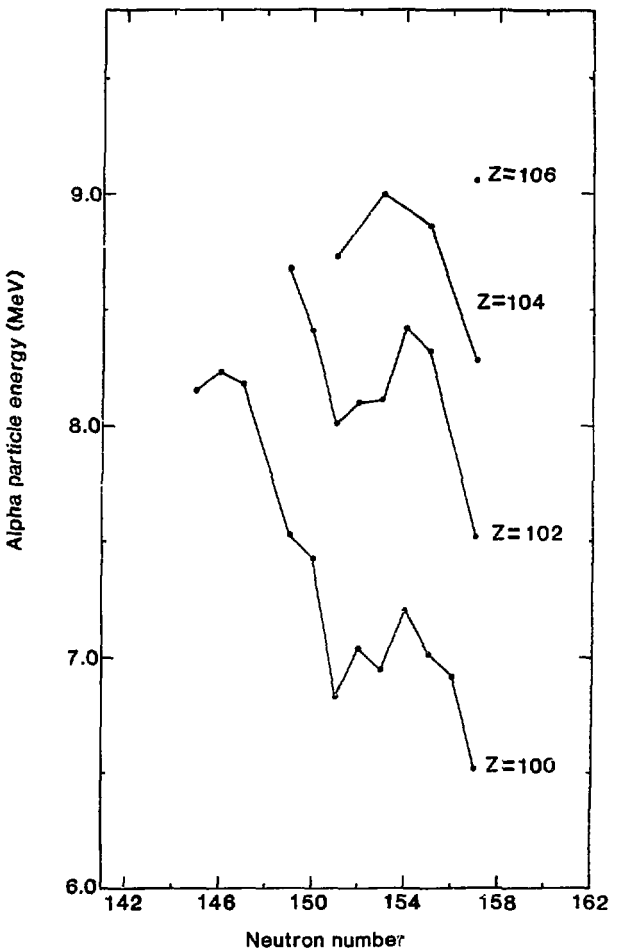
Alpha particle energy (MeV)
9.0
8.0
7.0
6.0
142
146
150
154
158
162
Neutron number
Z=106
Z=104
Z=102
Z=100

Figure 19

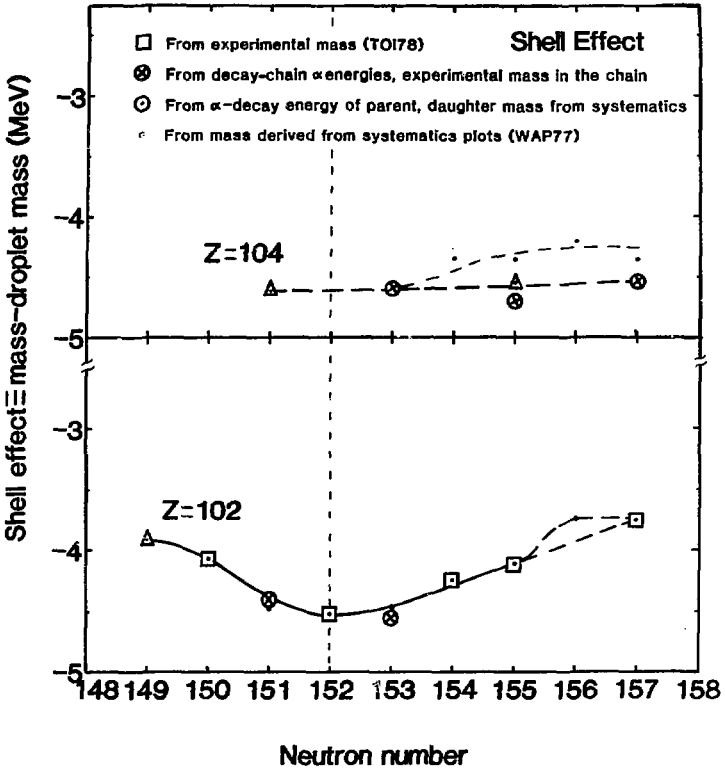
From experimental mass (TOI78)
Shell Effect
From decay-chain α energies, experimental mass in the chain
From α-decay energy of parent, daughter mass from systematics
From mass derived from systematics plots (WAP77)
Z=104
Z=102
Shell effect≡mass-droplet mass (MeV)
-3
-4
-5
148 149 150 151 152 153 154 155 156 157 158
Neutron number

Figure 20

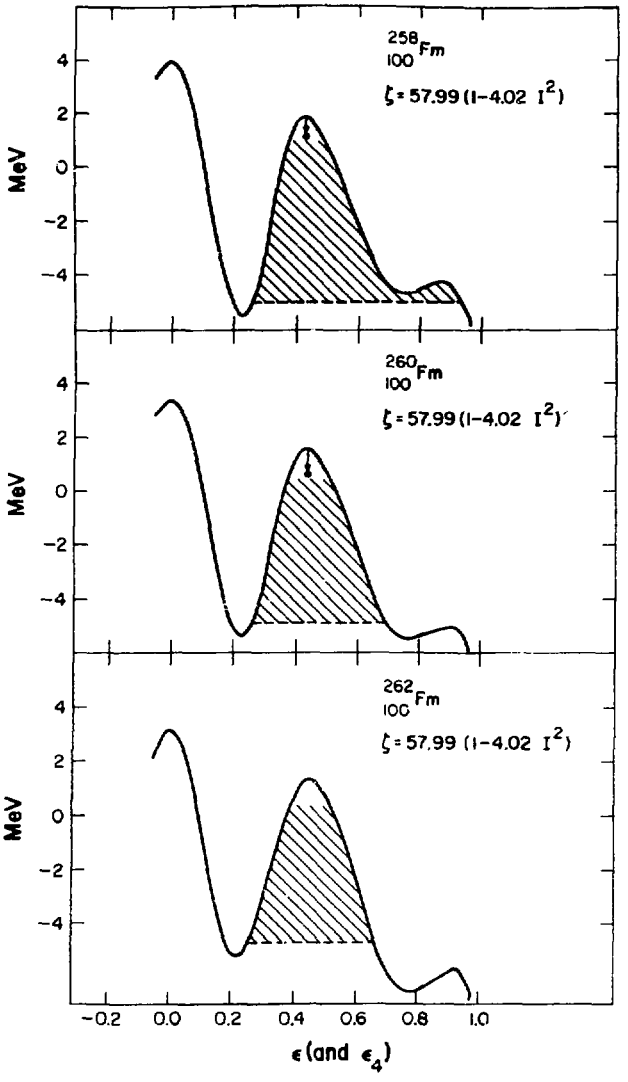
$^{258}_{100}Fm$
$\zeta = 57.99(1-4.02\ I^2)$
$^{260}_{100}Fm$
$\zeta = 57.99(1-4.02\ I^2)$
$^{262}_{100}Fm$
$\zeta = 57.99\ (1-4.02\ I^2)$
MeV
4
2
0
-2
-4
-0.2
0.0
0.2
0.4
0.6
0.8
1.0
ϵ (and ϵ_4)

Figure 21

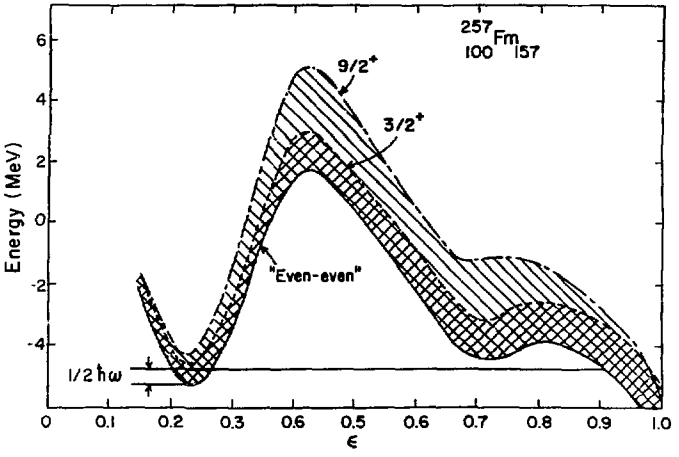
257 Fm 100 157
9/2+
3/2+
"Even-even"
1/2 ħω
Energy (MeV)
ε

a

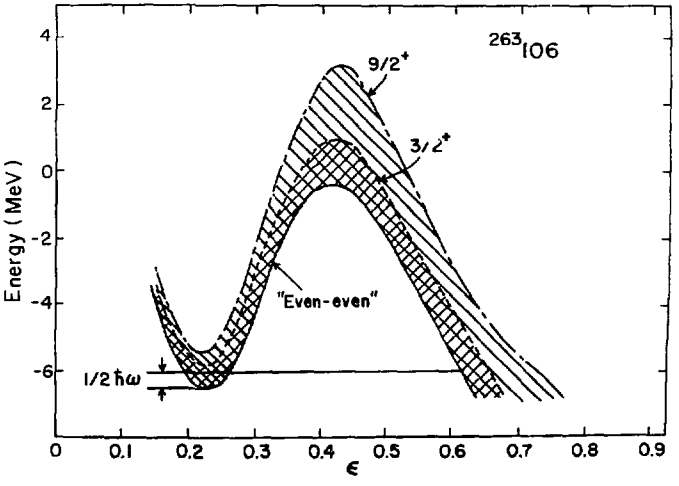
263 106
9/2+
3/2+
"Even-even"
1/2 ħω
Energy (MeV)
ε

Figure 22

b

VIII. Appendix

VIII.A. The JORPLE Code for Calculation of (HI,xn) Cross Sections and Comparison With Experimental Cross Sections

The JORPLE code is an indispensable tool in considering possible assignments for the new SF activities of Table 1. Comparisons of the experimental cross sections with the cross sections calculated by the JORPLE code can be made to see if the SF activities might be neutron-evaporation residues. The code uses a Jackson-Sikkeland-type model for predicting cross sections of compound-nuclear reactions followed by neutron evaporation (ALO72, 73; RAS71; SIK). It makes use of an empirical formula of Sikkeland et al. (SIK68) for the neutron-to-fission width ratio Γ_n/Γ_f to account for competition between fission and neutron emission. Other adjustable parameters include the nuclear radius parameter r_0, the diffuseness parameter D, and the nuclear temperature T. The JORPLE-code calculations for the maximum cross sections with respect to bombarding energy for the evaporation of four neutrons have been compared to extensive experimental cross-section data for heavy ions from ^{12}C up to ^{18}O bombarding actinide targets. With the parameters r_0=1.25 fermis, D=0.50 fermis, and T=0.95 MeV the calculations agree within a factor of three or better compared to experimental values. Certain exceptions among neutron-deficient nuclei have been noticed, however. Williams found that the JORPLE code overestimates the cross sections for some neutron-deficient isotopes in ^{10}B- to ^{12}C-induced reactions (WIL78, 79), and that a change in the adjustable parameters, especially Γ_n/Γ_f, would be needed to fit the

cross sections. Borggreen et al. (BOR70) noticed a similar overestimation of the cross sections for the production of neutron-deficient neptunium nuclei in the reaction 114-MeV $^{22}Ne + ^{209}Bi$.

The JORPLE code also does reasonably well in predicting the energies at which the excitation functions for neutron-evaporation products reach their maximum production cross sections, although discrepancies of up to ±3 MeV between experimental and calculated maxima have been observed for some carbon- and ^{18}O-induced reactions (LEI77) as well as one case with ^{15}N ions (see Figure 6c, DON66) bombarding actinide targets.

The JORPLE code does not predict the shapes of (HI,4n) reaction excitation functions as well as the maximum cross sections or the bombarding energies at the maxima, however. Figures 6a-c show a comparison of several experimental (^{15}N,4n) excitation functions (GHI70b, ESK71, DON66) with those calculated by the JORPLE code. In order to compare the excitation functions widths easily, the calculated excitation functions have been normalized to the peaks of the experimental ones. In every case the experimental excitation function is broader than calculated by the JORPLE code, and usually both on the low- and high-energy sides of the peak. These data indicate a weakness in the JORPLE code in predicting the shapes of the energy dependence of the cross sections. The fact that the shapes of excitation functions are not predicted well by the JORPLE code is important in discussing the excitation function for the ~20-ms SF activity in the reaction $^{15}N + ^{249}Bk$ in section IV.C.5.b.

VIII.B. Slight Corrections to the Existing Formulas for the Fraction of Activity Escaping a Target

On page 343 of reference ALE68 formulas are presented for the fraction F_F of activity escaping a target of thickness W if the recoil range is R_0 and the straggling parameter is ρ; $1 - F_F$ represents the fraction remaining in the target. The following formulas are nearly identical to those in reference ALE68, i.e., please note that the absolute value of y should be used in equation 2. Without this the formula would be incorrect for $W>R_0$. Also in the older reference WIN61 the equation analogous to equation 2 is incorrect.

$$1 - F_F = \frac{\sqrt{2}\, R_0 \rho}{W} \left[f\left(\frac{R_0 - W}{\sqrt{2}\, R_0 \rho}\right) - 2\, f\left(\frac{1}{\sqrt{2}\, \rho}\right) + f\left(\frac{R_0 + W}{\sqrt{2}\, R_0 \rho}\right) \right] \qquad (1)$$

$$\text{with} \quad f(y) = \frac{1}{2\sqrt{\pi}} \exp(-y^2) + 1/2\, |y|\, I(y) \qquad (2)$$

$$\text{and } I(y) \text{ is the error function} \quad I(y) = \frac{2}{\sqrt{\pi}} \int_0^y \exp(-u^2)\, du \qquad .(3)$$

For compound-nucleus recoils R_0 may be determined from the recoil energy using the Northcliffe and Schilling range tables (NOR70). The straggling parameter $\rho = \sqrt{\rho_s^2 + \rho_n^2}$ includes only two contributions from stopping in the target ρ_s and from neutron boil-off ρ_n if the

target foil is uniform in thickness. The formulas for ρ_s and ρ_n are given in reference WIN61. The fraction of activity escaping the target can then be calculated according to equation (1).

VIII.C. Detailed Arguments for Tentatively Assigning Three 5-s SF Activities

In section IV.C.1. three 5-s SF activities were discussed. Here in the appendix detailed cross-section arguments are made to suggest what their identities might be.

A possible assignment of the 4.5±0.5-s SF activity produced in the reaction 70-MeV ^{13}C +^{249}Bk/^{249}Cf is a ~1-per-cent electron-capture branch in ^{258}Lr(4.4±0.6 s) to the probable spontaneously-fissioning nucleus ^{258}No(1.2 ms). This possible assignment is suggested based on the closeness of the measured half-lives for SF (4.5±0.5 s) and for alpha decay (4.4±0.6 s, BEM76) of ^{258}Lr. The ~1-per-cent value is obtained from the ratio of the measured ~7-nb cross section for SF to the calculated total cross section of ~1 μb to produce ^{258}Lr from the ^{249}Bk portion of the target in the $^{249}Bk(^{13}C,4n)^{258}Lr$ reaction. Unpublished data from Eskola et al. (ESK81) show that the cross section for the $^{249}Cf(^{13}C,p3n)^{258}Lr$ reaction is 50-per-cent larger than the cross section for the $^{249}Cf(^{13}C,3n)^{259}Rf$ reaction with 70-MeV ^{13}C ions; but the calculated cross section for the $^{249}Cf(^{13}C,3n)^{259}Rf$ reaction is only 2 per cent of the $^{249}Bk(^{13}C,4n)^{258}Lr$ reaction cross section. On this basis and considering the 20-per-cent ^{249}Cf abundance in the target, the contribution to ^{258}Lr production is probably mainly from the ^{249}Bk portion of the target. The contribution to ^{258}Lr production from the reaction $^{249}Cf(^{13}C,p3n)^{258}Lr$ can then be neglected. At this low bombarding energy of 70 MeV, the excitation energy is insufficient to evaporate five neutrons in the reaction $^{249}Cf(^{13}C,5n)^{257}Rf$, accord-

ing to JORPLE code calculations.

According to Bemis et al. (BEM73) the production cross section for ^{257}Rf and observation of subsequent alpha decay in the reaction 73-MeV $^{12}C + ^{249}Cf$ is ~12 nb. Data from Eskola et al. (ESK71) for the same reaction $^{12}C + ^{249}Cf$ indicate that ^{257}Rf and ^{258}Lr are produced with roughly equal maximum cross sections, based on assumptions that these nuclei undergo alpha decay only. The latter assumptions are probably good approximations based on the following data. (1) The measured cross section is 12 nb for production of ^{257}Rf and observation of subsequent alpha decay with a 4.8-s half-life; for SF with the same half-life the measured cross section is only ~2 nb. (2) An upper limit of 1 per cent can be set on the electron-capture branch of ^{258}Lr. A maximum ~12-nb total production cross section for ^{258}Lr in the reaction $^{12}C + ^{249}Cf$ would imply a cross section of not more than 0.1 nb for SF due to ^{258}Lr production with 75-MeV ^{12}C ions if ^{258}Lr has a ~1-per-cent electron-capture branch to the spontaneously-fissioning nucleus ^{258}No(1.2 ms). Since the experimental cross section of ~2 nb for SF is much greater than 0.1 nb, the conclusion is that the SF events are probably not due to ^{258}Lr. If the SF events are due to ^{257}Rf, however, comparing the ~2-nb cross section for SF with the ~12-nb cross section measured for alpha decay, the SF branch would be ~14 per cent.

From the preceding discussion ^{258}Lr and ^{257}Rf may give rise to ~5-s SF activities. A 5.5-s SF activity (see section IV.B.3.) was produced in the reaction 98-MeV ^{18}O + (82-88% ^{249}Bk/12-18% ^{249}Cf). Since ^{258}Lr and ^{257}Rf would be produced in the unlikely nuclear reactions $^{249}Bk(^{18}O,\alpha 5n)^{258}Lr$ and $^{249}Bk(^{18}O,p9n)^{257}Rf$, $^{249}Cf(^{18}O,\alpha 6n)^{257}Rf$ and

$^{249}Cf(^{18}O,^{9}Li)^{258}Lr$, and considering the 12- to 18-per-cent abundance of ^{249}Cf in the target, this activity is probably yet another nuclide different from ^{258}Lr and ^{257}Rf.

IX. References

(ALE68) J. M. Alexander, Chapter 4 of Nuclear Chemistry edited by Yaffe, p. 273 (1968).

(ALE82) J. M. Alexander, private communication (1982).

(ALO72) J. R. Alonso, J. O. Rasmussen, Bull. Am. Phys. Soc. 17, p. 78 (1972).

(ALO73) J. R. Alonso, Gmelin Handbuch der Anorganischen Chemie, (Verlag Chemie, GmbH, Weinheim/Bergstrasse) Vol. Fb, part A 1, p. 28 (1973).

(BAC74) B. B. Back et al., Proc. of Third Symp. on Physics and Chem. of Fission, Vol. 1, IAEA-SM-174/201, Rochester, N.Y.; Aug. 13-17, 1973; Proc. published by Int'l. Atomic Energy Agency; Vienna, Austria; p. 25 (1974).

(BAR81) A. Baran et al., Nucl. Phy. A361, p. 83 (1981).

(BEL81) P. Belery et al., Nucl. Instr. and Meth. 179, p. 1 (1981).

(BEM73) C. E. Bemis, Jr. et al., Phys. Rev. Lett. 31, p. 647 (1973).

(BEM76) C. E. Bemis, Jr. et al., Phys. Div. Annual Report, Oak Ridge National Lab., Report ORNL-5137. p. 73 (1976).

(BEM77a) C. E. Bemis, Jr. et al., Phys. Rev. Lett. 39, p. 1246 (1977).

(BEM77b) C. E. Bemis, Jr. et al., Phys. Rev. C16, p. 1146 (1977).

(BEM79) C. E. Bemis, Jr. et al., Phys. Rev. Lett. 43, p. 1854 (1979).

(BEM81) C. E. Bemis, Jr. et al., Phys. Rev. C23, p. 555 (1981).

(BOH48) N. Bohr, Kgl. Danske Videnskab. Selskab, Mat.-Fys. Medd. 18, p. 8 (1948).

(BOR70) J. Borggreen et al., Phys. Rev. C2, p. 1841 (1970).

(DEM80) A. G. Demin, V. A. Druin, et al.; data presented in a talk by V. A. Druin at the Int'l. Symp. on the Synthesis and Properties of New Elements; Dubna, USSR; Sept. 23-27 (1980); Joint Inst. for Nucl. Research, Report D7-80-556, abstract on p. 25 (1980).

(DON66) E. D. Donets et al., Atomnaya Énergiya, 20, p. 223 (1966) (Russian); Sov. Atomic Energy 20, p. 257 (1966) (English).

(DON66a) E. D. Donets et al., Yad. Fiz. 2, p. 1015 (1966) (Russian); Sov. J. Nucl. Phys. 2, p. 723 (1966) (English).

(DRU73) V. A. Druin et al., Joint Inst. for Nucl. Research; Dubna, USSR; Report JINR E7-7023 (1973); Atomnaya Énergiya 35, p. 279 (1973)(Russian); Sov. Atomic Energy 35, p. 946 (1973) (English).

(DRU77) V. A. Druin et al., Joint Inst. for Nucl. Research; Dubna, USSR; Report JINR E7-10499 (1977).

(DRU78) V. A. Druin et al., Joint Inst. for Nucl. Research; Dubna, USSR; Report P7-12056 (1978).

(EGG78) R. C. Eggers, private communication (1978).

(EGG81) R. C. Eggers and L. P. Somerville, Nucl. Instr. and Meth. 190, p. 535 (1981): also in Lawrence Berkeley Lab. Report LBL-12060 (1981).

(ESK71) K. Eskola et al., Phys. Rev. C4, p. 632 (1971).

(ESK81) P. Eskola et al., unpublished data (1981).

(FLE64) G. N. Flerov et al., Phys. Lett. 13, p. 73 (1964).

(FLE65) R. L. Fleischer et al., J. Appl. Phys. 36, p. 3645 (1965).

(FLE67) G. N. Flerov et al., Atomnaya Énergiya 22, p.494 (1967) (Russian); Sov. J. Atomic Energy 22, p. 611 (1967).

(FLE68) G. N. Flerov et al., Sov. J. Nucl. Phys. 6, p. 12 (1968) (English); Yad. Fiz. 6, p. 17 (1967) (Russian).

(FLE71) G. N. Flerov et al., Proc. of Int'l Conf. on Heavy Ion Physics; Dubna, USSR; Joint Inst. for Nucl. Research, Report JINR D7-5769, p. 125 (1971) (Russian).

(FLE75) R. L. Fleischer et al., Nuclear Tracks in Solids; U. of California Press; Berkeley, Calif. (1975).

(GÄG80) H. Gäggeler et al., GSI Scientific Report 1979, GSI-80-3, p. 62, ISSN 0174-0814; Gesellschaft für Schwerionenforschung mbH; Darmstadt, West Germany (July, 1980).

(GAN67a) Yu. P. Gangrskiĭ et al., Yad. Fiz. 5, p. 22 (1967) (Russian); Sov. J. Nucl. Phys. 5, p. 16 (1967) (English).

(GAN67b) Yu. P. Gangrskiĭ et al., Yad. Fiz. 5, p. 535 (1967) (Russian); Sov. J. Nucl. Phys. 5, p. 380 (1967) (English).

(GHI69) A. Ghiorso et al., Phys. Rev. Lett. 22, p. 1317 (1969).

(GHI70) A. Ghiorso, unpublished data (1970).

(GHI70a) A. Ghiorso, Proc. Robert A. Welch Foundation Conf. on Chemical Research XIII, The Transuranium Elements - The Mendeleev Centennial; Nov. 17-19, 1969; Houston, Texas; p. 107-150 of Proceedings; W.O. Milligan, editor (1970).

(GHI70b) A. Ghiorso et al., Phys. Rev. Lett. 24, p. 1498 (1970).

(GHI70c) A. Ghiorso et al., Phys. Rev. Lett. 32B, p. 95 (1970).

(GHI71) A. Ghiorso et al., Nature 229, p. 603 (1971).

(GHI71a) A. Ghiorso et al., Phys. Rev. C4, p. 1850 (1971).

(GHI71b) A. Ghiorso et al., unpublished data (1971).

(GHI73) A. Ghiorso et al., Phys. Rev. C7, p. 2032 (1973).

(GHI74) A. Ghiorso et al., unpublished data (1974).

(GHI74a) A. Ghiorso et al., Phys. Rev. Lett. 33, p. 1490 (1974).

(GHI76) A. Ghiorso, unpublished results (1976).

(GHI76a) A. Ghiorso, private communication (1976).

(GHI80a) A. Ghiorso and D. Lee, unpublished results (1980).

(GHI80b) A. Ghiorso, unpublished results (1980).

(GHI81) A. Ghiorso and L. P. Somerville, unpublished data (1981).

(GHI81a) A. Ghiorso et al., 1979-1980 Annual Report of the Nucl. Sci. Div., Lawrence Berkeley Lab., LBL-11588, UC-34, p. 85 (1981).

(GHI81b) A. Ghiorso, private communication (1981).

(GHI82) A. Ghiorso, private communication (1982).

(GOU74) R. Gough, private communication (1974).

(GRO82) H. Groenig et al., Lawrence Berkeley Lab. Report LBL-13483; also to be published in Nucl. Phys. A in 1982; 1980-1981 Annual Report of Nucl. Sci. Div., Lawrence Berkeley Lab. (1982).

(HAH74) R. L. Hahn et al., Phys. Rev. C10, p. 1889 (1974).

(HOF79) D. C. Hoffman et al., unpublished data (1979).

(HOF79a) D. C. Hoffman, private communication (1979).

(HOF81) D. C. Hoffman et al., Phys. Rev. C24, p. 495 (1981).

(HUL71) E. K. Hulet et al., Phys. Rev. Lett. 26, p. 523 (1971).

(HUL80) E. K. Hulet et al., Phys. Rev. C21. p. 966 (1980).

(HUL81) E. K. Hulet et al., private communication (1981).

(HVE71) P. Hvelplund, Kgl. Dan. Vidensk. Selsk. Mat. Fys. Medd. 38, no. 4 (1971).

(KEL69) K. A. Keller and H. MÜnzel, Kernforschungszentrum Karlsruhe, Institut fÜr Radiochemie: Karlsruhe, West Germany; Report KFK 1059 (1969).

(LEE82) D. Lee et al., Phys. Rev. C25, p. 286 (1982); also 1979-1980 Annual Report of Nucl. Sci. Div., Lawrence Berkeley Lab. Report LBL-11588, UC-34, p. 82 (1981).

(LEI77) M. E. Leino, Phil. Lic. Thesis, U. of Helsinki: Helsinki, Finland (1977).

(LEI81) M. E. Leino et al., Phys. Rev. C24, p. 2370 (1981).

(LOU74, 75) R. Lougheed and E. K. Hulet, U. of California, Lawrence Radiation Lab. Report UCRL-75782, Sept. (1974); also in Proc. of Third Annual Conf. of the Nucl. Target Development Soc.; Chalk River, Ontario, Canada; Oct. 1-3, 1974 (1975).

(McFA80) R. M. McFarland, unpublished data (1980).

(McGA81) P. L. McGaughey, private communication (1981).

(MÖL70) P. Möller and S. G. Nilsson, Phys. Lett. 318, p. 283 (1970).

(MÖL72) P. Möller, Nucl. Phys. A192, p. 529 (1972).

(MÖL81) P. Möller, private communication (1981).

(MOO81) K. Moody, private communication (1981).

(MOS71) U. Mosel and H. W. Schmitt, Phys. Rev. C4, p. 2185 (1971).

(MÜN79) G. Münzenberg et al., Nucl. Instr. and Methods 161, p. 65 (1979).

(MÜN80) G. Münzenberg et al., GSI Scientific Report 1979, GSI 80-3, p. 59, ISSN 0174-0814; Gesellschaft für Schwerionenforschung mbH: Darmstadt, West Germany (July, 1980).

(MÜN80a) G. Münzenberg, private communication (1980).

(MÜN81) G. Münzenberg et al., private communication and Nucl. Instr. and Meth. 186, p. 423 (1981).

(MÜN81a) G. Münzenberg et al., Z. Physik A300, p. 107 (1981).

(MÜN81b) G. Münzenberg et al., Gesellschaft für Schwerionenforschung mbH, Darmstadt, West Germany; Report GSI-81-36, contribution to the conference Actinides--1981; Asilomar, California; Sept. 10-15 (1981).

(MÜN82) G. Münzenberg et al., Proceedings of the Int'l. Conf. of Nuclei Far From Stability; Helsingør, Denmark; June 8-13, 1981; to be published in early 1982.

(MUS77) M. G. Mustafa and R. L. Ferguson, Bull. of Am. Phys. Soc. 22, p. 611 (1977); also private communication discussed in reference BEM77a.

(MUS78) M. G. Mustafa and R. L. Ferguson, Phys. Rev. C18, p. 301 (1978).

(MYE77) W. D. Myers, Droplet Model of Atomic Nuclei, Plenum Publishing, New York (1977).

(NIT80) J. M. Nitschke, private communication (1980).

(NIT81) J. M. Nitschke et al., Nucl.Phys. A352, p. 138 (1981).

(NIT81a) J. M. Nitschke, 1979-1980 Annual Report of Nucl. Sci. Div., Lawrence Berkeley Lab., LBL-11588, UC-34, p. 181 (1981).

(NIT82) J. M. Nitschke, to be published in Nucl. Instr. and Meth. (1982).

(NIT82a) J. M. Nitschke, private communication (1982).

(NOR70) L. C. Northcliffe and R. F. Schilling, Nuclear Data Tables, Vol. 7, Nos.3-4, p. 233, Jan. (1970).

(NUR70) M. J. Nurmia et al., unpublished excitation function data (1970).

(NUR71) M. J. Nurmia, Nucl. Chem. Annual Report, Lawrence Berkeley Lab., LBL-666, p. 42 (1971).

(NUR74) M. J. Nurmia, private communication (1974).

(NUR81) M. J. Nurmia, private communication (1981).

(OGA69) Yu. Ts. Oganessian et al., Joint Institute for Nucl. Research: Dubna, USSR; Report P7-4797 (1969); Atomnaya Énergiya 28, p. 393 (1970) (Russian); Sov. Atomic Energy 28, p. 502 (1970) (English).

(OGA74a) Yu. Ts. Oganessian et al., Report D7-8224, Joint Inst. for Nucl. Research; Dubna, USSR (1974); also Report D7-8099 (1974) (Russian); Gesellschaft für Schwerionenforschung mbH: Darmstadt, West Germany; GSI-translation-19 (1974) (German).

(OGA75) Yu. Ts. Oganessian et al., unpublished data quoted in reference TER75 (1975).

(OGA80) Yu. Ts. Oganessian and Yu. A. Lazarev, data presented in a talk at the International Symposium on the Synthesis and Properties of New Elements; Dubna, USSR; Sept. 23-27 (1980).

(PAU74) H. C. Pauli and T. Ledergerber, Proc. Symp. on the Phys. and Chem. of Fission; Vol. I, Rochester, N. Y.; 1973; IAEA-SM-174/201; Proc. published by Int'l Atomic Energy Agency; Vienna, Austria; p. 463 (1974).

(POL68) S. M. Polikanov, Sov. Phys. Uspekhi 11, no. 1, p. 22 (1968).

(PRI62) P. B. Price and R. M. Walker, J. Appl. Phys. 33, p. 3407 (1962).

(RAN73) J. Randrup et al., Nucl. Phys. A217, p. 221 (1973).

(RAN76) J. Randrup et al., Phys. Rev. C13, p. 229 (1976).

(RAN82) J. Randrup and W. D. Myers, private communication (1982).

(RAS71) J. O. Rasmussen, K. Sugawara-Tanabe, Nucl. Phys. A171, p. 497 (1971).

(ROG62) P. C. Rogers, Technical Report 76 (NYO-2303); Laboratory for Nuclear Science, MIT; Cambridge, Mass.; June (1962).

(RUD78) N. Rud et al., Nucl. Instr. and Meth. 151, p. 247 (1978).

(SEG65,77) E. Segre, Nuclei and Particles, p. 44, W. A. Benjamin Press (1965); 2nd edition (1977).

(SIK) T. Sikkeland and D. F. Lebeck, unpublished results.

(SIK68) T. Sikkeland et al., Phys. Rev. 172, p. 1232 (1968).

(SIL73) R. J. Silva et al., Nucl. Phys. A216, p. 97 (1973).

(SOM80) L. P. Somerville, Proc. of Int'l. Conf. on Future Directions in Studies of Nuclei Far From Stability; Sept. 10-13, 1979; Vanderbilt Univ.: Nashville, Tennessee; Proc. published by North Holland, p. 337 (1980).

(SOM82) L. P. Somerville, to be published in a Lawrence Berkeley Lab. Report (1982).

(STE80) E. Stender et al., Radiochem. Radioanal. Lett. 42, p. 291 (1980).

(TER75) G. M. Ter-Akopyan et al., Nucl. Phys. A255, p. 509 (1975).

(TOI78) C. M. Lederer and V. S. Shirley (editors), Table of Isotopes, J. Wiley and Sons, Inc., New York (1978).

(WAP77) A. H. Wapstra and K. Bos, Atomic and Nuclear Data Tables 19, p. 175 (1977).

(WIL78) K. E. Williams, Ph. D. thesis, Lawrence Berkeley Lab. Report LBL-7714; Berkeley, California (1978).

(WIL79) K. E. Williams and G. T. Seaborg, Phys. Rev. C19, p. 1794 (1979).

(WIL80) J. B. Wilhelmy and D. C. Hoffman, private communication (1980).

(WIN61) L. Winsberg and J. M. Alexander, Phys. Rev. C121, p. 518 (1961).

(ZAR77) R. N. Zare, Scientific American 236, p. 86, Feb. (1977).

(ZVA70) I. Zvara, Proc. of Robert A. Welch Foundation Conf. on Chemical Research XIII, The Transuranium Elements - The Mendeleev Centennial; Nov. 17-19, 1969; Houston, Texas; p. 153-185 of Proceedings; W.O. Milligan, editor (1970).

X. Acknowledgements

"Praise the Lord!" "Give unto the Lord the glory due unto His name."---Psalm 29:2; 146:1. "Acknowledge Him in all thy ways and He shall direct thy paths."---Proverbs 3:6. I thank Christ Jesus, my Lord, for His guidance and strength in performing the experiments, analyzing the data, and for the joy of knowing Him throughout this writing, typing, and preparation of figures. In this regard I would like to thank many people for prayer support and encouragement including Eugene and Mary Somerville, Terry and Mary Jean Cheuvront, Roger K. Armstrong, Ryoichi and Chiaki Wada, Ryuichi Okayasu, Yutaka Yoshimura, Miyuki Watanabe, Ung So (Steven) Choi, Mary Taylor, Chris Peiper, Vivian Ho, Leon Archambault, John Ingersoll, Bonnie Jacobs....

I also want to express sincere thanks to Albert Ghiorso, from whom I learned nearly everything I know about experimental techniques and methods of research in nuclear science. Many of the experiments that I carried out or helped to carry out were suggested by Albert Ghiorso and Michael Nitschke. I also want to thank Matti Nurmia for staying overnight to help me in many experiments at the 88-inch cyclotron as well as for suggestions in writing this thesis. To Michael Nitschke, besides for designing the tape and drum apparatuses used in many experiments, I owe special thanks for assistance in understanding, interpreting, and writing up the results of our experiments. Professor Glenn T. Seaborg provided me the opportunity to do heavy-element research, supported me as a graduate student in Berkeley, and assisted me in this writing. In addition, he allowed me to

present our results at the International Conference on Future Directions in Studies of Nuclei Far From Stability in Nashville, Tennessee, where I had a unique opportunity to exchange views with Soviet counterparts in heavy-element research. I owe humble thanks to Albert Ghiorso, Matti Nurmia, Professor Glenn Seaborg, and Michael Nitschke for being patient enough to stick with me during seven years of work together.

Kim Thomas (now at Los Alamos), while she was graduate student, and Matti Nurmia deserve special thanks for teaching me the techniques of cutting, annealing, etching, and scanning mica track detectors. The late Richard C. Eggers wrote the first multi-component maximum-likelihood computer code which is used throughout this work in determining half-lives from our data. Thanks to Jose Alonso we have a JORPLE code for calculating compound-nucleus neutron-evaporation cross sections. Matti Leino wrote a fantastic computer code DGENE2 which could computer-simulate lots of drum or tape experimental data for the purpose of testing the maximum-likelihood code.

Peter Möller and Jørgen Randrup were very kind to discuss their theoretical calculations of element-104 spontaneous fission half-lives with me. Professor Herbert Steiner contributed many helpful suggestions that have strengthened both the science and organization of this thesis by 100 per cent. Ryoichi Wada and Professor Buford Price made helful suggestions for the style and organization of the thesis. To all these people, "Thank you!"

Kenneth Hulet and Ronald Lougheed of Lawrence Livermore National Laboratory and Kenton Moody of the Lawrence Berkeley Laboratory

prepared most of the radioactive curium, berkelium, and californium targets. Harry Harrington, Grace (Bette) Shipley, "Cal" Calhoun, Marshall Lombardo, Jim Haley, and Ken Biscay were helpful in keeping me safe in the handling of other radioactive materials.

Roy Benedict, Bill Shrum, and the rest of the 88-inch cyclotron and SuperHILAC operating crews deserve thankful acknowledgement for tuning our beams. The help of Al Wydler, Leon Archambault, Richard Leres, Gil Hartley, and David Ruiz with many technical, electrical, and computer problems is cheerfully acknowledged. Saburo Yashita and Ryoichi Wada stimulated several interesting discussions. Paul Hamilton assisted in proofreading and printing out this document.

I would also like to thank Linda England and Kathy Fugitt for assistance in scanning micas. Professor Buford Price and Edward Shirk deserve special thanks for the use of Lexan track detectors in early preliminary experiments and for helpful discussions about spontaneous-fission track detection.

To Jeanne Hassenzahl and Jean Wolslegel I want to express thankful appreciation for the use of Wang word processors to produce this document.

This work was supported by the Director, Office of Energy Research, Division of Nuclear Physics of the Office of High Energy and Nuclear Physics of the U.S. Department of Energy under Contract DE-AC03-76SF00098.

ASSIGNED SPONTANEOUS FISSION ACTIVITIES

Colors identify the type of spontaneous fission (SF).

- SF from the ground state
- SF from a deformed shape isomeric state
- SF from an ordinary isomeric state
- Electron capture + β^+-delayed SF
- β^--delayed SF
- No SF activity observed. But the lower limit for the partial SF half-life of the ground state is quoted.

? denotes assignment probable

?? denotes assignment uncertain du to insufficient evidence

Z (proton number)

Example:

isomer half-life — 2.34×10⁷ yr — i (isomer, fission isomer in this case)

isotope

ground state half-life — 2×10¹⁶ yr

partial SF half-life for the ground state

101

100

99

97

96

^{242}Fm 0.8ms?? | ^{243}Fm 146ms 250s | ^{244}Fm 3.3ms | ^{245}Fm 4.2s ≥40000s | ^{246}Fm 1.2s 15s

248 ? ≤0.06

7min? ≤3×10⁻⁹%SF

20.8d 1.64×10⁶yr

182.75d 6.08×10⁶yr

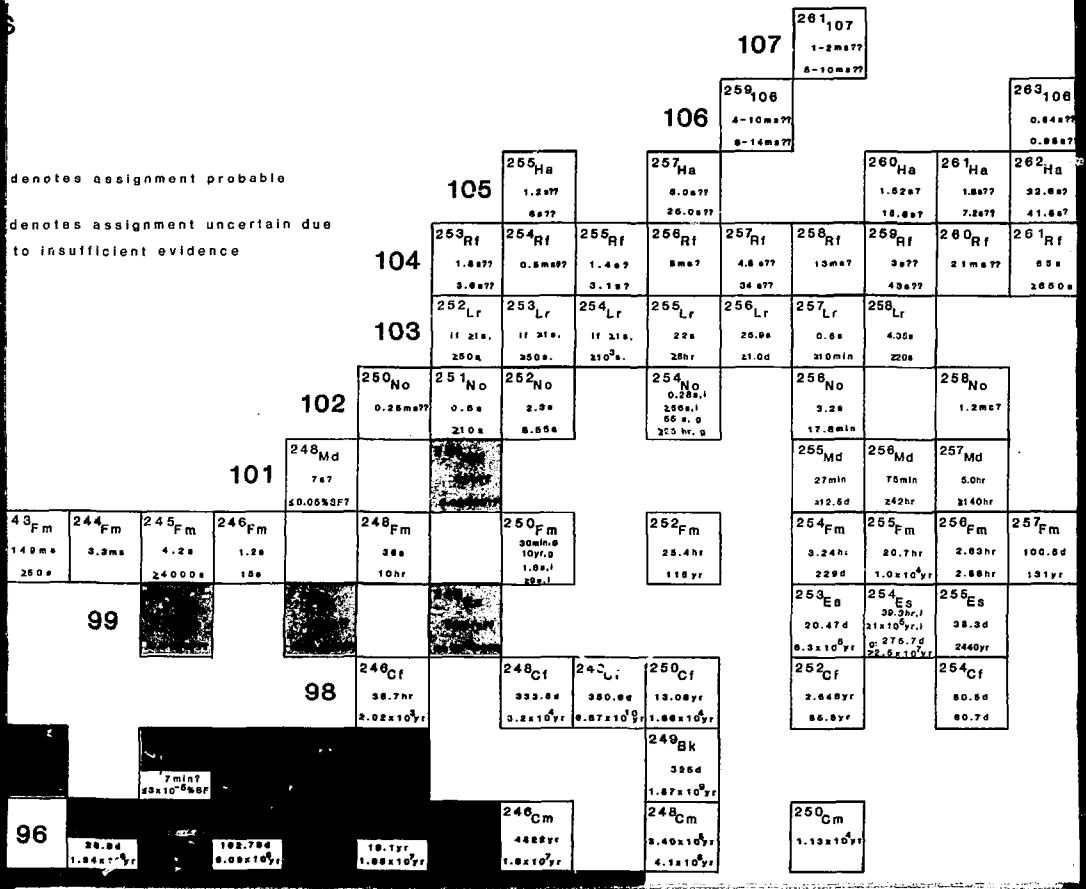
denotes assignment probable
denotes assignment uncertain due to insufficient evidence
107
106
105
104
103
102
101
99
98
96
261107 1-2ms?? 5-10ms??
259106 4-10ms?? 5-14ms??
263106 0.64s?? 0.96s??
255Ha 1.2s?? 6s??
257Ha 5.0s?? 26.0s??
260Ha 1.52s? 16.6s?
261Ha 1.8s?? 7.2s??
262Ha 32.6s? 41.6s?
253Rf 1.8s?? 3.6s??
254Rf 0.5ms?? 255Rf 1.4s? 3.1s?
256Rf 8ms? 257Rf 4.8 s?? 34 s??
258Rf 13ms? 259Rf 3s?? 43s??
260Rf 21ms?? 261Rf 65s ≥650s
252Lr If ≥1s, 250s 253Lr If ≥1s, ≥50s. 254Lr If ≥1s, ≥10^3s. 255Lr 22s 28hr 256Lr 25.9s ≥1.0d 257Lr 0.6s ≥10min 258Lr 4.0s 220s
250No 0.25ms?? 251No 0.8s ≥10s 252No 2.3s 8.5Ss 254No 0.28s,I 255s,I 55 s, g ≥23 hr, g 258No 3.2s 17.8min 258No 1.2ms?
248Md 7s? ≤0.05%SF? 255Md 27min ≥12.5d 256Md 75min ≥42hr 257Md 5.0hr ≥140hr
243Fm 149ms 250s 244Fm 3.3ms 245Fm 4.2s ≥4000s 246Fm 1.2s 15s 248Fm 36s 10hr 250Fm 30min,e 10yr,a 1.0s,I ≥2s,I 252Fm 25.4hr 118yr 254Fm 3.24hr 229d 255Fm 20.7hr 1.0x10^4yr 256Fm 2.63hr 2.86hr 257Fm 100.5d 131yr
253Es 20.47d 6.3x10^5yr 254Es 39.3hr,I 21x10^3yr,I g: 275.7d ≥2.6x10^7yr 255Es 38.3d 2440yr
246Cf 36.7hr 2.02x10^3yr 248Cf 333.5d 3.2x10^4yr 249Cf 350.6d 6.87x10^2yr 250Cf 13.08yr 1.66x10^4yr 252Cf 2.645yr 85.5yr 254Cf 60.5d 60.7d
249Bk 325d 1.87x10^3yr
7min? ≤3x10^-6%SF
246Cm 4482yr 1.8x10^7yr 248Cm 3.40x10^5yr 4.1x10^6yr 250Cm 1.13x10^4yr
28.8d 1.84x10^-5yr 162.79d 6.08x10^4yr 18.1yr 1.86x10^7yr

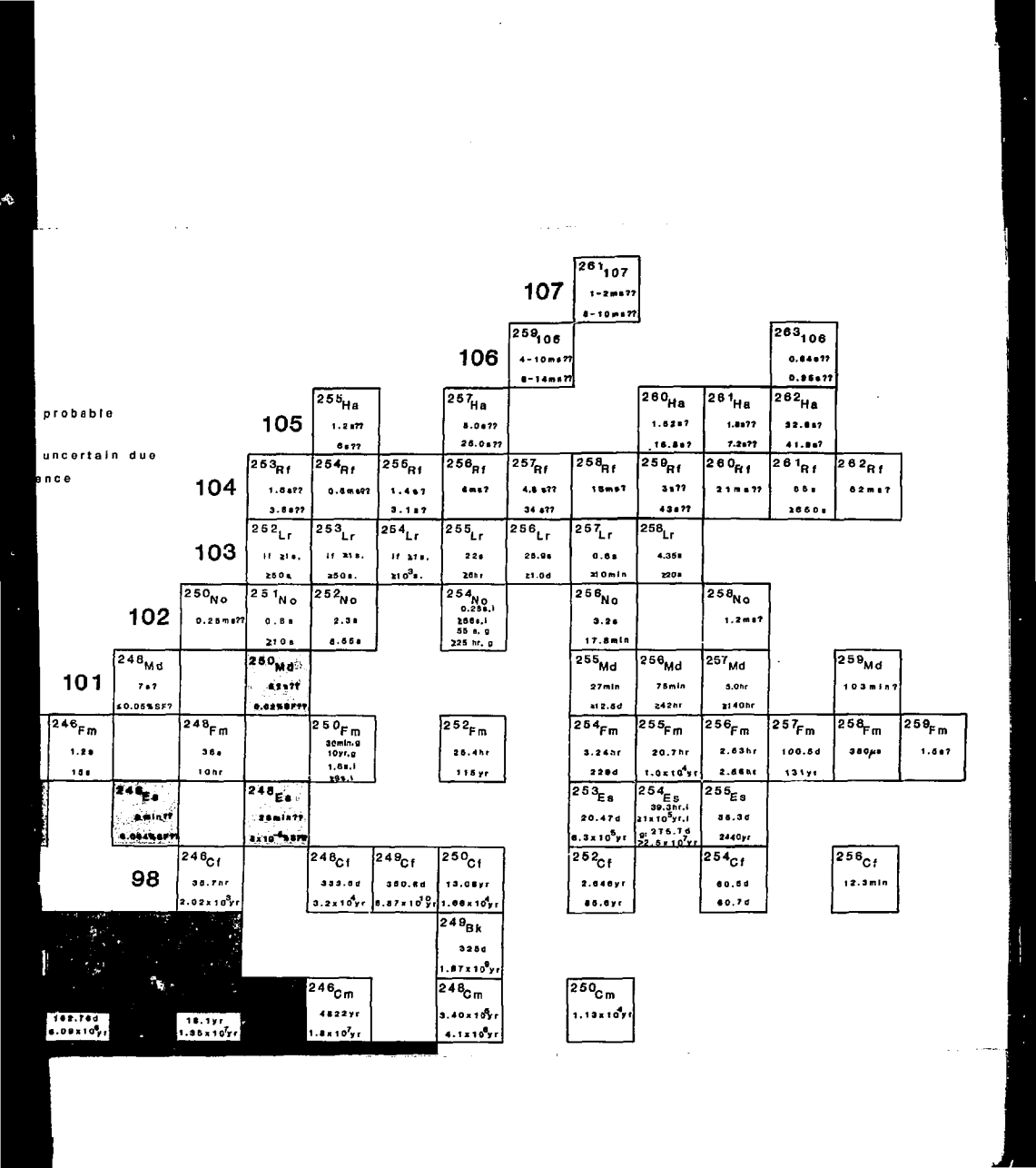
probable
uncertain due
ence
107
106
105
104
103
102
101
98
261107 1-2ms?? 8-10ms??
259106 4-10ms?? 8-14ms??
263106 0.64s?? 0.95s??
255Ha 1.2s?? 6s??
257Ha 5.0s?? 26.0s??
260Ha 1.52s? 16.8s?
261Ha 1.8s?? 7.2s??
262Ha 32.8s? 41.8s?
253Rf 1.6s?? 3.8s??
254Rf 0.6ms?? 256Rf 1.4s? 3.1s?
256Rf 6ms?
257Rf 4.8 s?? 34 s??
258Rf 15ms?
259Rf 3s?? 43s??
260Rf 21ms??
261Rf 65s ≥650s
262Rf 62ms?
252Lr 1.7 s. 250s.
253Lr 1.7 s. 250s.
254Lr 1.7 s. ≥10^3s.
255Lr 22s 26hr
256Lr 28.0s ≥1.0d
257Lr 0.6s ≥10min
258Lr 4.3s ≥20s
250No 0.25ms??
251No 0.8s 210s
252No 2.3s 6.55s
254No 0.29s,i 256s,i 55 s, g 225 hr, g
256No 3.2s 17.8min
258No 1.2ms?
248Md 7s? ≤0.05%SF?
250Md 52s?? 0.02%SF??
255Md 27min ≥2.6d
256Md 75min ≥42hr
257Md 5.0hr ≥140hr
259Md 103min?
246Fm 1.2s 15s
248Fm 36s 10hr
250Fm 30min,g 10yr,g 1.8s,i ≥95,i
252Fm 25.4hr 115yr
254Fm 3.24hr 220d
255Fm 20.7hr 1.0x10^4yr
256Fm 2.63hr 2.66hr
257Fm 100.5d 131yr
258Fm 380μs
259Fm 1.5s?
248Es 8min?? 0.04%SF??
248Es 25min?? 3x10^-4%SF??
253Es 20.47d 6.3x10^5yr
254Es 39.3hr,i 2.1x10^5yr,i or 275.7d 2.5x10^7yr
255Es 39.3d 2440yr
246Cf 35.7hr 2.02x10^3yr
248Cf 333.5d 3.2x10^4yr
249Cf 350.6d 8.87x10^39yr
250Cf 13.08yr 1.66x10^4yr
252Cf 2.646yr 85.5yr
254Cf 60.5d 60.7d
256Cf 12.3min
249Bk 328d 1.87x10^3yr
246Cm 4822yr 1.8x10^7
248Cm 3.40x10^5yr 4.1x10^6yr
250Cm 1.13x10^4yr
162.76d 6.09x10^6yr
18.1yr 1.35x10^7yr

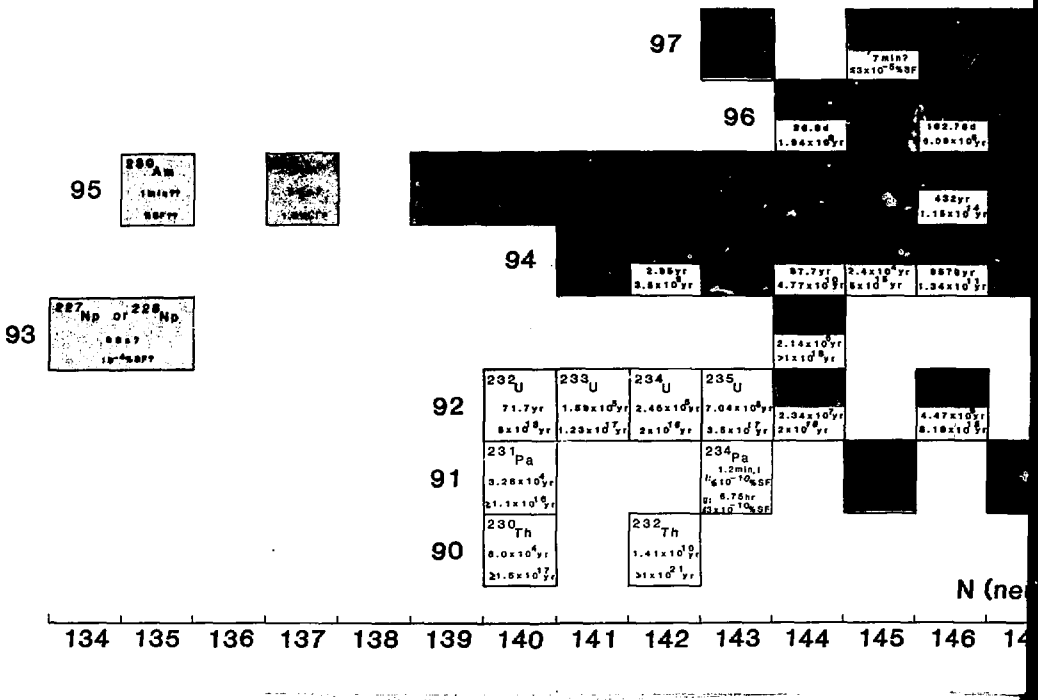
97
96
95
94
93
92
91
90
7min?
≤3x10⁻⁶%SF
98.8d
1.94x10⁶yr
102.70d
6.09x10⁶yr
239Am
11.9hr
98.8yr
432yr
1.15x10⁴yr
2.95yr
3.8x10⁶yr
87.7yr
4.77x10⁹yr
2.4x10⁴yr
8x10⁸yr
987yr
1.34x10¹³yr
227Np or 228Np
66s?
≤3x10⁻⁴%SF
2.14x10⁶yr
>1x10¹⁸yr
232U
71.7yr
≈1x10⁸yr
233U
1.59x10⁵yr
1.23x10¹⁷yr
234U
2.46x10⁵yr
2x10¹⁶yr
235U
7.04x10⁸yr
3.8x10¹⁷yr
2.34x10⁷yr
2x10¹⁸yr
4.47x10⁹yr
8.19x10¹⁵yr
231Pa
3.28x10⁴yr
≥1.1x10¹⁶yr
234Pa
1.2min,t
½≤10⁻¹⁰%SF
6.75hr
½≤10⁻¹⁰%SF
230Th
8.0x10⁴yr
≥1.5x10¹⁷yr
232Th
1.41x10¹⁰yr
>1x10²¹yr
N (ne
134
135
136
137
138
139
140
141
142
143
144
145
146
14

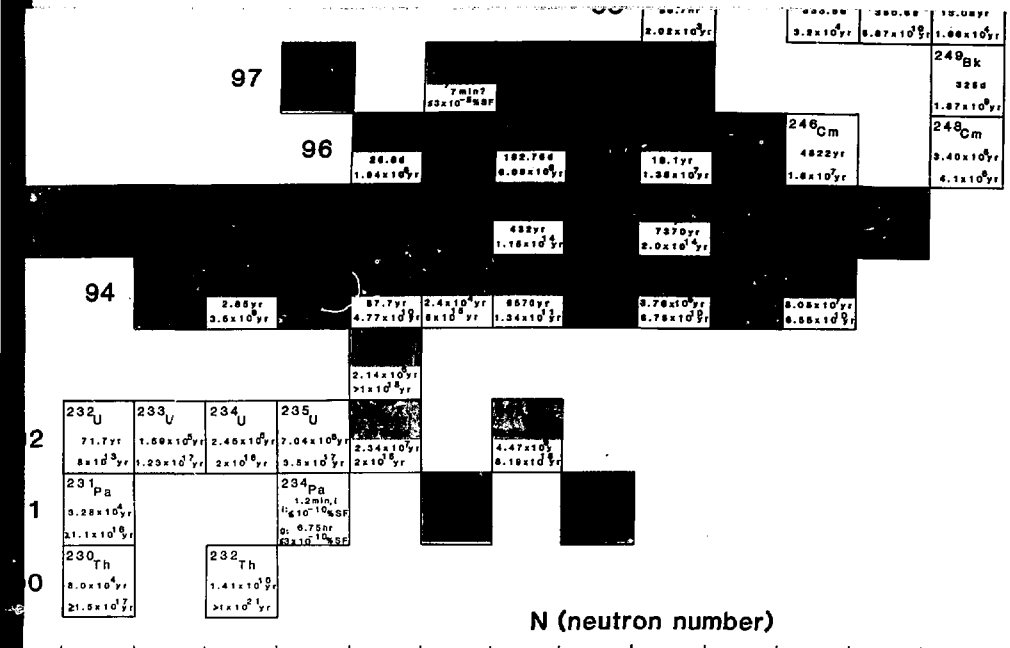
97
96
94
2
1
0
246Cm
4822yr
1.8x10^7yr
248Cm
3.40x10^5yr
4.1x10^6yr
249Bk
328d
1.87x10^9yr
232U
71.7yr
8x10^9yr
233U
1.59x10^5yr
1.23x10^7yr
234U
2.45x10^5yr
2x10^6yr
235U
7.04x10^8yr
2.34x10^7yr
2x10^6yr
231Pa
3.28x10^4yr
≥1.1x10^6yr
234Pa
1.2min,t
β: 6.75hr
230Th
8.0x10^4yr
≥1.5x10^7yr
232Th
1.41x10^10yr
N (neutron number)
139
140
141
142
143
144
145
146
147
148
149
150
151
152
153

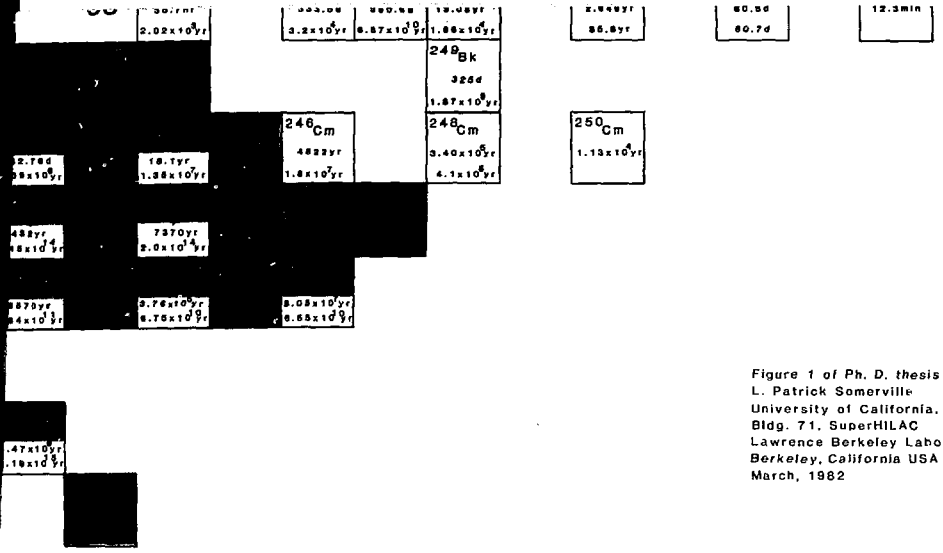

Figure 1 of Ph. D. thesis
L. Patrick Somerville
University of California, Berkeley
Bldg. 71, SuperHILAC
Lawrence Berkeley Laboratory
Berkeley, California USA
March, 1982

N (neutron number)

146 147 148 149 150 151 152 153 154 155 156 157 158 159

XBL 823-8490